Development, Characterization and Evaluation of Sorafenib Loaded Camel Milk Casein Nanoparticles

THESIS

Submitted in the partial fulfillment of the requirements

for the degree of

DOCTOR OF PHILOSOPHY

by

Ms. Aastha Mittal

2017PHXF0001P

Under the Supervision of

Dr. Uma S. Dubey

and

Co-Supervision of

Prof. Rajeev Taliyan

&

Dr. Sunil Kumar Dubey

BIRLA INSTITUTE OF TECHNOLOGY AND SCIENCE

PILANI – 333031 (RAJASTHAN) INDIA

2023

BIRLA INSTITUTE OF TECHNOLOGY AND SCIENCE, PILANI
PILANI - 333031 (RAJASTHAN) INDIA

CERTIFICATE

This is to certify that the thesis entitled "**Development, Characterization and Evaluation of Sorafenib Loaded Camel Milk Casein Nanoparticles**" submitted by **Aastha Mittal (2017PHXF0001P)** for the award of Ph.D. of the institute, embodies original work done by her under my supervision.

Signature of the Supervisor:
Name in capital letters: DR. UMA S. DUBEY
Designation: Associate Professor, Biological Sciences Department, BITS Pilani, Rajasthan
Date:

Signature of the Co-Supervisor:
Name in capital letters: PROF. RAJEEV TALIYAN
Designation: Professor, Department of Pharmacy, BITS Pilani, Rajasthan
Date:

Signature of the Co-Supervisor:
Name in capital letters: DR. SUNIL KUMAR DUBEY
Designation: General Manager, Medical Research, R & D Healthcare Division, Emami Ltd, Kolkata
Date:

Acknowledgement

Undertaking this Ph.D. has been a truly life-changing experience for me. It is an immense joy to express my gratitude to all who helped me through this fantastic journey and led to the successful completion of this thesis. First and foremost, I would like to acknowledge and thank my supervisor Dr. Uma S. Dubey, Department of Biological Sciences, Birla Institute of Technology and Science, Pilani, Rajasthan, for initially recruiting me for project JRF and further allowing me to pursue the doctoral program. Her exciting research idea, guidance, and consistent encouragement throughout the research helped me to complete the thesis. I am grateful for her caring, kind, understanding, and supportive nature. I am also thankful to her family for being gentle and kind, especially her husband, Prof. Balram Dubey, Professor, Department of Mathematics, BITS Pilani.

I also thank my Co-supervisors, Dr. Sunil Kumar Dubey and Prof. Rajeev Taliyan, Department of Pharmacy, for their advice and support throughout my research. I am grateful to Sunil sir for building confidence and energizing me at every stage. His helping and positive attitude helped me a lot in completing my work.

I am grateful to my Doctoral Advisory Committee (DAC) members, Prof. Sudeshna Mukherjee and Prof. Syamantak Majumder, for providing valuable suggestions, guidance, and comments during my presentations and for evaluating my thesis.

I express my deepest gratitude to Prof. V. Ramgopal Rao, Vice Chancellor, BITS Pilani, and Prof. Sudhir Kumar Barai, Director, BITS Pilani, Pilani campus for providing infrastructure, lab facilities, and administrative support from the institute. I sincerely thank Prof. S.K. Verma, Dean of Administration, BITS Pilani, for his constant administrative and academic support for fulfilling my Ph.D. thesis. I also express my gratitude to Prof. Shamik Chakraborty, Associate Dean, AGSRD, and Prof. Prabhat Nath Jha, Doctoral Research Convener (DRC), and Prof. Rajdeep Chowdhary, HOD, Department of Biological Sciences, BITS Pilani for their timely guidance and support regarding the academic formalities throughout the thesis work.

I would also like to thank the office staff of AGSRD for their support in various official procedures associated with the doctoral program at BITS Pilani. I acknowledge DST Rajasthan and BITS Pilani for providing me with the prerequisite fellowship and contingency grant.

I would also like to thank all the faculty members and research scholars of the Department of Biological Sciences for their guidance, help, and support during my coursework and research. A special thanks to the non-teaching staff – Mr. Mukesh, Mr. Ajay, and Dr. Iti Sharma for their help and cooperation in conducting my experiments.

I heartily acknowledge the cooperation, help, and support of my seniors Dr. Manohar Lal, Dr. Neelam Mahala, and junior Chetan Shrivastava. They are like family to me; their moral support and positive attitude helped me always be motivated. I thank them for teaching me all the basic cell culture-related techniques and necessary documentation work with detail and patience.

I would like to acknowledge the members of the cancer biology lab and all lab members of New Science Block. This CBG lab was like a second home to me. Here I have learned a lot about experimental techniques and research. I want to thank all the lovely lab seniors Dr. Subra Dash, Dr. Leena Fageria, and Dr. Heena Saini from whom I had cleared my doubts about basic experiments and data analysis. I would love to acknowledge all lab juniors – Mr. Sumukh, Ms. Ankita Daiya, Ms. Ankita Sharma, Ms. Mahima, Ms. Propanna, Ms. Subhashree, Mr. Chinmay, Ms. Simran, Ms. Lavanya, Ms. Ashima, Ms. Niyati, Mr. Yash, Mr. Rama, Ms. Harshita, Ms. Smita, for their love, respect, care, support, and assistance given during my experiments.

Special thanks to my close friends at BITS- Ms. Abhilasha, Ms. Sonia, Ms. Nidhi, Ms. Saumya, Mr. Anirudh, Mr. Ritobrata and Mr. Ashish who made the journey of my Ph.D very enjoyable and memorable. They have also been alongside to motivate me throughout all ups and downs. Without them, I can't imagine how I could have spent these beautiful years here.

My hearty thanks to the Department of Pharmacy for allowing me to work in their labs and to the research scholars of the Pharmacy department – Dr. Krishna, Rupesh, Dr. Swati, Dr. Shweta, Manisha, Mahipal, Arihant, Shobha, Pradyuth and Shrikant, for their kind support and guidance. I am grateful that they were always there to solve my any query. I am obliged and grateful to Rajesh for always helping and teaching me multiple aspects of pharmaceuticals and analytical and bioanalytical methods, besides helping in conducting *in vivo* animal experiments.

I would also like to thank Dr. Sushil, in charge of the animal house facility for his guidance in various processes related to animal handling and protocol approval. I would also like to acknowledge Vishal and Mukesh ji for training me in animal handling and their maintenance.

I also like to thank my special friends – Abhijeet, Sakshi, Rajesh, Ankita, and Shradha, for giving me their valuable time and advice, which directly and indirectly helped in this journey.

I also want to thank all the Meera Bhawan Hostel staff and mess staff of Meera Bhavan, specially Ritu, Mallika, and Indu mam, for their ever-ready help and care and for providing service as and when required.

I especially thank my parents, Mr. Mahesh Mittal, and Mrs. Anjana Mittal, for their patience, trust, and understanding. I specially appreciate that they perceived the value of this doctoral degree for me. They immensely contributed in the completion of this thesis by boosting my morale and bringing positivity in my moments of despair. Their blessings and sacrifices have inspired me to move forward in this journey. Love and thanks to my siblings, Mrs. Deeksha Dave and Akshat Mittal, for the faith and the encouragement they gave me in this journey.

I want to convey my heartfelt thanks to the Almighty. It is my faith in God that gave me optimistic hopes and kept my patience. This assignment would not have seen the light of day without his paramount blessings. Finally, I wish to thank everyone who directly or indirectly helped me in this endeavour.

Ultimately, I would like to thank and congratulate myself for attaining this achievement….. Well done…!!

Aastha Mittal

Abstract

Hepatocellular carcinoma (HCC), a primary liver cancer, is the third leading common cause of death worldwide. The major risk factors include chronic liver diseases like cirrhosis, long-term alcohol consumption, diabetes, hepatitis B, hepatitis C, and non-alcoholic fatty liver disease. Most patients with HCC are diagnosed very late when the disease has reached advanced-stages. Sorafenib, a kinase inhibitor drug, is approved for HCC. It has been shown to increase the survival rates of patients with advanced-stage liver cancer. However, because of sorafenib's poor water solubility, rapid metabolism, and low bioavailability, its clinical applications are constrained. The present study aimed to overcome these limitations of sorafenib through an improvised nanoparticulate drug delivery system. Casein, a major milk protein, possesses several exciting properties that make it a good candidate for drug delivery systems. Casein shows amphiphilic nature, self-assembling property, the ability to show sustained release and the capability to encapsulate hydrophilic and hydrophobic drugs. Camel milk was used as a source of casein protein because of its non-allergic potential, medicinal value and thermostable properties. Camel milk casein has a higher amount of hydrophobic protein, which enhances its drug delivery potential. In this study, we have developed and characterized sorafenib loaded camel milk casein nanoparticles. Subsequently, the efficacy of this sorafenib encapsulating camel milk casein nanoparticles has been studied *in vitro* in HepG2 cells by evaluating its cytotoxicity. Furthermore, pharmacokinetic and biodistribution studies of sorafenib loaded casein nanoparticles have been conducted using Swiss albino mice. Calcium chloride was used as a crosslinker to prepare the novel camel milk casein-based nanoparticles to encapsulate the hydrophobic drug sorafenib.

Initially, the resultant sorafenib-loaded camel milk casein nanoparticle was thoroughly characterized for size distribution, zeta potential, and morphology. Camel milk casein nanoparticles exhibited a particle size of around 230 nm with a uniform spherical shape and negative charge. The quantification of drug content in nanoparticles as well as the drug-protein binding studies was conducted by UV spectroscopy. The cytotoxicity and cellular uptake efficiency studies were performed in HepG2 cell lines. This sorafenib drug-loaded nanoparticle had a higher intracellular uptake of sorafenib than the free drug. The drug-loaded nanoparticles were also more cytotoxic in the mammalian hepatocarcinoma cell line, HepG2 as checked by MTT assay.

Subsequently, we evaluated the cytotoxicity and underlying mechanisms of apoptosis of sorafenib encapsulated in camel milk casein nanoparticles by conducting different apoptosis assays like DNA

fragmentation, Annexin Pi assay and checking the expression of apoptotic-related genes and proteins. Subsequently, the effect of the drug-loaded nanoparticles on cell cycle phase distribution has also been studied. Furthermore, the gene expression of apoptosis-related was also studied at the transcriptional and translational levels. Our study revealed that entrapment of sorafenib within casein nanoparticles exerted potent cytotoxicity against liver cancer cell lines by inducing cell cycle arrest, apoptotic cell death and generation of reactive oxygen species. The gene expression studies at the transcriptional level suggested the up-regulation of tumour suppressor 53, pro-apoptotic bax (bcl-2 associated X protein), and caspase-3 while decreased anti-apoptotic bcl2 (B-cell lymphoma-2) thus, hence confirming induction of apoptotic cell death. At the translational level, it was demonstrated that treatment increased the expression of proapoptotic bax protein and decreased the antiapoptotic protein bcl2 expression. We have also validated the absence of any toxicity of camel milk casein drug-loaded nanoparticles in normal cells taking HEK 293 cells as a model system. Further, we also calculated the therapeutic index of nanoparticles, which came out to be about two times higher as compared to the drug. Our results highlighted the feasibility of using camel milk casein nanoparticles as a nontoxic, biocompatible delivery vehicle with enhanced therapeutic outcomes.

Furthermore, we conducted an *in vivo* pharmacokinetic and distribution study of sorafenib-loaded camel casein nanoparticles in Swiss albino healthy mice. Before this, we developed a bioanalytical method of sorafenib quantitation in mice plasma and various tissues like the liver, kidney, lungs, heart, and spleen. Furthermore, the pharmacokinetic study upon intravenous administration of SFN-CasNPs in Swiss albino mice, showed that SFN-CasNP enhanced the bioavailability of sorafenib drug as exhibited by the enhanced area under the curve (AUC) and $t_{1/2}$ of the drug. Further, an enhanced accumulation of SFN-CasNPs in the liver and kidney (biodistribution studies) indicated their therapeutic usefulness in liver and kidney cancer that eventually could prove to be useful for clinical studies. Very importantly, we have observed less accumulation of drug-loaded nanoparticles in the heart as compared to the free drug. This indicates the safety of a nanoparticulate drug delivery system for the heart.

Therefore, it can be seen from above that in this study a novel, simple and reproducible method has been developed for synthesizing sorafenib-loaded camel milk casein nanoparticles. *In vitro,* cytotoxic studies in HepG2 cells show the strong anticancer effects of sorafenib and sorafenib encapsulated nanoparticles may be mediated via increasing the ROS level whereas cytotoxicity is induced by

apoptosis. Notably, the casein-encapsulated sorafenib nanoparticles did not show any significant cytotoxicity to normal HEK cells. Overall, this study has confirmed the benefit of sorafenib loaded casein nanoparticles by enhancing bioavailability, $t_{1/2}$ and more selective delivery to the liver while being free from cardiac toxicity.

Table of Contents

List of Figures

List of Tables

List of Abbreviations

Abbreviation	Description
DNA	Deoxyribonucleic acid
DLS	Dynamic light scattering
PDI	Poly dispersity index
C6	Coumarin 6
NAC	N-acetyl cysteine
NPs	Nanoparticles
FDA	Food and drug administration
EPR	Enhanced permeability and retention
P53	Tumour protein 53
PBS	Phosphate buffered saline
PI	Propidium iodide
PVDF	Polyvinylidene fluoride
RIPA	Radioimmunoprecipitation assay
EDTA	Ethylenediaminetetraacetic acid
PARP	Poly (ADP-ribose) polymerase
FTIR	Fourier transform infra-red
FBS	Fetal bovine serum
HBV	Viral hepatitis B
SEM	Scanning electron microscopy
RES	Reticuloendothelial system
ROS	Reactive oxygen species
FITC	Fluorescein isothiocyanate
SDS-PAGE	Sodium dodecyl sulfate-polyacrylamide gel electrophoresis
GLOBOCAN	Global cancer
MTT	(3-(4,5-Dimethylthiazol-2-yl)-2,5-diphenyltetrazolium bromide)
TI	Therapeutic index
DMSO	Dimethyl sulfoxide
EDTA	Ethylenediamine tetra acetic acid
HCl	Hydrochloric acid
NaOH	Sodium hydroxide
SDS-PAGE	Sodium dodecyl sulphate polyacrylamide gel electrophoresis
BSA	Bovine serum albumin
Bcl-2	B cell lymphoma-2
CUSO4	Copper sulphate
DCFDA 2',7'	Dichlorofluorescein diacetate
NCCS	National centre for cell science
CO2	Carbon dioxide
RNA	Ribonucleic acid
cDNA	Complementary DNA
PCR	Polymerase chain reaction

UV	Ultraviolet radiation
ANOVA	Analysis of variance
NRCC	National research centre on camel
HepG2	Hepatoma G2
RT-PCR	Reverse transcription polymerase chain reaction
Bax	BCL2 associated X
BITS	Birla institute of technology and science
HCC	Hepatocellular carcinoma
US	United States
HCV	Hepatitis C virus
NFLD	Non-alcoholic fatty liver disease
BCLC	Barcelona clinic liver cancer
RFA	Radiofrequency ablation
TACE	Trans arterial chemoembolization
ICIs	Immune checkpoint inhibitors
CTLA-4	Cytotoxic T lymphocyte-associated protein 4
PD-1	Programmed cell death protein 1
PD-L1	Anti-programmed death-ligand
TKIs	Tyrosine kinase inhibitors
MDR	Multidrug resistance
DDS	Drug delivery system
Pgp	Permeability glycoprotein
PK	Pharmacokinetics
ADME	Absorption, Distribution, Metabolism, and Excretion
NDDS	Nanoparticulate drug delivery system
HER2	Human epidermal growth factor receptor 2
EGFR	Epidermal growth factor receptor
PD	Pharmacodynamics
PDGF	Platelet-derived growth factor
VEGFR	Vascular endothelial growth factor receptor
MPS	Mononuclear phagocytic system
PLA	Poly (lactic acid)
PCL	Poly (ε-caprolactone)
PLGA	Poly (lactic-co-glycolic acid)
HPMA	N-(2-hydroxypropyl)-meth acrylamide copolymer
GRAS	Generally considered safe
α-la	α-Lactalbumin
β-lg	β-Lactoglobulin
CoQ10	Coenzyme Q10
EGCG	Epigallocatechin gallate
Lf	Lactoferrin
BBB	Blood brain barrier
CNS	Central nervous system
SFN	Sorafenib

TPGS	d-α-Tocopheryl polyethylene glycol 1000 succinate
Sora@siRNP	Sorafenib-loaded silica-containing redox nanoparticles
GI	Gastrointestinal
HSCs	Hepatic stellate cells
AUC	Area under curve
T1/2	Half time
MRT	Mean residence time
Co	Initial concentration
Ke	Elimination constant
Cl	Clearance
Vd	Volume of distribution
MQ	Milli-q
$CaCl_2$	Calcium chloride
ATR	Attenuated total reflection
ZP	Zeta potential
E.E	Encapsulation efficiency
MEM	Minimum essential medium
STR	Short tandem repeat
TBS	Tris buffer saline
HRP	Horseradish peroxidase
ECL	Enhanced chemiluminescence
SFN-CasNPs	Sorafenib-loaded casein nanoparticles
PE	Phycoerythrin
SEM	Standard error mean
CNP	Casein nanoparticles without the drug
PS	Phosphatidylserine
Bax	Bcl-2 associated X protein
RCC	Renal cell carcinoma
BCS	Biopharmaceutics classification system
IAEC	Institutional animal ethics committee
HPLC	High performance liquid chromatography
NCA	Non-compartmental analysis
C_0	Drug concentration at time 0
Cmax	Maximum plasma concentration
Z_λ	Elimination rate constant
T_{max}	Time to first occurrence of C_{max}
SD	Standard deviation
IS	Internal standard
FLT-CAS	Flutamide casein
TEM	Transmission electron microscopy
EE	Encapsulation efficiency

Chapter-1 : Introduction & Review of Literature

1.1 General Introduction

Cancer is characterized by uncontrolled growth and abnormal division of cells leading to disease progression and mortality. Its treatment by chemotherapy is often limited by non-specific drug delivery and the consequent side effects. Besides the disease itself, the side effects of cancer therapy also significantly increase morbidity in patients and lead to difficulty in compliance with complex therapeutic regimens. The utilization of nanotechnology-based drug delivery systems using natural biomolecules holds a very promising approach in chemotherapy.

Advancements in pharmaceutical and nanotechnology sciences have catapulted the importance of milk proteins much beyond their consumption for nutritional benefits. Milk components, especially its proteins, have played a vital role in the nutrition, growth, overall development and survival of infants across mammalian species. Camel milk is very nutritious and has various health and therapeutic benefits against diseases. It is known for its antimicrobial, anti-diabetic, immuno-modulatory, and anticancer activity due to the high level of bioactive molecules like lactoferrin, lysozymes, lactoperoxidases, peptidoglycan recognition proteins and most importantly, nanosized antibodies (Dubey et al. 2015; Mahala et al. 2022). Many milk proteins, especially casein micelles, serve as carriers of various important bioactive molecules present in milk. Casein's amphiphilic nature and flexible structure especially make it a very suitable molecule to act as a molecular transporter. Camel milk is preferred over cow's milk as it is significantly better for people with lactose intolerance or cow's milk allergy due to the absence of the protein beta-lactoglobulin, the causative agent of milk allergies in many people (Maryniak et al. 2018). Yet the individual protein fractions of camel milk have yet to be exploited for their nutritional value, medicinal properties and drug delivery potential.

Cancer ranks as the second leading cause of death globally. According to GLOBOCAN, 10 million cancer deaths occurred in 2020, and 19.3 million new cases have been reported (Sung et al. 2021). Predictions are that these cases will rise to 28.4 million by 2040. Amongst cancer-related mortality, lung cancer exhibits the highest count, being responsible for 1.8 million deaths (18%), followed by colorectal cancer (9.4%), liver cancer (8.3%), stomach cancer (7.7%) and female breast cancer

(6.9%) (Deo et al. 2022). Liver cancer is the third leading cause of cancer death worldwide, depicted in Fig 1.1. Improvisation in drug delivery for the treatment of liver cancer is the subject of study in the present thesis, as will be detailed later.

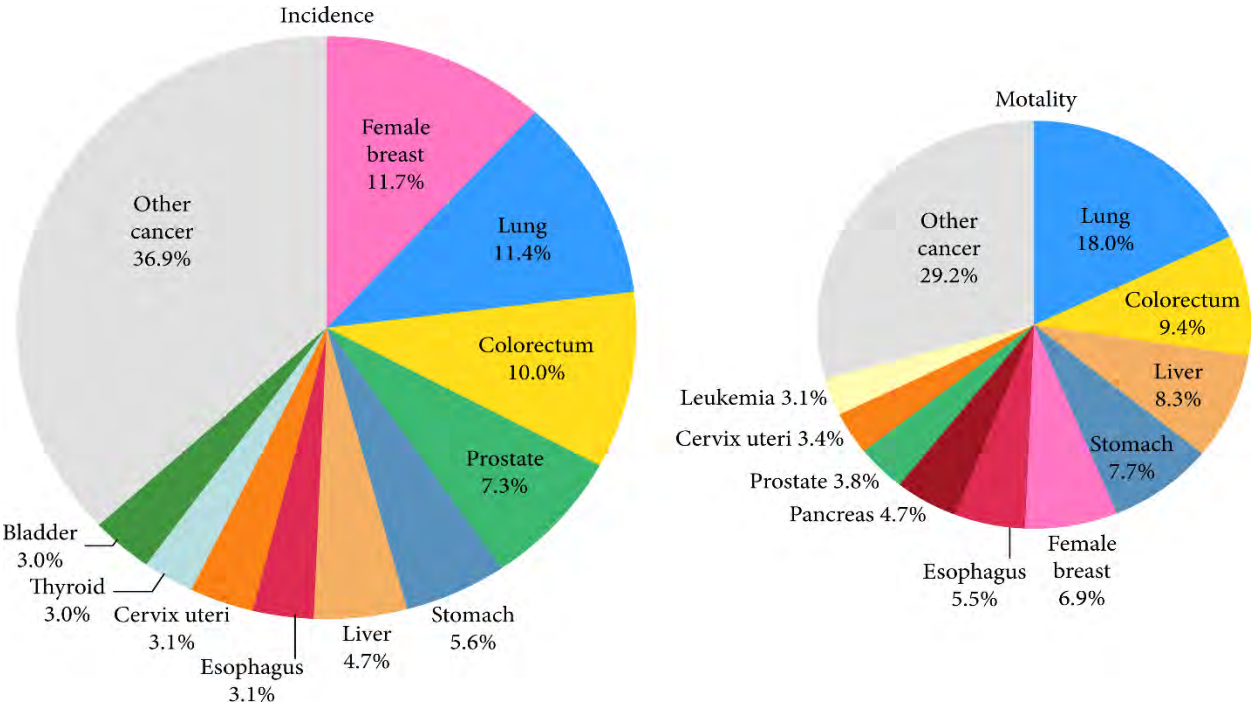

(Adapted from Sung *et al.*, 2021)

Figure 1. 1 Distribution of cancer incidence and mortality in 2020

Cancer cells are able to sustain proliferative signalling, evade growth suppressors and resist cell death. They show replicative immortality and are able to induce more blood vessel formation (angiogenesis) to fullfill their increased metabolic requirements. As the disease progresses, these cells invade the basal membrane and migrate to other organs (metastasis) (Hanahan et al. 2000). Metastasis and angiogenesis are prominent features of cancer the former being a significant cause of death from cancer (Nishida et al. 2006). These significant hallmarks of cancer have been depicted in Fig 1.2.

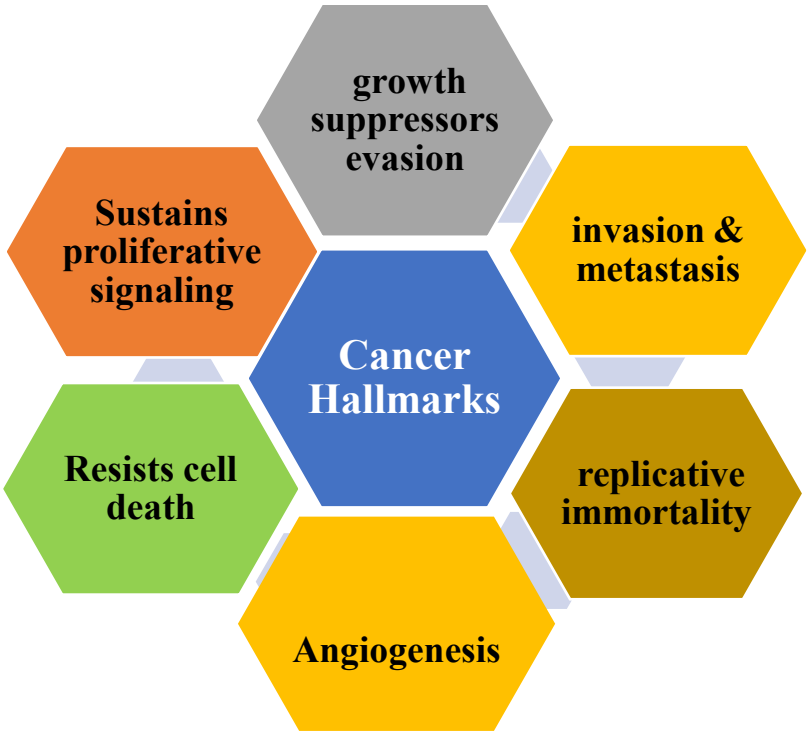

Figure 1. 2 Hallmark of cancer

1.2 Liver

Liver is one of the largest organs of our body, situated under the right rib beneath the right lung of the body and weighs around 1.2-1.4 kg. The liver plays a vital role in the production of bile, which helps in the breakdown and digestion of lipids (including fats and cholesterol). The liver stores and synthesizes multiple fat-soluble vitamins like A, D, E and K. Most importantly, it plays a vital role in the interconversion of macromolecules and detoxification of drugs, toxins, etc. It is also the central organ of blood detoxification, besides having many immunological functions (Chew et al. 2019). The detailed functions of the liver have been depicted in Fig. 1.3. Hepatitis A, B, and C, fatty liver disease, cirrhosis, liver cancer, hemochromatosis, and Wilson disease are the major liver diseases from which approximately 2 million people die yearly (Marcellin et al. 2018; Williams 2006).

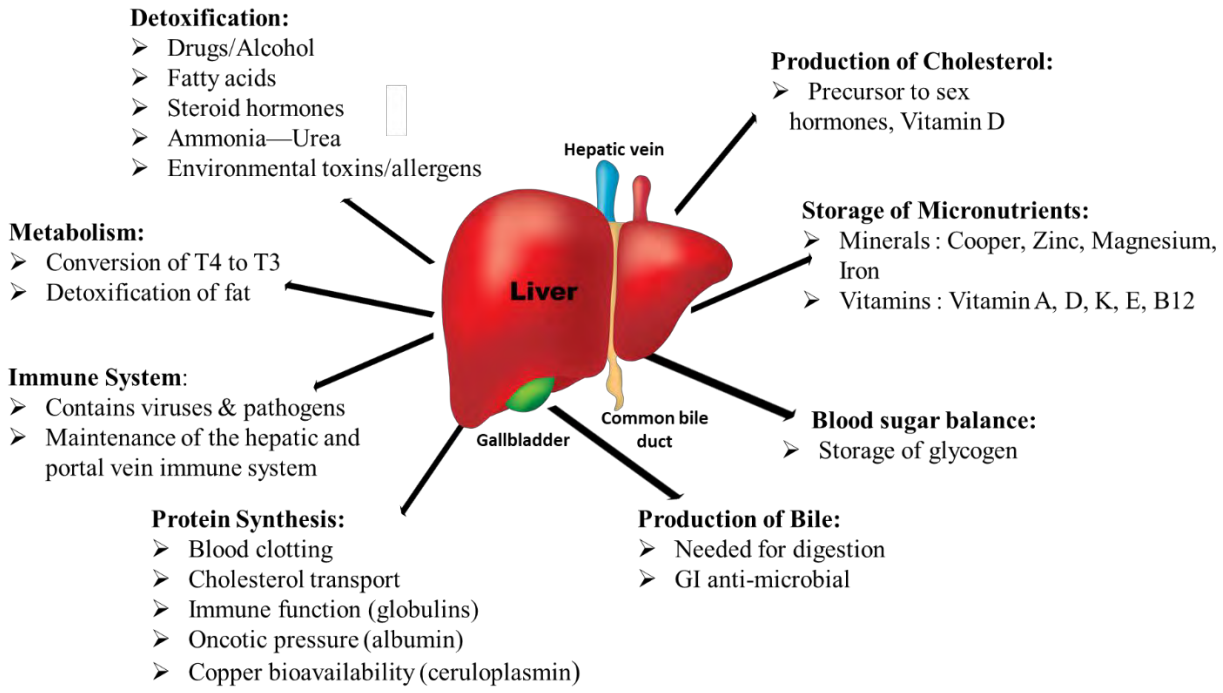

Figure 1. 3 Functions of the liver

1.3 Liver cancer

Cancers originating in hepatocytes are categorized as primary liver cancer, whereas when the cancer cells metastasize to the liver from other organs like the pancreas, colon, stomach, breast, or lung, it comes under the category of secondary liver cancer (Usmani et al. 2018). In the United States and Europe, secondary or metastatic liver tumours are more common than primary liver cancer.

Primary liver cancer includes hepatocellular carcinoma (HCC), cholangiocarcinoma and angiosarcoma (Ananthakrishnan et al. 2006). Approximately 80% of primary liver cancer belong to the category of (HCC). This is associated with chronic degenerative liver conditions, like cirrhosis and generally affects adults. Cholangiocarcinoma, which arises in bile duct cells in the liver, comprises 10-20% of primary liver cancer. Angiosarcoma is a fast-growing primary liver cancer that starts in the liver's blood vessels and is a rare type of primary liver cancer found in adults (Fig 1.4).

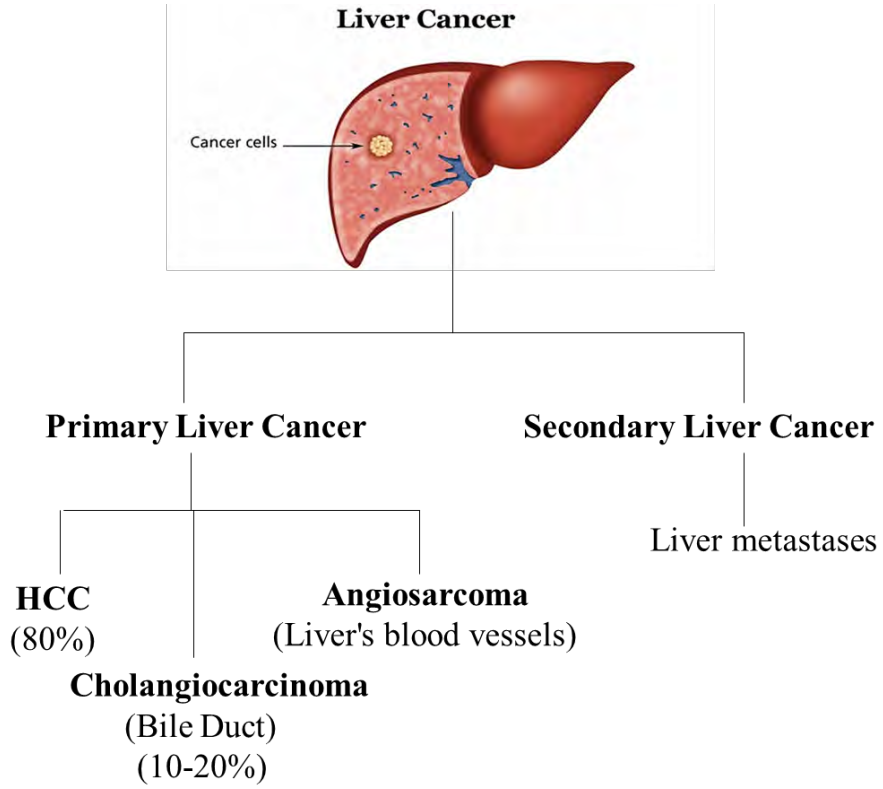

Figure 1. 4 Types of liver cancer

1.4 Prevalence of primary liver cancer

Primary liver cancer is the sixth most frequently diagnosed and the third most common cause of cancer-related death. Liver cancer is 2-3 times more common in males than females. In the last four decades, the incidence of liver cancer has at least tripled (Petrick et al. 2019). For men, liver cancer is the fifth most common cause of cancer incidence, whereas, for women, it is the seventh most common cause of incidence.

Most incidences of HCC occur in Eastern and South Eastern Asia (Mongolia, Thailand, Cambodia, and Viet Nam) and in sub-Saharan Black Africans (Egypt and Niger) (Singal et al. 2020). Hepatic viral infections are common in developing countries, Africa, Central East Asia and the United States. The important risk factors will be discussed in the future section.

Global data suggests an estimated 905,677 people were diagnosed with primary liver cancer, while 830,180 died in 2020 (Rumgay et al. 2022). Predictions suggest that this year in 2023, diagnoses of a total of 41,210 people (27,980 men and 13,230 women) and a total of 29,380 deaths (19,000 men and 10,380 women) from liver cancer are likely to occur just in the United States (Siegel et

al. 2023). However, incidence and cancer-specific mortality will continue to increase. The number of new cases and deaths from liver cancer could rise by more than 55% by 2040 (Mukthinuthalapati et al. 2021; Rumgay et al. 2022). Although considerable progress has been made in understanding liver cancer, it remains a challenging disease.

In India, the incidence of HCC is rising and is a concern for public health. The highest incidence of liver cancer was reported in parts of India, particularly Sikkim and Arunachal Pradesh, in 2014 (Shetty et al. 2022). The primary reason for the prevalence of liver cancer in Northeast India was hepatitis B & C infections in people. This prevalence and detection rate is getting higher with time. HCC in India also occurs in an advanced stage of cirrhosis, complicating detections and outcomes (Mondal et al. 2022).

1.5 Hepatocellular carcinoma (HCC)

HCC is recognised to be very most complex aggressive disease. Its tumours demonstrate considerable morphological and molecular heterogeneity (Li et al. 2016). It shows inter-tumoral heterogeneity among patients and intra-tumoral heterogeneity within the individual tumour. This heterogeneity complicates the available treatment options. Its heterogeneity and progression lead to metastasis, drug resistance, and poor clinical prognosis. Genetic heterogeneity and genetic drift, epigenetic environment, and genomic instability are the main reported reasons for tumour survival, even in cellular stress conditions (Llovet et al. 2008).

1.5.1 Epidemiology & risk factors for HCC

The worldwide incidence of HCC varies depending on its risk factors. The multiple risk factors associated with HCC development have been depicted in Fig 1.5. In the United States, cirrhosis is the most common underlying cause of HCC, with 80% of patients diagnosed having underlying cirrhosis. The hepatitis-causing virus is transmitted through infected blood and body fluids. This is one of the main causes of liver cirrhosis, which ultimately results in liver cancer (Yang et al. 2019). Chronic infections lead to persistent liver inflammation. Long-term infections with hepatitis B virus (HBV) and hepatitis C virus (HCV) are associated with developing HCC. Excessive alcohol consumption, non-alcoholic fatty liver disease (NFLH), obesity, aflatoxin, smoking and type 2 diabetes are some other important risk factors that drive HCC initiation and progression through different mechanisms (Paradis et al. 2023).

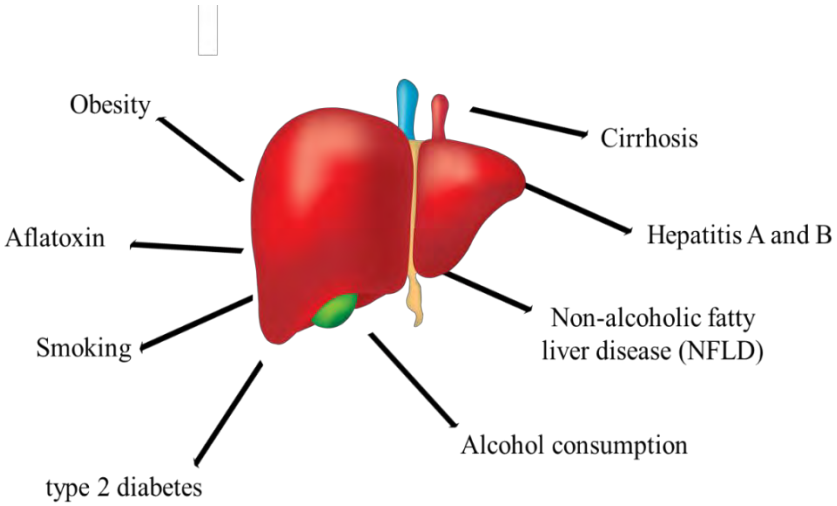

Figure 1. 5 Risk factors for HCC

The geographical distribution of HCC according to risk factors has been depicted in Fig 1.6. Major incidences of HCC occur in Eastern and South-Eastern Asia and in sub-Saharan Black Africans. Hepatic viral infections are common in developing countries, Africa, Central East Asia, and the United States (Mukthinuthalapati et al. 2021). However, hepatitis B can be prevented by vaccination and safe hygiene. Our surroundings, lifestyle, age (<60), and food intake play a significant role in tumorigenesis. These factors may change the genetic and signalling networks that control the functioning of cells. Chronic alcohol consumption can lead to alcohol-induced cirrhosis followed by the transformation of hepatocytes. Alcohol intake is an etiological factor in Central and Eastern Europe (Huang et al. 2023). Aflatoxin, a carcinogenic toxin produced by the fungus, can contaminate certain food items like grains (rice, wheat), corn, nuts, and soybeans. Its intake, either directly or via the food supply chain, can cause liver cancer (Mart et al. 2023). This fungus generally grows in tropical countries that are humid and have a warm climate. A detailed understanding of all possible risk factors inducing hepatocarcinogenesis could be helpful in preventing this disease.

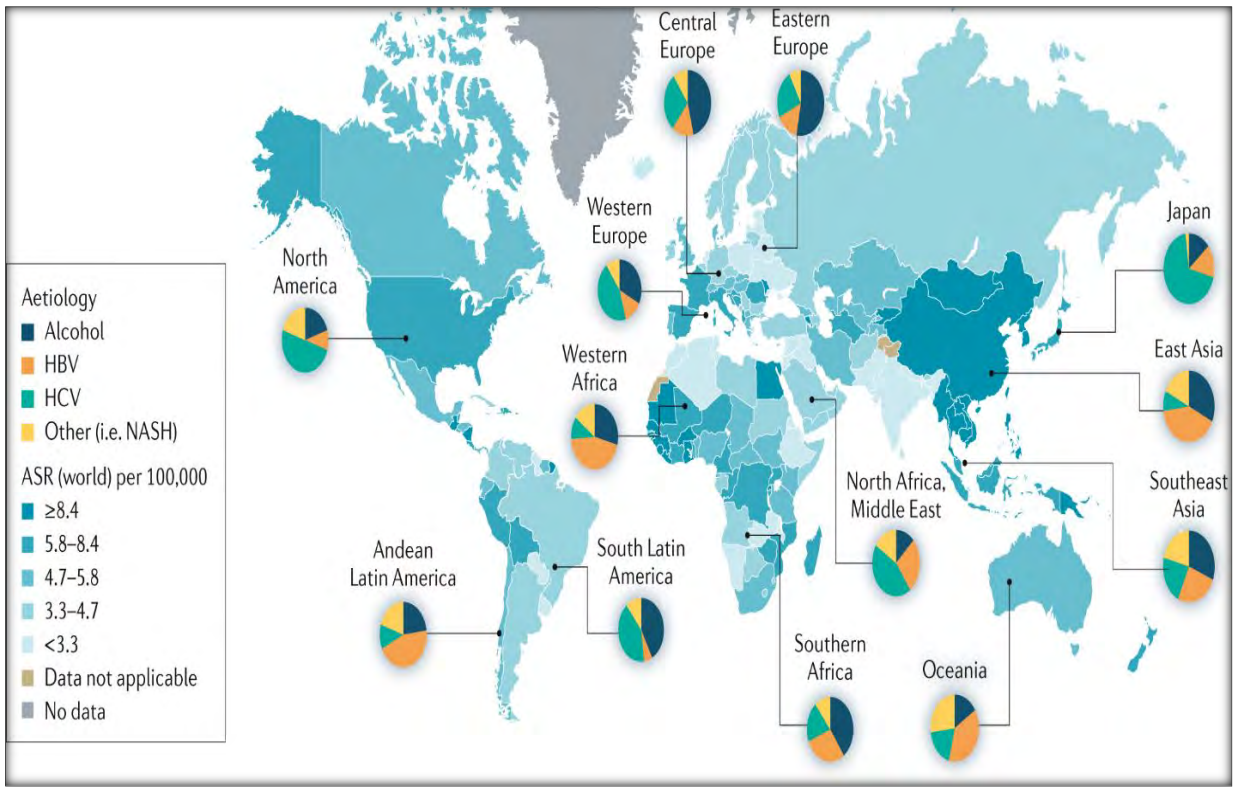

(Adapted from Llovet et al. 2021)

Figure 1. 6 Geographical distribution of HCC Incidence according to etiological factors

1.5.2 Staging of HCC

Treatment of liver cancer is given according to the stage of the disease. Staging of liver cancer tells about the tumour size, its location, and the advancement or invasiveness of the disease (Pons et al. 2005). Amongst various staging systems, The Barcelona Clinic Liver Cancer (BCLC) staging system is quite widely used. Different stages of liver cancer as per the BCLC staging system are shown in Table 1.1.

Table 1.1 Staging of HCC

BCLC Stage	Tumour Burden	Function of liver
Very early stage (O)	Tumour size is ≤2 cm	normal functioning of the liver
Early stage (A)	Single or multi tumours with a size less than 3 cm	normal functioning of the liver
Intermediate stage (B)	Multiple tumours in the liver	normal functioning of the liver
Advanced stage (C)	Vascular invasion or extrahepatic spread	normal functioning of the liver
End stage (D)	Maximum HCC burden	impaired liver function

1.5.3 Treatment of HCC

Standard treatment options available for the early and intermediate stages of HCC are surgery, liver transplantation, radiofrequency ablation (RFA), and transarterial chemoembolization (TACE) (Méndez-Sánchez et al. 2021). However, in advanced HCC, the treatment becomes limited. However, chemotherapies, molecular targeted therapy, and immunotherapy are often given in the advanced stage when surgical sectioning is impossible. The treatment options have been described below and depicted in Fig 1.7, per the disease progression.

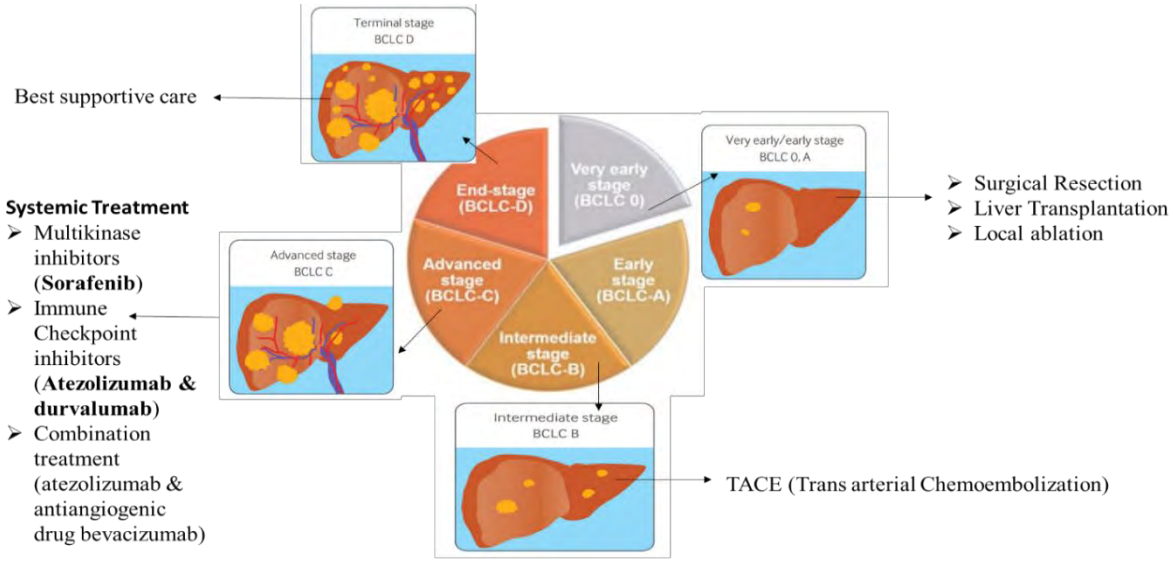

(Adapted from Yang, J. D., & Heimbach, J. K. (2020)

Figure 1. 7 Standard treatment of liver cancer

1.5.3.1 Surgery & Liver Transplantation: Surgical treatment is possible only in non-metastasized hepatic tumours**.** It is the best possible direct treatment option in the early stage of the disease while the liver function is still fine. The side effects may include pain, weakness, fatigue, and temporary liver failure. Besides surgery, liver transplantation is also an additional option when fewer tumours grow with smaller sizes (Liu et al. 2015). Problems like an insufficient suitable liver donor, donor's liver rejection by the host body and its infection are always a cause of concern (Hartke et al. 2017).

1.5.3.2 Radiofrequency ablation (RFA): It is a heat or thermal therapy used in an early stage of HCC to destroy primary or metastatic tumours in the liver. A needle-like probe is placed on the tumour site that delivers electromagnetic energy (Ryan et al. 2016). The generation of an electric field through electromagnetic energy causes agitation of the ions in the target tissue, resulting in frictional heat. Permanent tissue destruction occurs at temperatures of 45°C- 60°C. However, RFA is ineffective for enormous tumour burdens. Moreover, it has a high chance of recurrence after treatment.

1.5.3.3 Trans Arterial Chemoembolization (TACE): TACE is widely used to treat the intermediate stages of HCC. It is considered a first-line treatment. In TACE, the catheter is passed through blood vessels until it reaches the liver's hepatic artery to deliver the embolic agents to block the blood vessels that feed the tumour and facilitate the chemotherapeutics drugs that can act on the liver tumour (Chang et al. 2020). TACE is performed when surgical resection of the liver is not possible.

1.5.3.4 Immunotherapy: Immunotherapy involves treatment with agents or drugs that can modify the immune system to recognise and act against tumour-specific antigens on cancer cells. It is now recognized that immune checkpoints prevent a detrimental immune response against healthy cells. United States Food and Drug Administration (US FDA) approved immunotherapy includes Immune checkpoint inhibitors (ICIs)**.** To maintain homeostasis, liver immune cells utilise various checkpoint proteins like cytotoxic T lymphocyte-associated protein 4 (CTLA-4), programmed cell death protein 1 (PD-1), and anti-programmed death-ligand (PD-L1) (Johnston et al. 2019). Monoclonal antibodies like pembrolizumab and nivolumab are used against PD-1. For anti-CTLA-4, drugs like tremelimumab and a combination of nivolumab and ipilimumab are used, while inhibitor drugs for PD-L1 atezolizumab, avelumab, and durvalumab are used. Recently, approval

was given for a combination treatment of HCC. A combination treatment of immune checkpoint inhibitor atezolizumab (Tecentriq) and antiangiogenic drug bevacizumab (Avastin) has been very recently used (Mandlik et al. 2023). Cancer immunotherapy has a critical role to play in HCC treatment. But, there is still enough scope for significant improvements in this context.

1.5.3.5 Molecular targeted therapy: With advances in tumour biology and molecular genetic profiling, several signalling pathways and molecular mechanisms have been identified as responsible for initiating and promoting HCC. Kinases are a family of enzymes involved in protein phosphorylation or growth factors phosphorylation. These proteins regulate cellular machinery like proliferation, differentiation, cell cycle, migration, and apoptosis. Any dysregulation, mutation, and hyperactivation of kinases can lead to abnormal growth of cells and the spread of cancer. The kinase inhibitors are a large group of unique and potent antineoplastic agents specifically targeting protein kinases. These kinases are altered in cancer cells, accounting for their abnormal growth. Kinase inhibitors may also block the growth of new blood vessels (angiogenesis) that tumours need to grow. Molecular targeted therapy plays an important role as it inhibits various kinases that are involved in cancer progression. Amongst tyrosine inhibitors, Sorafenib was approved as the first targeted therapy for advanced HCC treatment in 2007 worldwide (Fig 1.7). Another drug, Lenvatinib, an oral multi-targeted tyrosine kinase inhibitor, has also been approved to treat advanced HCC after ten years and post-phase III trials (Kudo 2020).

In contrast, other multikinase inhibitor drugs, such as regorafenib, cabozantinib, and ramucirumab, have been developed as second-line therapy (Bteich et al. 2019). The development of approved tyrosine kinase drugs for HCC has been depicted in Fig. 1.8. The other tyrosine kinase inhibitors (TKIs) such as sunitinib, erdafitinib, erlotinib, anlotinib, pazopanib, tivantinib, brivanib, and linifanib have been tested in phase III trials. Still, the outcome of these trials was far from satisfactory (Ikeda et al. 2018). Moreover, small molecular chemotherapy in HCC also suffers from the drawbacks of dose-limiting toxicities, development of multidrug resistance (MDR) and unfavourable side effects like the formation of other cancers. Therefore, there is a desperate need for a developing drug delivery system (DDS) to overcome these limitations and improve overall survival.

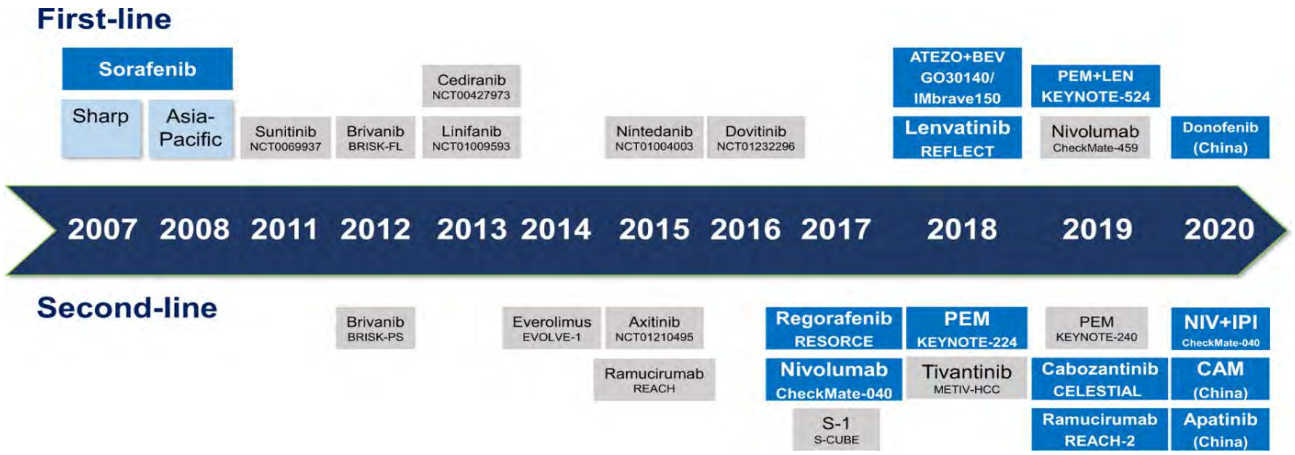

(Adapted from Huang, Ao, et al. 2020)

Figure 1. 8 Approved molecular targeted drugs for HCC

1.6 Sorafenib and its mechanisms of action

Sorafenib tylosate is an FDA-approved, small-molecule, targeted anticancer drug. Other than liver cancer, it is also used in the treatment of renal and thyroid cancers. Sorafenib is found to not only improve the quality of life of the patient but also enhance survival. It is commercially available in the market under the brand name Nexavar in tablet form and is recommended to be taken orally (Llovet et al. 2008).

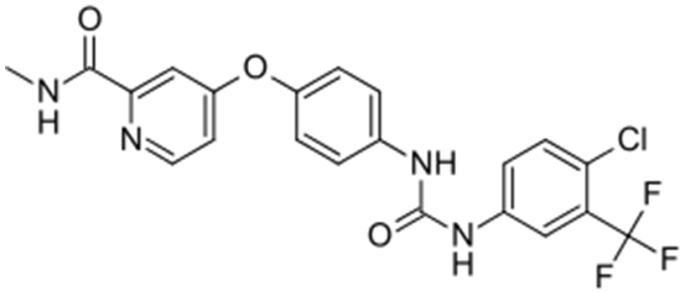

(Adapted from Tseng, et al. 2013)

Figure 1. 9 Molecular structure of sorafenib

Sorafenib is an inhibitor of several kinases involved in tumour cell proliferation, growth and angiogenesis. These kinases include Raf, vascular endothelial growth factor receptor 2 (VEGFR) and platelet-derived growth factor receptor (PDGFR). Raf is serine/threonine kinase, which, when activated by Ras (membrane-localized protein), stimulates gene transcription in the nucleus, leading to various tumour-promoting cellular effects. Vascular endothelial growth factor (VEGF) is the primary mediator of normal and tumour-associated angiogenesis. It exerts this effect through

several mechanisms, including induction of endothelial cell division and migration, promoting endothelial cell survival through protection from apoptosis and reversing endothelial cell ageing. VEGF interacts with receptors (VEGFR 1,2,3) on the endothelial cell surface, leading to autophosphorylation of intracellular receptor tyrosine kinase and further activating a cascade of downstream proteins (Niu et al. 2010). PDGF has its receptor on the surface of capillary endothelial cells. The binding of PDGF to the receptors has several effects on endothelial cell motility and apoptosis (Raica et al. 2010). Sorafenib also induces autophagy, which further helps suppress tumour growth (Prieto-Domínguez et al. 2016).

1.6.1 Clinical limitations of sorafenib

The clinical use of sorafenib is limited by its low and variable oral bioavailability. Sorafenib is a lipophilic and poorly water-soluble molecule. Its poor oral absorption is caused by its low solubility (Kong et al. 2021). The absolute sorafenib bioavailability has not been evaluated adequately. However, one study reported its absolute bioavailability too low, around 8.3% (Yang et al. 2016). Its mean relative bioavailability after administration of tablet dosage forms was found to be 38 - 49 % compared to an oral solution.

Another problem is that it undergoes high presystemic hepatic metabolism. Therefore, a higher daily dose of 800 mg has to be given. It also has a high efflux by virtue of the permeability glycoprotein (Pgp). Furthermore, it shows altered pharmacokinetics and lower bioavailability (28%) after taking food. Its use is associated with several adverse effects, such as dermatological reactions (hand-foot skin reaction, rash or itching of the skin), gastrointestinal problems, diarrhoea, liver dysfunction, hair thinning, weight loss, hypertension, fatigue, abdominal pain, and nausea. Adverse reactions may lead to reduced doses, interrupted treatment, reduced efficacy and patient compliance (Raut et al. 2022). Some of these solubility and bioavailability-related issues can be addressed by encapsulating this drug with a suitable nanocarrier system, as has been done in the present thesis.

1.7 Therapeutic index

It can be seen from above that there is an acute need to create a suitable drug delivery system that can enhance its drug therapeutics index and possibly reduce the side effects associated with its consumption. With a low therapeutic index, anticancer drugs or their active molecules exhibit adverse effects in normal tissues, which limits their efficacy (Olusanya et al. 2018). Using

nanoparticles as a nanocarrier in drug delivery systems provides a platform for delivering drugs with increasing anti-cancer efficacy, reducing their side effects, and improving therapeutic index through selective targeting of tumour tissues. The therapeutic index quantitatively measures the drug's safety and efficacy. It is a ratio that compares the blood concentration at which a drug becomes toxic and the concentration at which it is effective. The larger the therapeutic index (TI), the safer or more effective the drug is (Lynch 2022). The TI is calculated by considering the cytotoxicity of a drug (or viability of a treated cell) in normal cells and in cancer cells in an *in vitro* experiment. Therapeutic index = (IC50 normal (non-neoplastic) cell lines) / (IC50 cancer (neoplastic) cell line) (Deepa et al. 2012). TI is defined here as the ratio of the drug concentration that inhibits 50% viability of the normal cells to the concentration that inhibits 50% viability of tumour cells. In this respect, biodegradable nanoparticles with a limited life span as long as therapeutically needed would be optimal.

1.8 Pharmacokinetic and biodistribution study and their applications

Medications are prescribed in order to give maximum therapeutic outcomes with minimal side effects, if any. Pharmacokinetics (PK) deals with drug absorption, distribution, metabolism and excretion, whereas pharmacodynamic**s** (PD) is the study of a drug's molecular, biochemical, and physiologic effects or actions. Actually, pharmacokinetics studies the effect that an organism has on the drug, whereas pharmacodynamics studies the action of the drug on the organism. The chemical and physical properties of the nanoparticles, including size, surface charge, and surface chemistry, are important factors that determine their PK and biodistribution. The Pharmacokinetics study of drugs provides the estimation of the locations and concentrations of a drug in different areas of the body. By studying it, safe drug dosing can be estimated.

Nanotechnology has been increasingly employed in drug delivery. The tissue distribution of nanoparticles largely defines their therapeutic effect and toxicity. Currently, optimal drug delivery systems are being explored to increase the drug dissolution rate, enhancing absorption and bioavailability (Arti et al. 2022). Bioavailability is one of the vital pharmacokinetic properties of a drug. When the drug is administered in a dose, the part that reaches the systemic circulation unchanged is called its bioavailability (Toutain et al. 2004). The blood concentration of any drug is often correlated with its efficacy and toxicity. The pharmacokinetic profiles of a free drug and the drug encapsulated in the nanoparticles often differ. Together study of pharmacokinetics and

biodistribution helps analyze plasma or tissue drug concentration profiles, monitor their level, compare them with their nanoformulations and optimize the dosage. Therefore, monitoring nanoparticles' pharmacokinetics and biodistribution are essential to understanding and predicting their efficacy and side effects. Undesirable biodistribution or pharmacokinetic behaviour can lead to toxicological or side effects on the body. Pharmacokinetics studies provide information on the administered food compound or drug's circulation throughout the body for the entire duration of exposure. It encompasses the drug's absorption, distribution, metabolism, and excretion (ADME) (Li et al. 2019).

1.9 Nanoparticulate drug delivery system (NDDS) in cancer

Nanotechnology is a new field of science that takes advantage of the peculiar properties of matter at the nanoscale range. The extreme surface area to / volume ratio of nanoparticles allows them to interact efficiently with their environment. Nanoscale drug delivery systems can be very suitably used to transport drugs either passively or actively to the tumour site, thereby playing an essential role in diagnosing and treating tumours. The challenge of crossing the blood-brain barrier could also be possible due to the use of a nano-drug delivery system (Gupta et al. 2012).

Nanoparticles target the tumour cells either actively or passively (Fig 1.10). In passive targeting, the retention of nanoparticles at the tumour site is mainly due to the enhanced permeability and retention (EPR) effect. According to this, the size of the nanoparticles influences their uptake and enhances their retention at the tumour site due to the leaky vasculature and defective lymphatic drainage system in a tumour. Unlike low molecular weight drugs, it does not extravasate out of blood vessels at this size (Ejigah et al. 2022). In active targeting, the nanoparticles as drug carriers are designed to target specific cancer cells by attaching ligands against specific receptors present on them (Zwicke et al. 2012). Transferrin and folic acid receptors are overexpressed in many types of cancers and can serve as targets for active transport. Other common targets include human epidermal growth factor receptor 2 (HER2) and epidermal growth factor receptor (EGFR) (Large et al. 2019). It has been observed that nanoparticles coated with anti-HER2 monoclonal antibodies (Herceptin), which had been loaded with paclitaxel, showed significantly higher tumour accumulation of paclitaxel in a disseminated ovarian cancer model compared with free paclitaxel (Cirstoiu-Hapca et al. 2010).

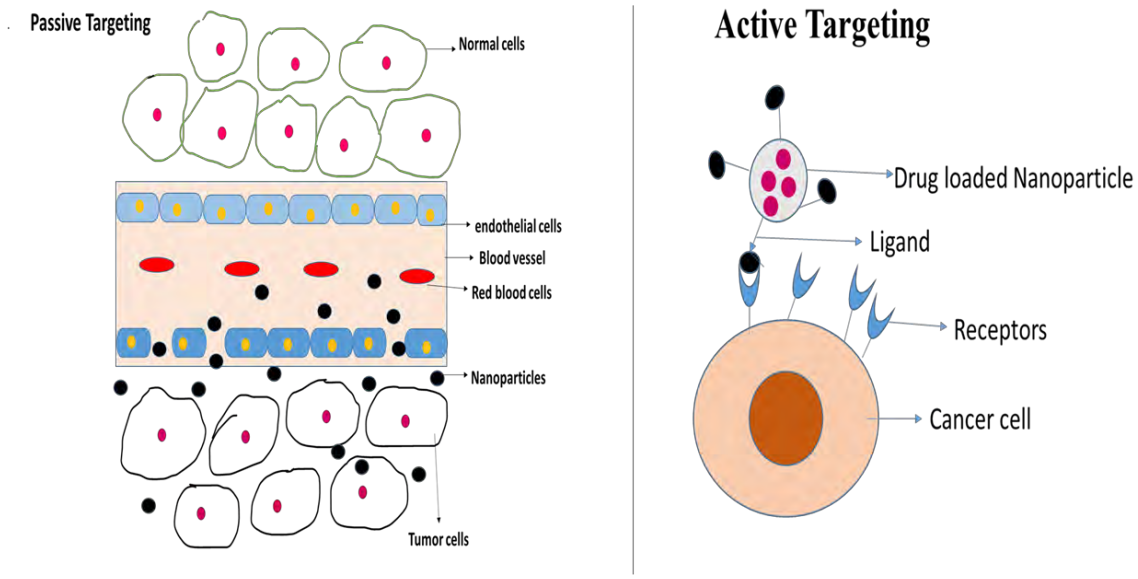

Figure 1. 10 Active and Passive targeting of nanoparticles to cancer cells

Nanocarriers such as liposomes, micelles, polymeric nanomaterials, mesoporous silica, gold, and magnetic nanoparticles have improved biomedical applications, including gene and drug delivery (Edis et al. 2021). Polymeric particulate systems are derived from biodegradable and biocompatible polymers but are synthesised within a nano range to protect drugs against *in vitro* and *in vivo* degradation. Reduced liver metabolism and renal clearance of drug-encapsulated nanoparticles often result in prolonged blood circulation with an increased chance of accumulation in the target tissue. They also facilitate the release of the drug in a controlled manner. In addition, the polyethylene glycol (PEG) modification can protect them from blood clearance by the mononuclear phagocytic system (MPS) by preventing opsonisation (Alexis et al. 2008). Nanoparticulate drug delivery systems have also established benefits in cancer treatment and management by demonstrating good pharmacokinetics and, hence better bioavailability of water-insoluble drugs. Its usage also limits the unnecessary accumulation of the drug in various non-target organs, thereby improving the biodistribution to the target organ (Narvekar et al. 2014). Besides this, polymeric nanoparticles can be made to possess intelligent responses upon being stimulated by variations in temperature, pH, redox, light, enzyme activity, etc. (Alsehli 2020).

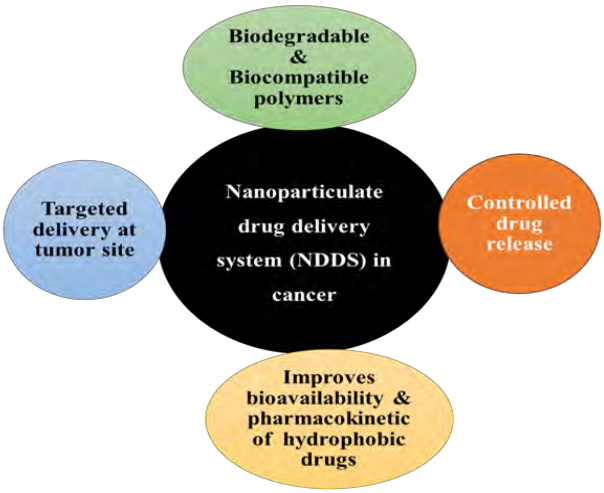

Figure 1. 11 Advantages of nanoparticulate drug delivery system in cancer

Many current cancer chemotherapy regimens can only prolong the patient's life instead of being able to cure the disease completely. High dosages of chemotherapeutic drugs cause severe side effects due to the non-specific *in vivo* distribution and limited efficiency. The solubility of the drug has a significant role in its final biodistribution, efficiency, and uptake. Solubilizing agents, such as dimethyl sulfoxide (DMSO), are added to the system to increase solubility *in vitro*. However, this compound leads to neurotoxicity *in vivo*. Even at low concentrations, this toxicity restricts the applications of free drugs for treatment (Shihong Shen et al. 2017).

Efforts have been made to reduce side effects by employing biological and pharmacological strategies. It is a great challenge to balance the two by designing novel delivery systems for selective distribution. Doxil (liposomal doxorubicin), Marqibo (Liposomal vincristine), Onivyde (liposomal irinotecan), Abraxane (albumin-particle bound paclitaxel), Eligard (leuprolide acetate), Vyxeos (liposomal cytarabine and daunorubicin), DaunoXome (liposomal daunorubicin) are some FDA- approved nanotechnology-based medicines for various cancers available in the market for clinical use (Rodríguez et al. 2022).

Bioavailability is one of the vital pharmacokinetic properties of a drug. It is approximated that about 65 billion dollars are wasted per year because of the poor bioavailability of drugs. Several new anticancer drugs act by blocking or turning off signals. Some examples of such drugs are tyrosine inhibitors dasatinib and sorafenib, or monoclonal antibodies bevacizumab and rituximab. These drugs generally have poor water solubility and tend to distribute and accumulate in the

peripheral tissues, translating into significant systemic toxicity. Nanoparticulate systems of such drugs have been explored but not thoroughly characterized for improved dissolution rate, cytotoxicity, bioavailability, and stability. In the present thesis, camel milk casein-based nanoparticle has been used as a suitable drug delivery system for enhancing the bioavailability and solubility of sorafenib, as will be discussed later in detail.

1.9.1 Types of Nanoparticles

Over the years, poor solubility has been the major drawback for drugs in the developmental stage and even in many marketed drugs. Due to low solubility, high doses of drugs have to be administered to obtain the desired efficacy. This leads to unwanted clinical complications, especially in the case of anticancer drugs. Researchers have tried to overcome this limitation by enhancing the solubility and dissolution rate of poorly soluble drugs. Various techniques have been used, such as size reduction, salt formation, complexation, use of surfactants, and solid dispersions. Solid colloidal microscopic particles ranging from 1 to 1000 nm are included in nanoparticulate systems. Drugs may be embedded, dissolved, encapsulated, entrapped or adsorbed in a suitable matrix. This may be a polymeric or lipidic matrix (Shitole et al. 2022). Currently, natural as well as synthetic polymers are employed for drug delivery. Nanoparticles can be prepared from different sources of materials like proteins (Gelatin, Albumin, Lectins, Legumin, and Casein), polysaccharides (Alginate, Dextran, Chitosan, Agarose, Pullulan), and synthetic polymers e.g. poly (lactic acid) (PLA), poly(ε-caprolactone) (PCL), poly (lactic-co-glycolic acid) (PLGA), N-(2-hydroxypropyl)-methacrylamide copolymer (HPMA) and poly (styrene-maleic anhydride) copolymer (Cheng et al. 2021). Besides being biodegradable and biocompatible, polymers should be compatible with the body regarding adaptability (non-toxicity) and immunological tolerance (non-antigenicity).

1.10 Significance of milk proteins as a nanocarrier for drug delivery system

Milk is the most consumed primary functional food due to its health benefits. Milk is an essential source of calcium, phosphorus, vitamins A, B12 and D and various proteins. Its proteins are essential in making milk nutritious and helping to fight many conditions like metabolic disorders, hypertension, cancer, and infectious diseases, besides helping in growth and development (Haug et al. 2007).

Owing to milk protein's unique structural and functional properties, they are now being significantly explored for their role in nutraceuticals and drug delivery. Naturally available milk proteins are inexpensive and can be polymerized to yield drug delivery systems for great therapeutic benefit. Hydrophobic molecules can be bound to milk proteins via hydrogen bonding, hydrophobic interactions, and van der Waals forces. The binding sites are located on the surface (the so-called hydrophobic pockets) or inside the inner cavities of globular protein structures. Milk and its derived protein nanocarriers come under the category of GRAS (Generally considered safe) (Mehla et al. 2021).

1.10.1 Milk whey and its components in drug delivery

Milk consists of two main protein fractions, casein and whey, which differ in chemical constituents and physical properties. Casein is separated from whey proteins by acidic precipitation at pH 4.6 (Yen et al. 2015). Whey proteins include α-lactoalbumin (α-la), β-lactoglobulin (β-lg), immunoglobulins, lactoferrin, lactoperoxidase, etc. (Davoodi et al. 2016; Mahala et al. 2023). They belong to the category of water-soluble globular proteins. Nanoparticles have been prepared from whole whey proteins to encapsulate antioxidants such as soy isoflavones and Coenzyme Q10 (CoQ10). This has improved solubility, stability, and oral bioavailability (Liu et al. 2022). Studies about encapsulating astaxanthin, 3,3'-Diindolylmethane, vitamin D3, resveratrol, and β-carotene have been reported. Likewise, a BSA-based nanoparticle was prepared to deliver survivin-siRNA resulting in brilliant antitumor and biocompatibility in vitro (MCF-7 cells) and *in vivo* (Wang et al. 2021). The whey protein β-lactoglobulin has received tremendous research interest as a transport vehicle for hydrophobic substances like vitamin D, fatty acids, β-polyphenols like EGCG (epigallocatechin gallate) from green tea, and folic acid (Maulana et al. 2022).

1.10.2 Lactoferrin in drug delivery

Lactoferrin (Lf) is an exciting whey protein present in milk. It is an iron-binding glycoprotein that belongs to the transferrin family (Mahala et al. 2022). This biodegradable protein has antibacterial, anticancer, antioxidant, and immunomodulatory properties (Guzmán-Mejía et al. 2023). It is now widely explored as a drug nanocarrier because of its net positive charge at physiological pH (7.0-8.0) and its stability in the gastrointestinal tract (Ahmed O. Elzoghby et al. 2020). The presence of its receptors in the intestine and on several tumour cells facilitates the increased oral absorption and bioavailability of hydrophobic drugs and nutraceuticals (Tran et al. 2023). Lactoferrin-based

amphiphilic micelles were synthesized with zein protein to encapsulate the anticancer drugs rapamycin and wogonin, which showed enhanced *in vitro* cytotoxicity and cellular uptake on MCF-7 cells (Sabra et al. 2018). Furthermore, they also exhibited an enhanced anticancer efficacy in Ehrlich ascites tumor animal model.

In addition, the drug dasatinib also showed sustained drug release with increased in vitro cytotoxic effect against the human breast cancer cell line, MDA-MB-231. This suggested the potential of utilizing lactoferrin-based nanoparticles as efficient drug delivery systems. LF nanoparticles were also developed for oral nanoformulation of gambogic acid (Zhang et al. 2013) and oleanolic acid (Xia et al. 2017) for their enhanced anti-tumour effect, improved oral absorption, pharmacokinetic profile, and bioavailability in rats. Some Lf nanoformulations have been designed to transport drugs across the blood-brain barrier (BBB) to the central nervous system (CNS). These are helpful for the treatment of Alzheimer's and Parkinson's disease (Kumari et al. 2017).

1.10.3 Casein as a drug delivery molecule

The milk protein casein is abundantly present in the micellar form (Fig. 1.12). These casein micelles in human milk work as natural nano vehicles by delivering calcium and amino acids from the mother to neonates (Ranadheera et al. 2016).

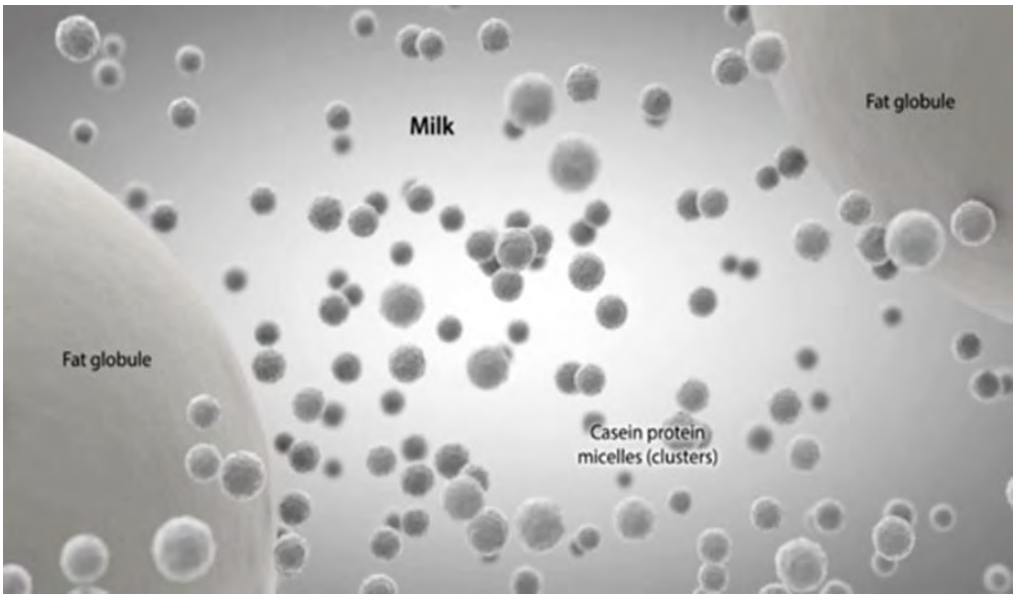

Figure 1. 12 Casein micelles in milk

(Adapted from www.foodhighs.com)

Calcium phosphate complexes generally stabilize casein micelles. The high phosphate content of the casein family allows it to bind with calcium and form calcium phosphate salts. Casein micelles comprise phosphoprotein, a heterogeneous mixture of 4 significant components, including alpha casein (αs1-casein and αs2-casein), beta-casein, gamma-casein, and kappa-casein (Yelubaeva et al. 2017) depicted in Fig. 1.13. Each has amino acid composition, molecular weight, and physiochemical and functional properties.

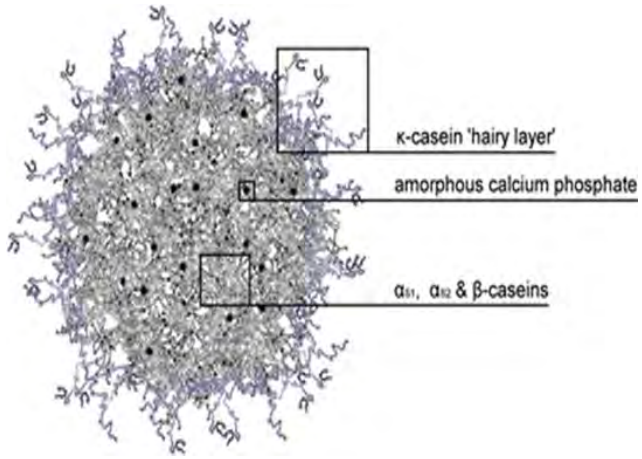

(Adapted from de Kruif CG et al. 2003)

Figure 1. 13 Casein micelle structure

Casein does not have a proper secondary and tertiary structure but has a high proline content. The open structure of casein allows it to self-assemble into spherical micelles flexibly and has a diameter of 150–180 nm. In an aqueous solution, it has a hydrophobic core inside and a hydrophilic-charged κ-casein layer outside. The hydrophobic core of casein micelle consists of alpha- (αs1- and αs2-casein) and beta-casein. Hydrogen bonding, hydrophobic and electrostatic interactions are involved in forming casein micelles (Sadiq et al. 2021). The hydrophobic core binds calcium, and the hydrophilic layer provides stability. Due to these structural and physiochemical properties, casein protein from bovine milk is widely explored as a nanocarrier for various bioactive compounds (Morris 2002). The amphiphilic structure also leads to the thermal stability of casein micelles. Bioactive compounds with water solubility and stability-related limitations fail to show their complete efficiency in providing essential health benefits. The unique property of casein, its porosity and amphiphilic nature facilitates its more efficient interaction with hydrophobic and hydrophilic molecules. It has already offered advantages for the nanoencapsulation of bioactive and pharmaceutical drugs like flutamide (Elzoghby et al. 2013),

ω-3 fatty acids, curcumin (Sahu et al. 2008), vitamin A, vitamin D (Maryniak et al. 2018), β-carotene etc.

1.11 Camel milk's casein as a drug delivery molecule

Earlier studies have shown that as a nano-drug delivery system, camel milk casein is safe, natural, biodegradable, and non-immunogenic (Sadiq et al. 2021). Camel milk casein peptides on hydrolysis show antioxidant properties. A higher presence of β-casein in camel milk is beneficial. It tends to possess highly hydrophobic amino acids, which could show high encapsulation of hydrophobic drugs with hydrophobic interactions (Farah et al. 1989). An earlier study has reported that camel milk beta-casein micelles increase curcumin solubility and cytotoxicity when encapsulated in camel milk β-casein (Esmaili et al. 2011). Comparatively speaking, β-casein constitutes about 65% of the total casein in camel casein, whereas only about 34% in bovine casein. In fact, camel milk has a wide range of casein micelles sizes from 20 to 300 nm in diameter compared to 40–160 nm in cow's milk. As a result, camel casein is likely to show more promising delivery effects, enhanced solubility and bioavailability of hydrophobic drugs and bioactive molecules as compared to bovine milk. However, as per the existing literature, the application of camel milk casein is not yet thoroughly studied. Its role as a delivery vehicle for drugs and nutraceuticals is yet unexplored. Given its high application, a lot of work needs to be done in this area.

1.12 Current status of therapeutic nanoparticulate delivery of sorafenib

Polymeric nanoparticles, encapsulating sorafenib, serve as a novel delivery platform and exhibit immensely promising potential for enhanced cancer therapy. In a study conducted by (Li et al. 2020), a novel sorafenib-loaded d-α-tocopheryl polyethylene glycol 1000 succinate (TPGS) nanoparticle showed robust stability and SFN release in a pH-based manner. It also exhibits higher cellular uptake and cytotoxicity than free unencapsulated SFN. Furthermore, it significantly inhibited tumour growth *in vivo* without apparent side effects. In another study, sorafenib-loaded silica-containing redox nanoparticles (sora@siRNP) were given orally to protect them from harsh gastrointestinal (GI) conditions (Tran et al. 2022). siRNP improved antiproliferative and antifibrotic effects against hepatic stellate cells (HSCs) and showed low toxicity against normal endothelial cells. They also showed an improved level of sorafenib uptake in the liver. A study showed that sorafenib-encapsulated PEG-PLGA nanoparticles also influenced

immune cells in the tumour microenvironment (D. Zhang et al. 2022). It has the ability to restrict tumour growth after intravenous administration in mice. Researchers also explored its active targeting by attaching the hGC33 antibody to SFN-loaded polyethylene glycol-b-PLGA polymer nanoparticles against glypican-3, an overexpressed membrane protein on HCC cells. Results showed inhibition in cell migration, cell cycle progression, and proliferation by inhibiting the Ras/Raf/MAPK and the Wnt pathways in tandem with GPC3 molecules. They also inhibited the growth of liver cancer in vivo and improved the survival rate of tumour-bearing mice.

Theranostics therapy refers to pairing diagnostic biomarkers with therapeutic agents that share a specific target in diseased cells or tissues. Interestingly, a team of researchers (Huang et al. 2022) recently performed a dual functionality study of sorafenib-loaded $Cu_{2-x}Se$ nanoparticles. Sorafenib was encapsulated in photothermal cored $Cu_{2-x}Se$ nanoparticles exhibiting a photothermal effect. Its anticancer activity was enhanced by this coordination with the targeted drug. This study provided insight into using $Cu_{2-x}Se$-based theranostics agents for biomedical applications in photothermal therapy.

Furthermore, various multifunctional pH-sensitive nanoparticles with surfaces modified with antibodies for targeted delivery have been formulated. They have shown good biocompatibility and high efficiency in tumour killing. For example, when modified for pH-sensitive and targeted delivery, sorafenib showed a higher synergistic effect with doxorubicin (Duan et al. 2018). Also, sorafenib nanoformulation, when conjugated with VEGFR, can kill tumours through the pH-sensitive release of this drug. A higher antitumor effect in this conjugated form has been observed than in free sorafenib. These studies highlight the significance of proper encapsulation of sorafenib to get an optimal benefit for its use in cancer therapy.

2. Gaps in Research

Many existing FDA-approved chemotherapeutic drugs have low water solubility, due to which they suffer from poor oral bioavailability, pharmacokinetic variability, and toxicity. Despite numerous studies on sorafenib nanoparticulate drug delivery in liver cancer, HCC remains a disease with a poor prognosis. Furthermore, drug delivery systems for tyrosine kinase drugs remain largely uninvestigated. It can be observed from earlier studies that although a few polymeric nanoparticles loaded with sorafenib have been tested but their potential has not been explored. It is known that both polymeric and metallic nanoparticles increase ROS production *in vivo*, leading

to cytotoxicity even in normal cells besides exhibiting unpredictable reactions and interactions. Overcoming these limitations by developing a suitable natural nanoparticulate drug delivery system could increase the therapeutic index and safety of sorafenib. Most importantly, it would provide additional opportunities for HCC patients. It is important to note that camel milk casein's amphiphilic and stable nature makes it a very relevant model for drug delivery in cancer therapy. This novel system is yet to be explored as a drug delivery system.

Chapter- 2: Aims and Objectives

Many existing FDA-approved chemotherapeutic drugs have low water solubility, due to which they suffer from poor oral bioavailability, pharmacokinetic variability, and toxicity. Sorafenib, a water-insoluble and multikinase inhibitor used to treat hepatocellular carcinoma, is limited by its low oral bioavailability. Casein is a biocompatible dietary protein of pharmaceutical relevance. Due to its amphiphilic nature, self-assembling property, ability to show sustained release and capability of encapsulating hydrophilic and hydrophobic drugs, it can be a suitable nanocarrier. The broad objective of the current study is to develop a novel drug delivery system to enhance the efficacy of sorafenib. To fulfil this broad objective, the following specific objectives are proposed:

Objective 1: To synthesise, characterize, and conduct a cellular uptake study of sorafenib-loaded camel casein nanoparticles.

For this, camel milk protein is first separated into casein protein by acid precipitation. Further, this casein was visualised by SDS-PAGE. Firstly, casein nanoparticles were developed and then loaded with the drug sorafenib. Characterization of drug-encapsulated casein nanoparticles and only casein nanoparticles was done by dynamic light scattering (DLS), zeta potential analysis, scanning light microscopy (SEM), and FTIR (Fourier-transform infrared) spectroscopy. The drug content in nanoparticles, as well as the drug-protein binding studies, were conducted by UV-Vis spectroscopy. *In vitro* cytotoxicity (MTT and DAPI) was performed on HepG2 cells. Later on, the cellular uptake study was studied by fluorescence microscopy.

Objective 2: To study the cytotoxicity and associated mechanisms induced by sorafenib and sorafenib-loaded camel casein nanoparticles in HepG2 cells.

Initially, cytotoxicity studies were performed in HepG2 cell lines *in vitro*. Mechanisms of apoptosis were studied by phase contrast microscopy, DNA fragmentation assay, cell cycle analysis, and annexin Pi assay. Its ability to induce reactive oxygen species was studied by ROS assay. Lastly, the expression of cancer-related genes like p53, bcl-2, bax, & caspase 3 was studied at the transcription level by RT-PCR and apoptosis-related protein like caspase 3, PARP, BAX, and BCl-2 was studied by western blotting. The therapeutic index of drug-loaded camel casein nanoparticles has also been compared with only sorafenib.

Objective 3: To conduct *In vivo* Pharmacokinetics and Biodistribution studies of sorafenib-loaded camel casein nanoparticles in Swiss albino mice

Pharmacokinetics and biodistribution studies followed the development of the bioanalytical method, which was done by HLPC. Pharmacokinetic studies have been done through intravenous dosing. Multiple pharmacokinetic parameters like area under the curve (AUC), half time ($t_{1/2}$), mean residence time (MRT), initial concentration (Co), elimination constant (Ke), clearance (Cl), the volume of distribution (Vd) were analysed through Phoenix Winolin software. Biodistribution of sorafenib was also performed in various tissues- kidney, liver, heart, spleen, and lungs. The quantification of the drug in tissues was done by HPLC.

Chapter- 3: To synthesise, characterize, and cellular uptake study of sorafenib-loaded camel casein nanoparticle

3.1 Introduction

Nanotechnology holds great potential in the diagnosis, treatment, and management of cancer (Din et al. 2017; William H. et al. 2015). The distinctive properties of nanoparticles (NPs), like small size, tailored surface, improved solubility and administration through different routes, are of utmost importance (Krishna et al. 2019). These characteristics override the drawbacks of utilizing conventional chemotherapeutic agents (Hejmady et al. 2020; Patra et al. 2018; Rajesh et al. 2009). Different nanocarriers have been employed in drug delivery to enhance various biomedical applications (Krishna et al. 2020). Milk whey proteins such as alpha-lactalbumin, -lactoglobulin, lactoferrin, caseins, etc., have all been investigated to deliver medications, nutraceuticals, and other bioactive molecules. These GRAS natural derivatives are suitable for drug transport, safety, and improved therapeutic index of anticancer treatments due to their biocompatibility, amphiphilicity, wide availability, lack of toxicity, non-antigenicity, and low cost (Lohcharoenkal et al. 2014).

Casein nanoparticles can deliver both hydrophilic and hydrophobic drug molecules due to their micellar properties. They are also helpful for the controlled release of oral medications because of their pH-dependent behaviour. Furthermore, casein's unfolded structure makes it conveniently accessible for proteolysis, ensuring good release by proteolytic enzymes in the gastrointestinal tract. Additionally, caseins can penetrate the cell membrane in an energy-independent fashion, which can enhance cellular uptake on oral administration. Physiological degradation products of casein produce immunomodulatory peptides, antioxidants, and ACE inhibitors (which optimize blood pressure regulation). These characteristics make casein a good candidate for use as an encapsulating matrix for anticancer agents (Głąb et al. 2017; Sahu et al. 2008).

Camel milk has been traditionally consumed worldwide for its nutritional benefits and medicinal properties. It also has therapeutic and prophylactic benefits against cancer (Dubey et al. 2015; Al haj et al. 2010). Camel milk proteins have more thermal stability and pH hydrolysis resistance (Atri et al. 2011). Camel milk casein is in micellar form, is readily biodegradable, has an amphiphilic character, is an antioxidant, and has a molecular chaperon-like activity (Kumar et al.

2016). Earlier, camel casein has been used as an effective nano vehicle for curcumin, and its application has been suggested in functional health food formulations (Esmaili et al. 2011). Camel milk casein has the potential to bind with both polar and non-polar compounds and serve as a suitable nanocarrier for other physiological compounds, including drugs.

HCC is the most common type of primary liver cancer and the most common cause of death in people with cirrhosis (Balogh et al. 2016). Kinases are essential in tumour cell signalling, angiogenesis, and apoptosis (Krishna et al. 2021). Sorafenib is a promising anticancer drug with the properties of a multikinase inhibitor. It acts against several solid tumours by preventing cell proliferation, tumour growth, and angiogenesis (Jindal et al. 2019). However, sorafenib is a small-molecule drug with poor aqueous solubility and low bioavailability. Being a small-molecule drug, it may be distributed throughout the whole body and be rapidly metabolized, leading to adverse effects (Babos et al. 2018). Camel milk reduces drug-induced hepatic and renal toxicity, whereas casein-derived peptides are important pharmaceutically active and immunomodulatory molecules (Głąb et al. 2017; Kumar et al. 2016). Therefore, in this chapter, we have explored using casein-derived nanoparticles from camel milk to encapsulate sorafenib. For this, we have initially developed and characterized camel casein nanoparticles. Later we studied the bioavailability and cytotoxicity of sorafenib-loaded casein nanoparticles in the HepG2 cell line.

3.2 Methodology

3.2.1 Camel milk sample collection

Camel (*Camelus dromedarius*) samples were collected from 'Sarika Raika MilkBhandar', Jaipur, India. The sample was collected under aseptic conditions and stored at -20 ^{0}C in a sterile container until further use.

3.2.2 Isolation and purification of casein protein from camel milk

Isolation of casein from camel milk was done according to the process described earlier (Kumar et al. 2016; Salami et al. 2011) with slight modification (Fig 3.1). Briefly, fat was removed from the milk by centrifugation at 8000 rpm for 30 min. at 4 ºC. The supernatant containing skimmed milk was collected for further use. Whey and casein were separated by acid precipitation with 1N HCl at pH 4.6 and centrifugation at 12000 rpm for 30 min. at 4 ºC. The precipitated casein was washed thrice with distilled water. The precipitated casein pellet was kept at -20 ºC until further use and

solubilized according to the reported method (Ashkan Madadlou et al. 2009), briefly described as follows.

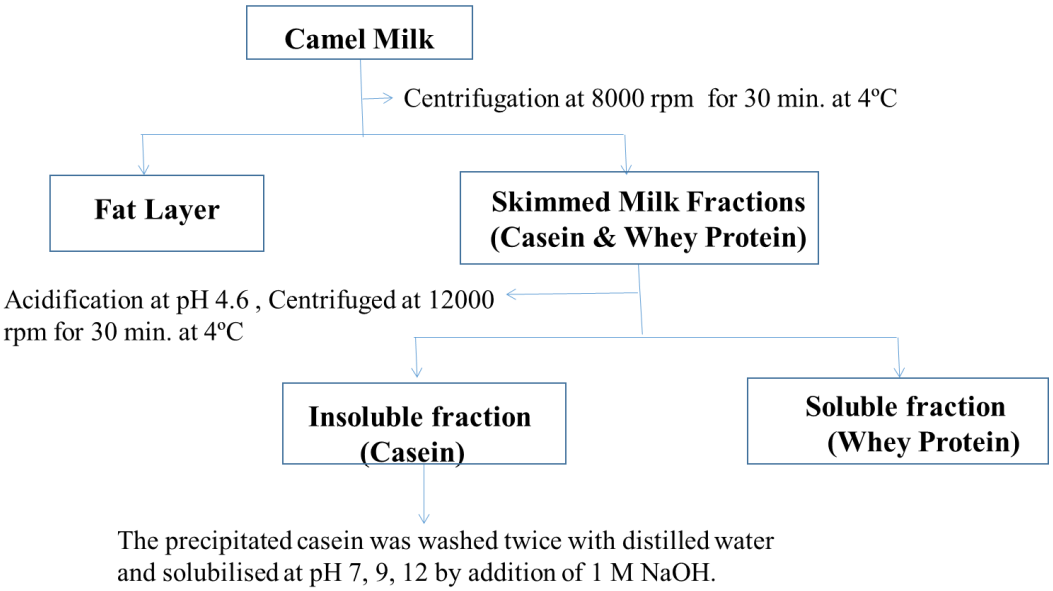

Figure 3. 1 Method of isolation of casein protein from camel milk

Casein solution (5%) was prepared by adding 10 g casein protein to 200 mL of deionized water (pH 7.0), stirring at 1000 rpm for 60 min at room temperature. Sodium azide (0.03%) was added to prevent any microbial contamination. The solution was stored at 4 ^{0}C for 10-12 hours for complete hydration. The pH of the solution, originally 6.48, was then adjusted to 7, 9 or 12 separately by slowly adding 1N sodium hydroxide solution with constant stirring.

3.2.3 Polyacrylamide gel electrophoresis

Skimmed milk and isolated camel milk casein protein were analyzed by SDS-PAGE on 12% gel under reducing conditions using a Bio-Rad mini gel electrophoresis unit run at 80 V. Before the electrophoresis, skimmed milk and casein protein samples were diluted to 2 µg/µL with the sample buffer. Sample denaturation was done for 5 min. at 100 °C, and protein samples were loaded into each well. Proteins in the gel were stained by Coomassie Brilliant Blue R-250, and the gel image was viewed using a gel documentation system (BioRad). Separated proteins were validated for identification using the molecular weight marker.

3.2.4 UV- Vis spectroscopy

Quantitative analysis of sorafenib and casein was performed using a UV-Vis spectrometer. Stock solutions of casein and sorafenib drugs were prepared in Milli Q water and methanol, respectively. The UV – Vis absorption spectra were recorded on a UV-2700 spectrophotometer (Shimadzu Co., Kyoto, Japan) over a wavelength range of 200-300 nm. The wavelength (λ) range of these compounds was estimated from the calibration curve. The binding of the sorafenib drug with casein micelles was analyzed by UV- Vis spectrophotometry.

3.2.5 Synthesis of camel milk casein nanoparticle

Casein nanoparticles were prepared according to an earlier reported method with some modifications (Sona Gandhi 2018). Five percent casein solution was mixed with the drug sorafenib of concentration (1 mg/mL) 200 µL and was stirred at 900 rpm at room temperature for one hour. This was followed by adding 50 µL (10 mM) $CaCl_2$ until the solution became turbid. Further, it was kept for 6 to 7 hours on a magnetic stirrer to remove methanol. This same has been explained pictorially in Fig. 3.2.

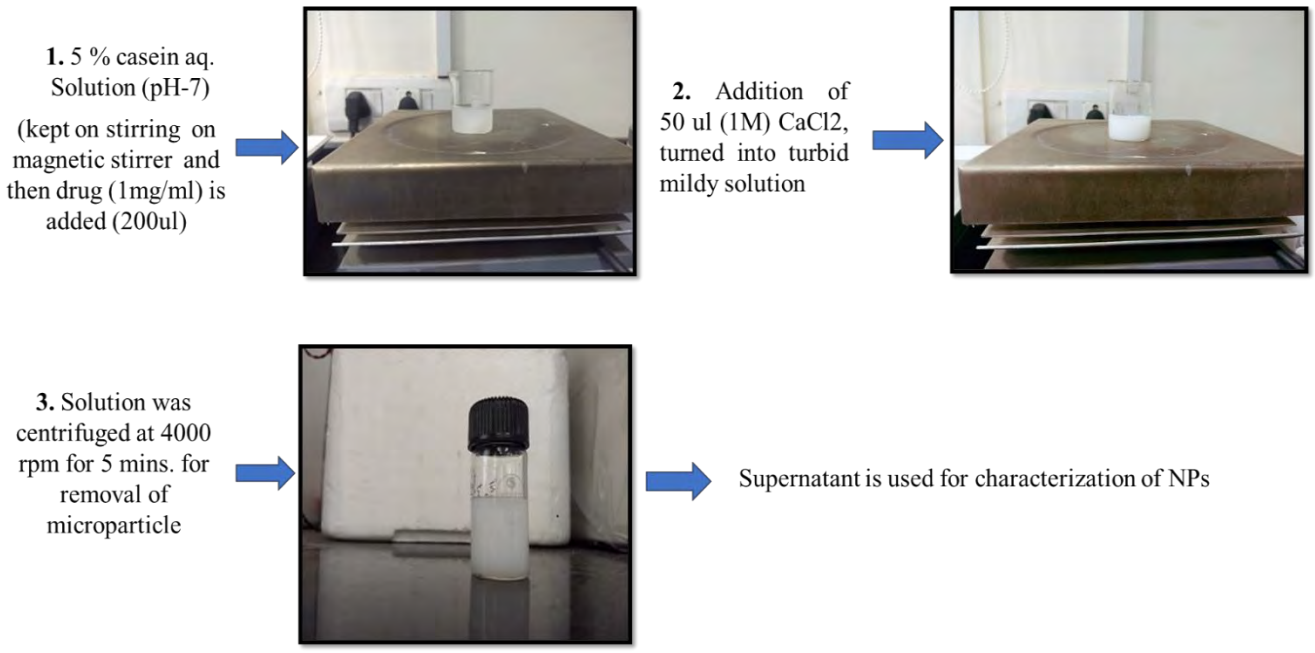

Figure 3. 2 Pictorial representation of the synthesis of camel milk casein nanoparticle (A) 5% casein solution with sorafenib drug. (B) Turbid mild casein solution upon addition of calcium chloride ($CaCl_2$) (C) Casein nanoparticle

3.2.6 Characterization of camel milk casein nanoparticle

3.2.6.1 FTIR study

The chemical functionality and interaction between the casein nanoparticle and sorafenib were investigated by FTIR spectroscopy. Briefly, the spectra of casein, sorafenib, their mixture (1:1), and sorafenib-loaded casein nanoparticles were recorded using a Fourier Transformed-IR system (Alpha Bruker's) equipped with a germanium attenuated total reflection (ATR) system. Lyophilized Solid samples of each were placed directly in the FTIR sample holder in direct contact with the ATR crystal. In transmittance mode, IR spectra were obtained in the spectral region of 4,000 cm^{-1} to 500 cm^{-1}.

3.2.6.2 Physical property analysis & scanning electron microscopy of camel milk casein nanoparticles

The prepared casein nanoparticles were characterized for their size, polydispersity index (PDI), and zeta potential using a Zetasizer, Nano series (Nano-ZS, Malvern, UK). The casein nanoparticle diameter and surface charge/ZP were measured in water pH (6.2–7.4) at 25 ^{0}C with a scattering angle of 90 ^{0}C. Morphology was examined by scanning electron microscopy (SEM) at a voltage of 20 kV after coating with gold under a vacuum. Drops of nanoparticle samples were put on slides and dried under nitrogen gas. Then, these slides were placed on aluminium stubs fixed by double-sided tape and placed in the vacuum chamber of SEM (Thermo Scientific^{TM} Apreo scanning electron microscope). Slides were seen from 30,000 x to 10,000 x magnifications.

3.2.6.3 Drug encapsulation efficiency

To quantify the drug content, 1 mL aliquot of the nanoparticle solution containing the drug was centrifuged at 10,000 rpm for 20 minutes at 4^{0}C. Now, the pellet was dissolved in methanol to precipitate the protein. Subsequently, it was vortexed for 1 hour and centrifuged at 6000 rpm for 10 minutes. The drug concentration in the pellet was determined using a UV-Vis spectrophotometer. Results have been presented as means ± SEM of three independent experiments performed in duplicate. The encapsulation efficiency (E.E.) was calculated by using the following formula:

E.E. (%) = (Mass of a drug in nanoparticles/mass of drug used in formulation) × 100 (Equation 1.)

3.2.7 Cell culture-associated studies

3.2.7.1 Culture of cells

HepG2 cells procured from NCCS, Pune, India was, cultured at 37°C, 5% CO_2, in minimum essential medium (Invitrogen) supplemented with 10% fetal bovine serum (Invitrogen) and 1% antibiotics solution - Penicillin (100 UML^{-1}) and streptomycin (100 μgmL^{-1}; Invitrogen). Trypsin- EDTA solution (0.05%) was used to detach cells. The cells were grown to 70% confluence in tissue culture flasks (Tarson), detached using trypsin EDTA solution, rinsed in phosphate buffer saline, and transferred in an entirely fresh medium. Subsequently, they were analyzed for cellular uptake, viability, and morphological changes.

3.2.7.2 Cellular internalization study

Coumarin-6 (green-fluorescent dye) entrapped casein nanoparticles were prepared in the same way as described above in section 3.2. HepG2 cells were seeded on coverslips in six-well plates and treated with the 3 µg/mL of coumarin-6 entrapped casein nanoparticles at 37 ^{0}C for 4 h and 6 h, respectively. The cells were washed twice with PBS to remove nanoparticles not taken up by the cells and fixed with methanol for 10 minutes. Subsequently, they were stained with DAPI (2 µg/mL) for 3–5 min and washed twice with PBS. Cells were mounted using glycerol and examined under a fluorescence microscope (Zeiss Axio Scope A1) using filters for DAPI and FITC. The merged image was also obtained for better visualization.

3.2.7.3 Cytotoxicity assay

MTT (3-(4, 5-dimethylthiazol-2-yl)-2,5-diphenyltetrazolium Bromide) assay was used to determine the cytotoxicity of the drug, sorafenib and its loaded casein nanoparticles. Briefly, HepG2 cells were seeded at a density of 8000 cells/well in a 96-well plate. After reaching 70% confluence, cells were treated with different concentrations of sorafenib and its loaded casein nanoparticles for 24 hours. MTT was added to cells and incubated for 4 hrs at 37 ^{0}C. Subsequently, the media was discarded, and 150 µL of DMSO was added to each well. The colour intensity was measured at 570 nm wavelength using a microplate reader (Multiskan #Thermo scientific). Each determination was carried out in triplicate, and at least two independent experiments were carried out. Cell viability was calculated using the following formula.

% Cell Viability = O.D of treated cells/O. D of control untreated cells *100……Equation (2)

3.2.7.4 DAPI staining

HepG2 cells were implanted on a coverslip in a 6-well plate and incubated with only sorafenib and casein-encapsulated sorafenib at 10 μM and 20 μM concentration for 24 h. Cells were washed twice with PBS, fixed with ice-cold methanol, and washed twice with PBS. Next, cells were stained with DAPI (2 μg/mL) and incubated for 10 min at room temperature in the dark. The cells were washed with PBS two times and visualized under a fluorescence microscope (ZEISS Axio Scope A1 microscope). The apoptotic bodies were observed.

3.2.7.5 Statistical analysis

Graphs and statistical analysis of data were performed by using GraphPad Prism 8 software. The data are given as the mean values ± SEM. Comparisons among inter and intra-groups were analysed using one-way and two-way ANOVA followed by the Bonferroni post-test. $P<0.05$ was considered to indicate a statistically significant difference. All experiments were repeated at least three times and performed in triplicates.

3.3 Results and Discussion

3.3.1 Solubility and SDS PAGE analysis of camel milk casein protein

Camel milk casein was obtained at its isoelectric pH of 4.6 at room temperature. It is a hydrophobic protein and insoluble in water. At high pH (7, 9, and 12), casein will have a net negative charge (due to the ionization of its acidic side chains). Therefore, it was soluble after adding 1 N NaOH at all three pH values, as shown in Fig. 3.3 (A).

Camel milk casein is a major dietary phosphoprotein of 4 types, namely, αs1 casein, αs2 casein, β casein, and *k* casein. The electrophoretic migration of camel milk casein has been depicted in Fig 3.3 (B) at the three different pH studied. The molecular weight of α-caseins, β-casein, and *k*-casein was observed to be about 28 kDa, 26 kDa, and 22 kDa, respectively, at each pH as expected and reported earlier (Kappeler et al. 1999; Yelubaeva et al. 2017). It was also clearly seen that the bands corresponding to whey protein in camel skimmed milk decreased or disappeared in casein protein, depicting the relative purity of the isolated casein protein.

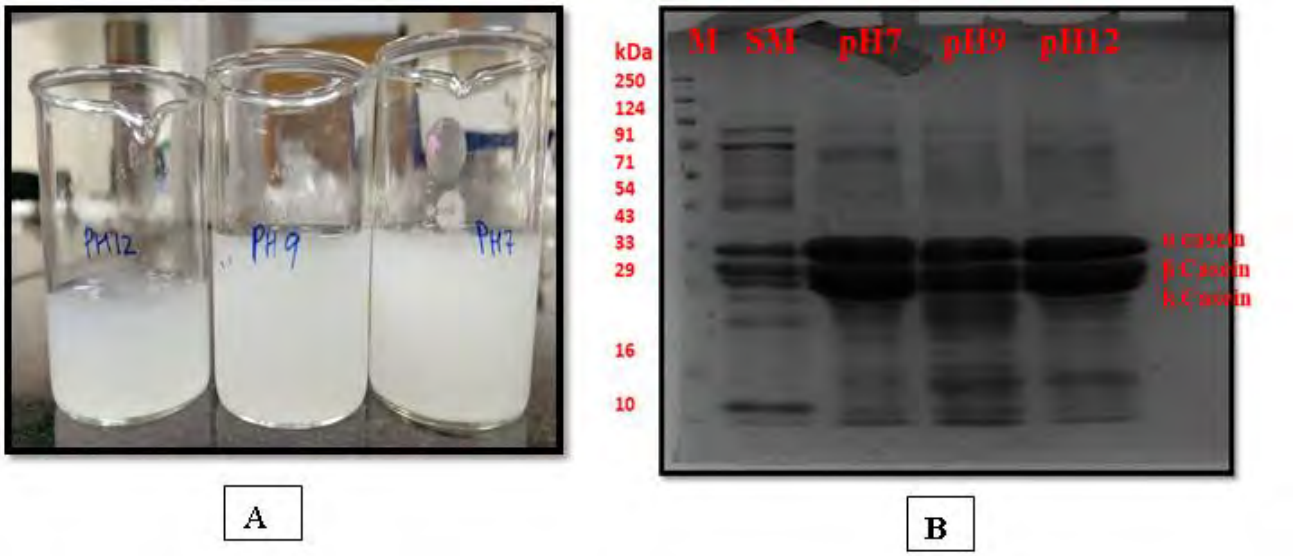

Figure 3. 3 (A) Solubilization of camel milk casein solution at pH 7, 9, and 12. (B) SDS- PAGE image of solubilized casein at pH 7, 9, and 12. The molecular weight marker has been loaded in the 1st lane, skimmed camel milk (SM) in the 2nd lane and camel milk casein at pH 7, 9, and 12 have been loaded in lanes 3, 4, and 5, respectively

3.3.2 UV-visible spectroscopic analysis of camel milk casein and sorafenib

Spectrum analysis of the drug sorafenib, camel milk casein, and the drug mixed with casein (not as nanoparticle) was analyzed by UV-Vis spectroscopy; the respective of λ_{max} was determined and has been depicted in Fig 3.4. Casein (1 µg/mL) exhibits maximum absorption at the wavelength of 275 nm, as shown in Fig. 3.4 (A). It can be explained by the presence of the aromatic side-chains of amino acids like tryptophan (Trp), tyrosine (Tyr), and phenylalanine (Phe) residues, which absorb in this range of wavelength (Antosiewicz et al. 2016). Sorafenib showed maximum absorbance at 264 nm at all studied concentrations ranging from 1-6 µg/mL. This corresponds to earlier studies (Onur 2018) and has been shown in Fig. 3.4 (B).

To investigate the effect of sorafenib interaction with camel milk casein for any structural changes induced in the mixture, the UV spectra of casein were plotted by taking various concentrations of sorafenib in Fig. 3.4 (C). The maximum absorption peak of only casein was at 275 nm, and it remained unchanged in the presence of sorafenib at the concentration range studied. With the increase in sorafenib concentration, the absorbance of casein gradually increased from 0.6 to 0.9 at the same λ_{max} (275 nm). This suggests that the drug has changed the polarity of the microenvironment around Trp and Tyr residues of casein, but this does not cause its conformational

change in casein (D. Li et al. 2011; Yue et al. 2012). The linear calibration curve obtained by measuring the absorbance of the sorafenib at various concentrations has been shown in (Fig. 3.4 (D) has good linearity with a correlation coefficient of R^2=0.998.

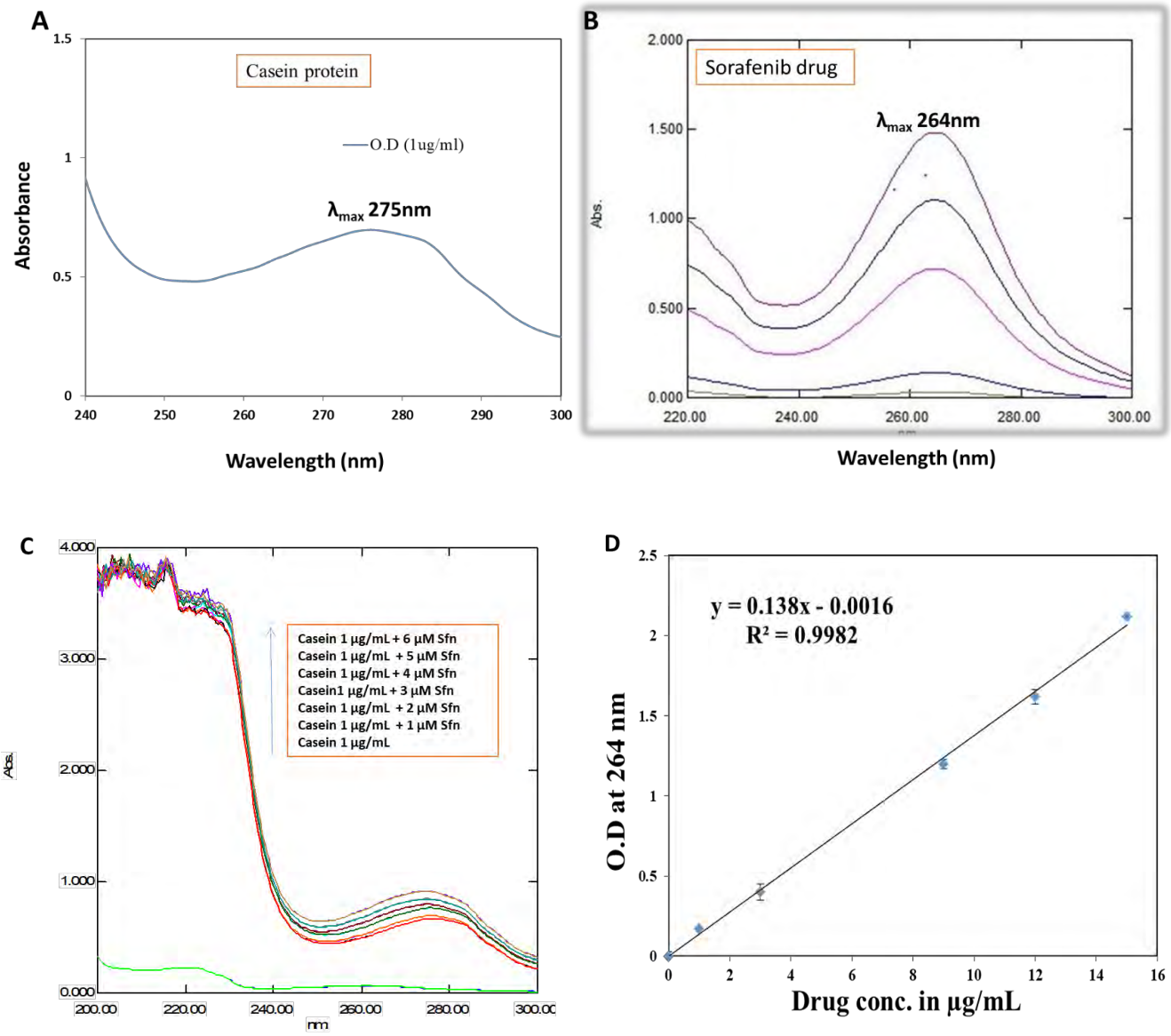

Figure 3. 4 UV-Visible spectrum (A) UV spectra of camel casein milk protein (B) UV spectra of sorafenib at various dilutions (C) UV spectra of casein (1 µM) in the absence and presence of different concentrations of Sorafenib drug (1 µM - 6 µM) and (D) Calibration curve of sorafenib drug.

3.3.3 Synthesis of camel casein nanoparticle

In this study, we have indigenously prepared novel camel milk casein nanoparticles and have explored its use as a carrier for the anticancer drug sorafenib. Casein self-assembles into spherical

micelles at pH 7 when dissolved in water, and sorafenib gets encapsulated into the hydrophobic core of casein micelle (M. Corzo-Martínez1 et al. 2015). This is further stabilized by adding calcium chloride solution, which maintains micellar integrity (M.G. Sosa-Herrera et al. 2012). The solution formed was mildly turbid due to densely formed casein nanoparticles (Penalva et al. 2015). A pictorial depiction of the synthesis of nanoparticles done by us has been described earlier in section 2.6 (Fig 3.2), and its features are described subsequently. No exogenous cross-linkers and toxic chemicals were used in the process of preparation.

3.3.4 Characterization of camel milk casein nanoparticle

3.3.4.1 FTIR spectra analysis of sorafenib loaded camel milk casein nanoparticle

The chemical analysis of the drug sorafenib, casein, physical mixture of casein and drug, as well as the drug-loaded casein nanoparticle was subjected to analysis by FTIR spectroscopy, as shown in Fig. 3.5. The mixture was also used to investigate any possible chemical association, change in composition, or compatibility between the drug and its carrier. The initial bands higher than 3608 cm^{-1} are due to the solvent system in all four panels. The uppermost panel represents the sorafenib band. The bands at 3062 cm^{-1} and 2928 cm^{-1} (due to the C-H stretching band of aromatic and aliphatic CH, respectively) are evident. The sorafenib band at 1696.4 cm^{-1} is characteristic of the amide group (C=O). Absorption bands of casein (2nd panel from top) are at 3273 cm^{-1} (amide band) and at 1639 $cm^{-1,}$ which is mainly associated with the C=O stretching vibration and depends on the backbone conformation and hydrogen bonding. Casein also exhibits another characteristic band at 1442 $cm^{-1,}$ which may be attributed to the carboxylate group (O-C-O). The major absorption bands shown in casein and drug spectra were also found in their physical mixture spectrum (3rd panel from the top) and casein-loaded nanoparticle (4th panel from the top). FTIR spectral analysis we conducted revealed that the specific functional groups of casein as a carrier and the drug sorafenib in the nanoparticles have almost identical chemical characteristics of the pure casein and drug bound together. The FTIR spectrum of the sorafenib-loaded casein nanoparticles indicates that there was no significant chemical interaction between the sorafenib and casein. This indicated that sorafenib was well encapsulated in casein nanoparticles. This result aligns with the spectrometric analysis done earlier in section 3.3.2.

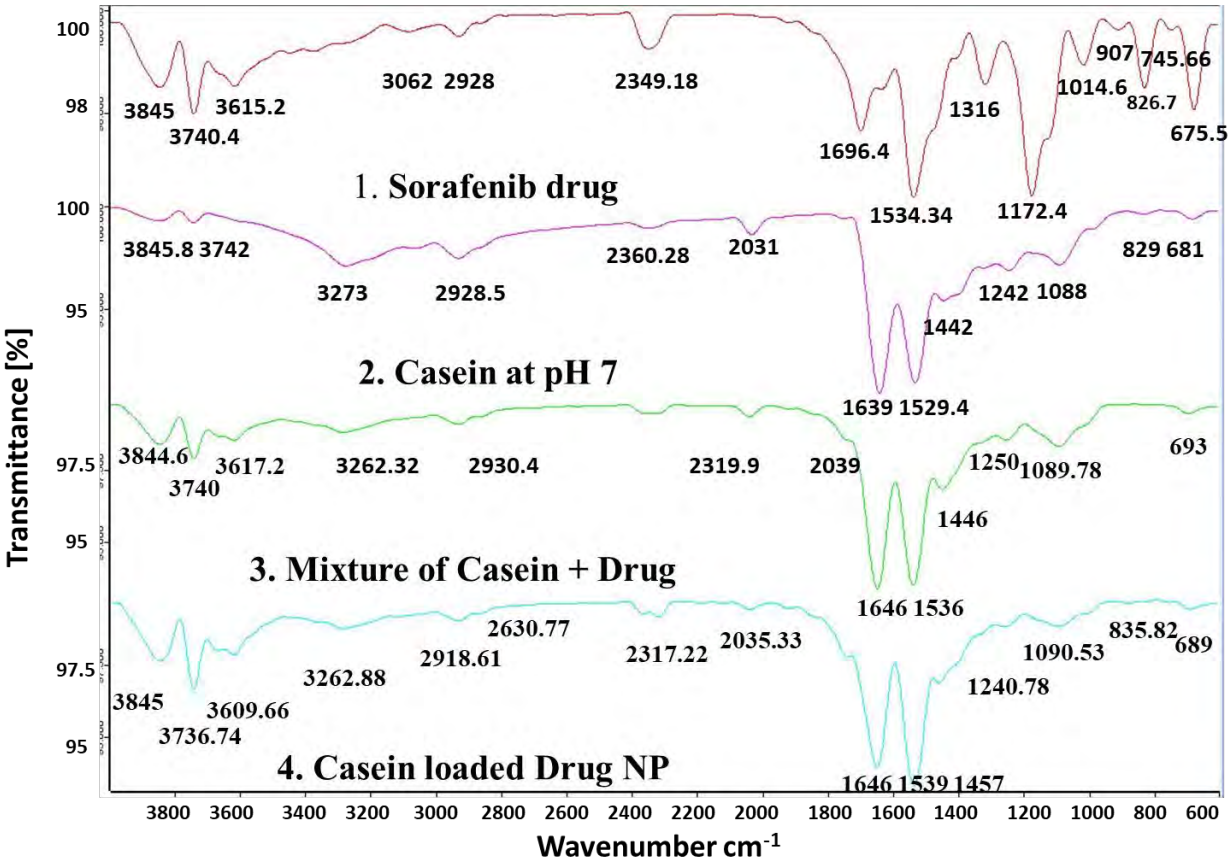

Figure 3. 5 FTIR spectra of 1. Sorafenib drug, 2. Casein at pH 7, 3. A physical mixture of casein and drug, 4. Drug-loaded casein nanoparticle (NP)

3.3.4.2. Physical & morphological studies of unloaded and sorafenib loaded camel casein nanoparticles

The novel camel casein nanoparticles were analyzed to determine their particle size, distribution, and zeta potential using the Malvern zeta sizer, as shown in Fig. 3.6 and Table 3.1. Camel milk casein nanoparticles were found to have an average particle size (hydrodynamic diameter) of 192 ± 5.4 nm with a polydispersity index of 0.22, whereas sorafenib loaded camel casein nanoparticles had a slightly greater size, i.e., 212 ± 6 nm with a narrow polydispersity index of 0.23 (shown in Table 3.1). This indicates that the particles were uniform and monodispersed. The entrapment efficiency of drug-loaded nanoparticles was observed to be 51.5 ± 3.2%. The magnitude of zeta potential determines the colloidal stability. The zeta potential of a nanoparticle also represents its surface charge. The zeta potential of the casein nanoparticles was found to be negatively charged (data shown in Table 3.1) because of the ionized carboxylic groups of sodium caseinate at pH 7. The negative surface charge is also indicative of low toxicity as compared to the positively charged

nanoparticle, which internalizes the cells by various mechanisms which need to be explored further (Tang et al. 2018).

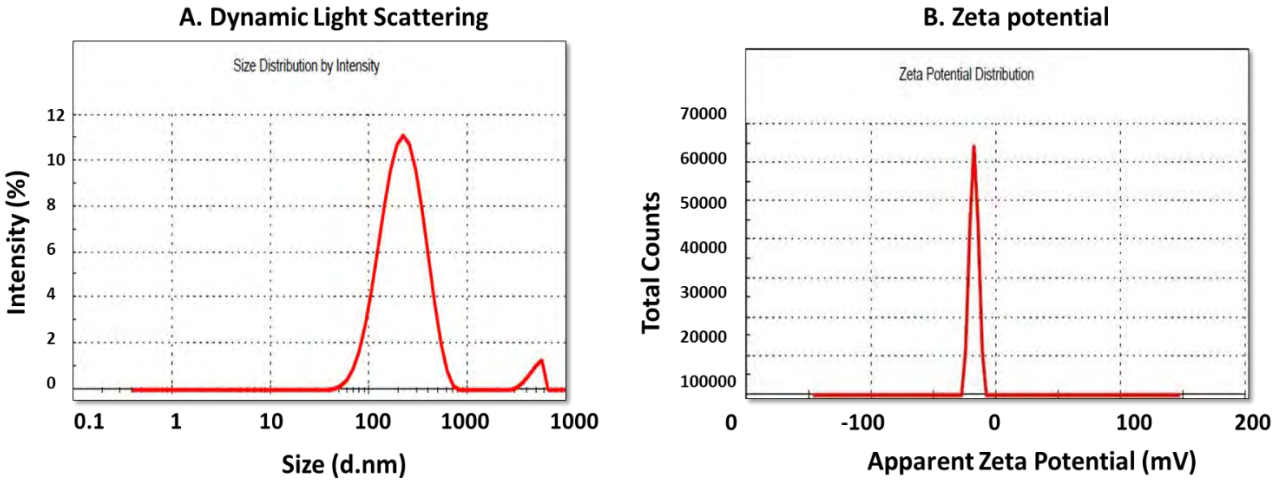

Figure 3. 6 Measurement of nanoparticle (A) size and (B) zeta potential of casein nanoparticle by dynamic light scattering (DLS)

Table 3.1 Characterization of nanoparticles

NPs	D_h (nm)	PDI	ZP (mV)	EE %
Casein NP	192 ± 5.4	0.21	–23 ± 1.5	-
Sorafenib-CasNPs	212 ± 6	0.22	–20 ± 1.2	51.5 ± 3.2

Note: D_h: average hydrodynamic diameter; PDI: polydispersity index; ZP: zeta potential; EE: drug encapsulation efficiency. Data represent mean ± SD (n=3)

The shape of the camel casein nanoparticle was analyzed using scanning electron microscopy (SEM). A smooth surface and spherical shape of the nanoparticles were observed, as has been shown in Fig. 3.7. The size of particles in terms of diameter ranges between 160–220 nm, which is in agreement with the dynamic light scattering studies done earlier (Penalva et al. 2015).

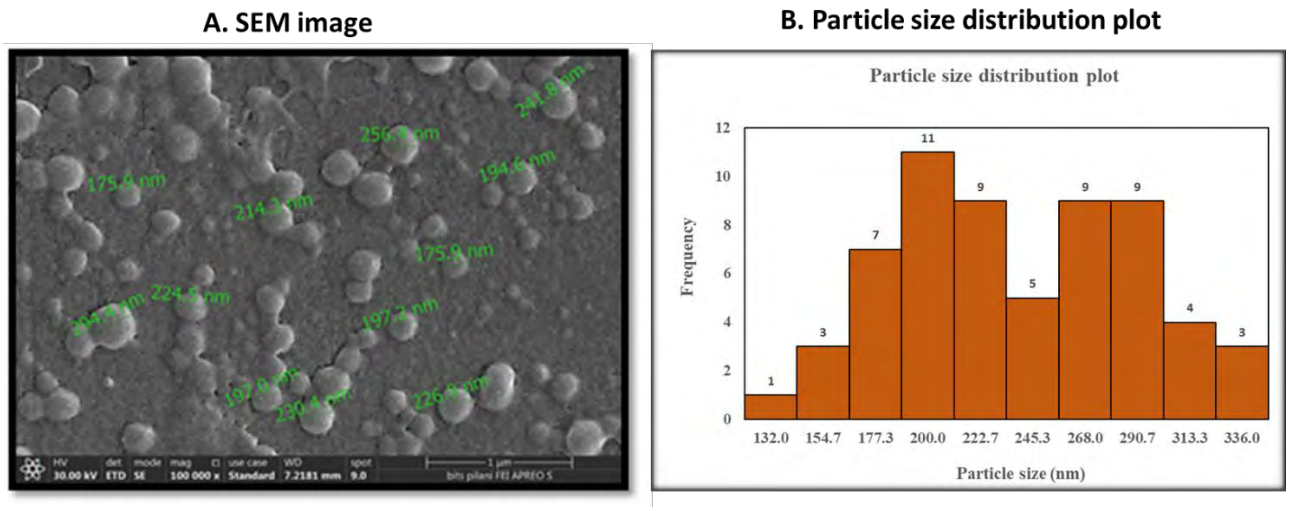

Figure 3. 7 A) Scanning electron microscopic image of camel milk casein nanoparticles and B) Particle size distribution plot of camel milk casein nanoparticles

3.3.5 Cellular internalization study

Coumarin-6 encapsulated casein nanoparticle was used to study cellular uptake as it is a suitable fluorescent probe. The resulting fluorescence images depict that coumarin-6 dye-loaded nanoparticles were effectively taken up by the cells (Fig. 3.8). Coumarin-6 dye-loaded nanoparticles showed a preferentially higher accumulation in the cytoplasm as compared to the nucleus of HepG2 cells after 4 h (Fig. 3.8 (A) and 6 h (Fig. 3.8 (C) of incubation, compared to the only dye-treated cells (Fig. 3.8 (B & D). It can also be seen that the fluorescent intensity of coumarin-6 encapsulated casein nanoparticles also increased within 2 h (between 4 h and 6 h) of the time interval. This enhanced cellular internalization associated with the nanoparticles could translate to better therapeutic efficacy.

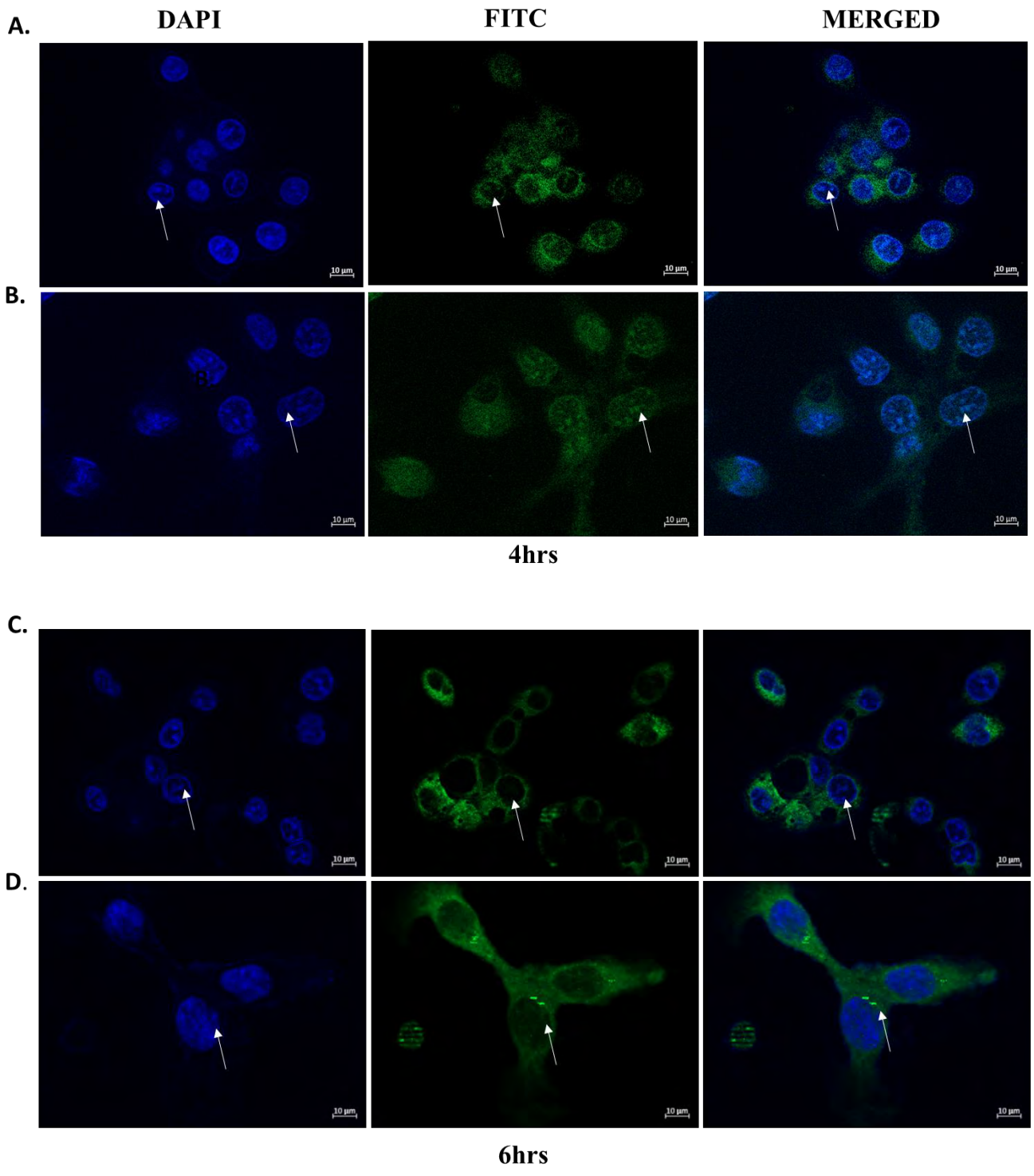

Figure 3. 8 Internalization study of fluorescent dye (coumarin) loaded casein nanoparticle by fluorescence microscopy on HepG2 cells. (A) Fluorescent images of HepG2 cells after 4 hours incubation with coumarin loaded casein nanoparticle (B) HepG2 cells after 4 hours incubation with free coumarin (C) Fluorescent images of HepG2 cells after 6 hours incubation with coumarin

loaded casein nanoparticle and (D) HepG2 cells after 6 hours incubation with free coumarin. The scale bar is 10 µm.

3.3.6 Cellular toxicity study of drug-loaded camel milk casein nanoparticles

Cytotoxicity of our novel drug-loaded casein nanoparticles was evaluated in the HepG2 cell line by the MTT assay after 24 h. Improved cytotoxic efficacy of sorafenib in the HepG2 cell line *in vitro* was observed as compared to the untreated control, as has been shown in Fig. 3.9. According to the results, the IC_{50} concentrations were determined as ~14 µM for sorafenib and ~9 µM for sorafenib loaded casein NPs respectively. Sorafenib-loaded casein NPs had a remarkable activity on HepG2 cells at 10 µM concentration (48.5% cell viability), whereas it has been observed that when treated with non-encapsulated sorafenib, there was (58% cell viability) at the same concentration. This can be due to better internalization of drug-loaded nanoparticles into the cells than the only drug. Further, it was observed that the cytotoxicity increased with increasing drug concentration in a statistically significant manner.

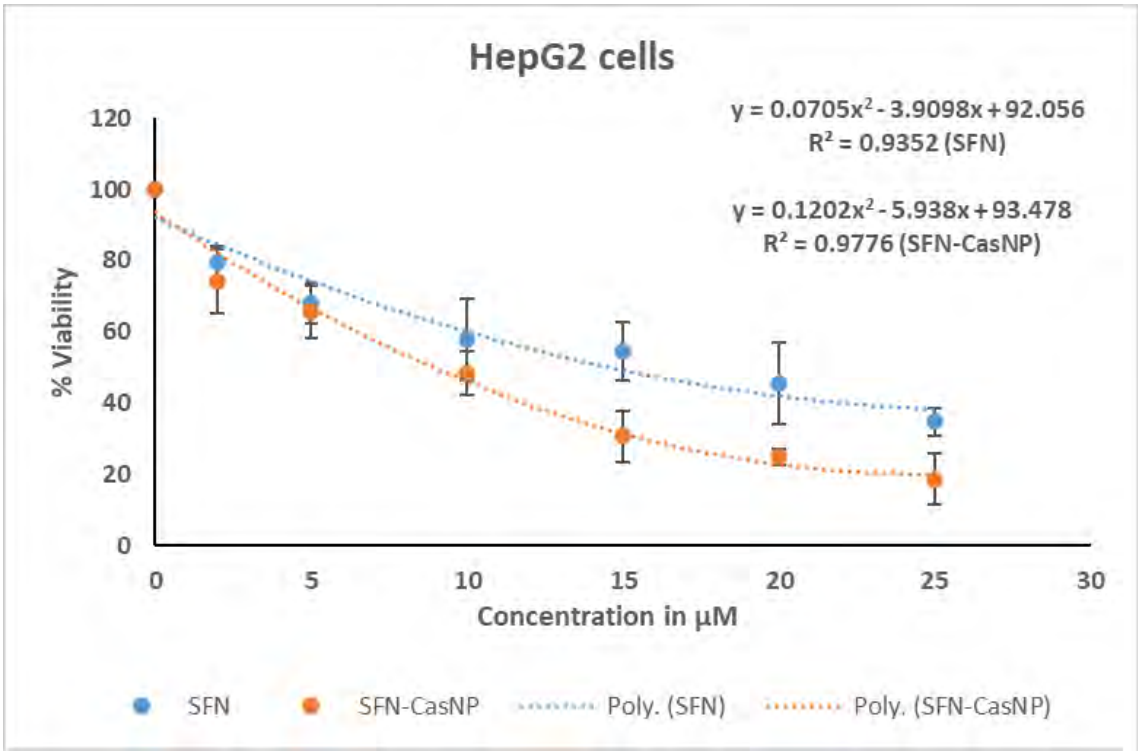

Figure. 9 Cell viability of HepG2 cells treated with Sorafenib loaded casein nanoparticle and free Sorafenib.

To gain further insight into the mechanism involved, the cells were stained with DAPI, a nuclear stain. Cell shrinkage, nuclear fragmentation, and margination of the nucleus were observed in cells

after treatment with the drug-loaded casein nanoparticle as well as with only sorafenib, as can be observed in Fig. 3.10. In untreated control cells, the nucleus was seen normal without any condensation of nuclear material.

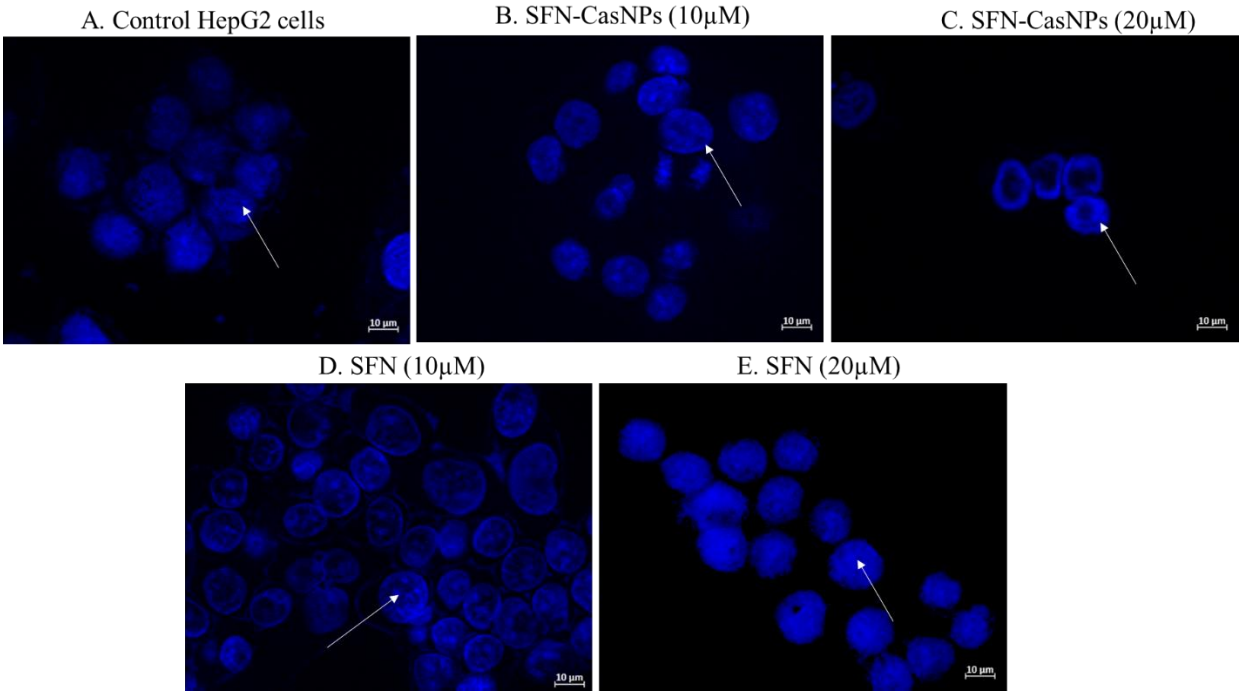

Figure 3. 10 Fluorescence images of DAPI stained HepG2 cells treated with drug-loaded casein nanoparticle and only drug sorafenib. Magnification 60x. (A) Control cells without any treatment, (B) Cells treated with sorafenib loaded casein np (conc. 10 µM), (C) Cells treated with sorafenib loaded casein np (conc. 20 µM), (D) Cells treated with sorafenib (conc. 10 µM), (E) Cells treated with sorafenib (conc. 20 µM). The scale bar is 10 µm.

3.4 Conclusion

In the present study, novel camel milk casein nanoparticles were developed by us and loaded with the drug sorafenib, to overcome its poor solubility and bioavailability. We have successfully developed the camel milk casein nanoparticles with a particle size of around 230 nm with a uniform spherical shape and negative charge. This drug-loaded nanoparticle had a higher intracellular uptake of sorafenib as compared to the uptake of the only drug. The drug-loaded nanoparticles were found to be more cytotoxic and induced apoptosis in the mammalian hepatocarcinoma cell line, HepG2. In the subsequent chapters, the focus is on the cytotoxicity and the *in vivo* pharmacokinetic studies of this novel sorafenib loaded camel milk casein nanoparticle-based anticancer drug delivery system developed.

Chapter- 4: To study the *in vitro* cytotoxicity of sorafenib-loaded camel casein nanoparticles

4.1 Introduction

HCC is the most common primary liver malignancy and is the third leading cause of cancer-related death worldwide (Yang et al. 2010). Sorafenib is the first FDA-approved oral multi-tyrosine kinase inhibitor drug administered in patients with renal and hepatocellular carcinoma (Mou et al. 2021). Kinases are involved in the phosphorylation of proteins or growth factors that facilitate cellular signalling and regulate the cell cycle. Any dysregulation in kinases can eventually lead to cancer. Kinase inhibitors such as sorafenib have immense therapeutic potential. Sorafenib induces apoptosis, suppresses cell growth, and inhibits tumour-associated angiogenesis. Its anticancer activity improves the overall survival of patients with advanced HCC (Liu et al. 2006; Ma et al. 2022). The optimal utilization of sorafenib is restricted by its low water solubility and bioavailability. Several studies have reported its toxicity-related adverse effects leading to reduced patient compliance (Yang et al. 2016; Zhang et al. 2014).

Casein is the major colloidal phosphoprotein in milk and exists in micellar form. It is an amphiphilic molecule with structural and physicochemical characteristics suitable to be used as a carrier molecule, besides being biodegradable and non-toxic. The rationale for using milk casein protein as nanoparticulate drug delivery lies in its size, biocompatibility, biodegradability, amphiphilic characteristics, and stability (Elzoghby et al. 2013; Mittal et al. 2021). Casein carries a negative charge and exhibits stability due to proline residue, explicitly found in beta-casein (Sadiq et al. 2021). Camel milk casein has four constituent components, namely, αS1-casein, αS2-casein, β-casein, and κ (kappa). Beta-casein is found in a maximum amount (65%) higher than bovine milk (36%). It possesses high hydrophobicity, which would be helpful in binding hydrophobic drugs and increasing their solubility and hence bioavailability (Swelum et al. 2021). Another essential property of camel milk casein is the presence of a wide range of micelles size (20 to 300 nm in diameter) as compared to the 40–160 nm range found in cow's milk (Farah et al. 1989; Swelum et al. 2021).

Moreover, unlike bovine milk, camel milk proteins do not induce allergic responses (Maryniak et al. 2018). Based on the suitable properties of camel milk casein, we hypothesized that encapsulation of sorafenib in camel milk casein nanoparticles would have an enhanced cytotoxic

effect on liver cancer cells compared to the drug given without any carrier. Being a natural biomolecule, it may reduce the toxic effect on normal cells.

In the previous chapter, we have already synthesized casein NP from camel milk and characterized it in terms of its particle size, zeta potential, and morphology by scanning electron microscopy (SEM) (Mittal et al. 2021).

However, we have further optimized casein nanoparticles for better drug encapsulation efficiency and checked their stability here. The current work aims to evaluate the cytotoxic efficiency of sorafenib against the human hepatoma cancer cell line, HepG2, using camel milk casein nanoparticles as a carrier. The underlying mechanisms of apoptosis have also been investigated in various dimensions. Subsequently, the effect of the drug-loaded nanoparticles on cell cycle phase distribution has been studied. Furthermore, the induced alteration of gene expression of apoptosis-related genes is studied at the transcriptional and translational levels. Lastly, we have studied the toxicity of this drug-loaded nanoparticle in HEK 293 cells and calculated the therapeutic index, taking the latter as a model system for normal cells.

4.2 Methodology

4.2.1 Optimization, synthesis, and storage stability of casein nanoparticles

The synthesis of SFN-CasNPs was optimised to improve its drug encapsulation efficiency. Two parameters, casein protein composition (5%, 4%, and 3%) and volume of 10 mM $CaCl_2$ (20, 30, 40, 50) µL were chosen. With each parameter size, zeta, PDI, and EE% were calculated. The most optimal conditions were used for further studies. Accordingly, nanoparticles were synthesized, and storage stability was checked for a month by keeping the nanoparticles at 4 ^{0}C.

4.2.2 Cell culture

STR profiled HepG2 (liver) and HEK 293 (kidney) cells that were purchased from the National Centre of Cell Science (NCCS), Pune, India. Cells were cultured in minimum essential medium (MEM) supplemented with 2 mM L-glutamine, 100 U/mL penicillin, 100 µg/mL streptomycin, 0.1 mM non-essential amino acids, 1 mM sodium pyruvate, and 10 % FBS. A temperature of 37 ^{0}C in an atmosphere of 5% CO_2 was maintained in the CO_2 incubator for cell culture and growth. Cells were detached from the flask and dishes with the help of trypsin.

4.2.3 Phase-contrast microscopy

Either HepG2 cells or HEK293 cells were seeded at a density of 2×10^6 cells/well in a 6-well plate. Sorafenib-loaded casein nanoparticles treatment was given at 70% confluency of the cells. After 24 hrs, the changes in cell morphology were examined under an inverted microscope (Carl Zeiss) at 20x magnification, and images were captured using Zeiss software (Zen 3.4).

4.2.4 DNA fragmentation assay

Cells were seeded in a 6-well plate at 2×10^6 cells/well density. Further, DNA was isolated from HepG2 cells after 24 h treatment with casein protein, sorafenib, and sorafenib-loaded casein nanoparticles, respectively. Both adherent and floating cells were harvested, pelleted down, and washed with PBS. Cell pellets were then treated with 100 µL of DMSO and mixed well. This was followed by the addition of an equal volume of TE (Tris-EDTA) (pH 7.4) buffer containing 2% SDS (sodium dodecyl sulfate) (Sigma-Aldrich). After that, it was, centrifuged at 12000 rpm for 15 minutes at 4 ^{0}C. The DNA supernatant was subjected to 2% agarose gel electrophoresis for DNA fragmentation analysis (Pandey et al. 2012).

4.2.5 Annexin V-FITC/Propidium iodide apoptosis assay and cell cycle phase distribution analysis by flow cytometry

For performing annexin pi and cell cycle assay, HepG2 Cells (2×10^6 cells/well) were plated in two different 6-well plates and treated with drug-encapsulated nanoparticles (15 µM) or with the free drug (15 µM) for 24 h. After treatment, for annexin pi assay, cells were harvested by trypsinization, washed with PBS, and resuspended in 500 µL of 1X binding buffer (Thermo Fisher Scientific). Subsequently, 5 µL of AnnexinV-FITC (Thermo Fisher Scientific) and 5 µL of propidium iodide (PI) (Sigma-Aldrich) are added and incubated in the dark for 20 minutes. Then samples were acquired and analysed.

For analysing the distribution of cells in the phases of the cell cycle, after the above-mentioned treatment, cells were harvested as described earlier. After that, the cell pellet was resuspended in 100 µL PBS and fixed with 900 µL 70% ethanol overnight at -20 ^{0}C. Subsequently, cells were centrifuged at 1500 rpm; the pellet was resuspended in PBS (pH 7.4), 5 µL PI dye was added, and incubated for 10 min in the dark. Experimental analysis depicting the percentage of cells in the sub-G1, G0/G1, S, and G2/M phases was performed by flow cytometry (CytoFLEX, Beckman

Coulter). The histogram of the percentage of cells in each phase of the cell cycle was acquired from CytExpert software and represented in a bar diagram.

4.2.6 Reactive oxygen species (ROS) assay

DCFDA (2', 7'-dichlorofluorescein diacetate), a fluorogenic dye that measures ROS activity within the cell, was used for this assay. In the presence of ROS, DCFH is rapidly oxidized to highly fluorescent DCF. Quantitative estimation of DCF is used to determine cell ROS levels (Liou et al. 2010; Kalyanaraman et al. 2012). Approximately 7000 cells/well were seeded in a 96-well plate and treated with either drug-loaded casein nanoparticle or free drug for 24 h. Also, 5 mM NAC (*N*-acetyl cysteine) (Sigma-Aldrich), a ROS scavenger, was added one hour before treatment. To these cells, 100 µL of DCF-DA dye (20 µM) (Sigma-Aldrich) was added after 24 hr of treatment and incubated for one hour at 37 ^{0}C in the dark. Fluorescence was measured using a microplate reader (Fluoroskan Ascent) at an excitation wavelength of 485 nm and an emission wavelength of 530 nm. Correspondingly, an MTT assay was also performed, giving similar treatment to cells, in the absence and presence of NAC, to estimate cell viability as described in the next section, 4.2.7.

4.2.7 Cell viability assay

MTT is a colourimetric assay based on reducing a yellow tetrazolium salt (3-(4, 5-dimethyl thiazol-2-yl)-2, 5-diphenyltetrazolium bromide) to purple formazan crystals by metabolically active cells and used as an indicator of cell viability, proliferation, and cytotoxicity. Briefly, HEK 293 cells were harvested, counted, and seeded at 7000 cells per well in the 96-well plate for 24 hours. The following day, cells were treated with various concentrations of the sorafenib-loaded casein nanoparticles and free sorafenib for 24 hours. Untreated cells served as a negative control. Subsequently, 20 µL of 5 mg/mL MTT (Sigma) reagent was added to each well and incubated for 4 hours. Lastly, the media was removed, and 150 µL of dimethyl sulfoxide (DMSO) was added to the wells to solubilize the formazan crystals. The resulting coloured solution is quantified by measuring absorbance at 570 and 630 nanometers using a microplate reader (Multiskan™ Thermo Scientific™). Each determination was carried out in triplicate, and at least two independent experiments were carried out. Cell viability was calculated using the following formula:

% Cell viability = O.D of treated cells/O.D of untreated control cells × 100.

4.2.8 RNA isolation, cDNA preparation, and qRT-PCR

Standard protocols were followed for the extraction of RNA from HepG2 cells. Briefly, cells were lysed with Trizol reagent and incubated for 45 minutes on ice. The cell suspension was transferred to a fresh tube, followed by adding 200 µL of chloroform and incubated for 5 minutes at room temperature. The suspension was centrifuged at 12000 rpm for 15 minutes at 4 ºC, and the upper aqueous layer was transferred to a fresh tube. An equal volume of isopropanol was added, and the mixture was incubated overnight at -20 ºC. Subsequently, it was centrifuged at 12000 rpm for 15 minutes at 4 ºC. The resulting RNA pellet was washed with 70% ethanol. The pellet was air-dried and resuspended in DNase-free water**.** Genomic DNA contamination was removed by treating with DNase (Thermo Scientific) for 30 minutes at 37 °C. The RNA concentration of this DNA-free sample was determined by measuring the absorbance at 260 nm. RNA quality was determined by measuring the 260/280 ratio in a nanodrop (Thermo Scientific, USA).

cDNA was synthesized immediately by a high-capacity cDNA reverse transcription kit (Thermofisher). 1 µg of RNA per 20 µL reaction mixture was used for cDNA preparation. Briefly, the reaction was conducted with 2 µL 10x RT buffer, 0.8 µL 25x dNTPs mix (100 mM), 2 µL 10x RT random primer, 1 µL reverse transcriptase, 1 µL RNAse inhibitor, and 3.2 µL sterile nuclease-free water.

qRT-PCR was performed on the amplified cDNA template. The latter was further checked for the expression of BAX, BCl2, Caspase-3, and p53 genes using SYBR® Green PCR master mix reagents (Biorad, USA) on the CFX connect RT-PCR system (BioRad). β-actin was used as a housekeeping gene**.** Details about primers, like their size, forward and reverse sequences, and annealing temperature, are mentioned in Table 4.1**.** A pre-denaturation was done for 5 min at 95 °C, followed by 35 cycles of 30 secs each at 94 °C for denaturation. The annealing temperature of gene-specific primers was for 30 seconds, then extension at 72 °C for one minute, and a final extension at 72 °C for 3 minutes. Fold change in gene expression was calculated with CT values of treated and untreated cells. It was quantified by the $2^{-\Delta\Delta CT}$ method, where ΔCT= CT of target gene – CT of the housekeeping gene, ΔΔCT= ΔCT treated cells - ΔCT control cells.

Table 4. 1 Details of primer sequence (Bcl-2, Bax, Caspase-3, β-actin, p53)

S.No.	Gene name	Forward sequence	Reverse sequence	Band size (bp)	Annealing Temperature Tm (^{0}C)
1.	Bcl-2	5′-TGTGGCCTTCTTTGAGTTCG-3′	5′-TCACTTGTGGCCCAGATAGG-3′	281	60
2.	Bax	5′-TTTGCTTCAGGGTTTCATCC-3′	5′-CAGTTGAAGTTGCCGTCAGA-3′	246	62
3.	Caspase 3	5′-TTGATGCGTGATGTTTCTA-3′	5′-CAATGCCACAGTCCAGTTC-3′	223	54.8
4.	β-actin	5′-TATTGGCAACGAGCGGTTCC -3′	5′-GGCATAGAGGTCTTTACGGATGTC -3′	139	54.5
5.	p53	5′-GTTCCGAGAGCTGAATGGG-3′	5-ACTTCAGGTGGCTGGAGTGA-3′	92	65

4.2.9 Western blotting

HepG2 cells were seeded in a 6-well plate, and treatment was given with a dose of 15 μM for both drug-encapsulated nanoparticle and free drug for 24 hours. Cells were incubated with RIPA lysis buffer and proteinase inhibitor cocktail. Subsequently, the protein lysate was collected by a scraper, sonicated for a few seconds and centrifuged at 12000 rpm, 4 °C for 20 min. The protein concentration of the lysate was measured by Bradford assay. This was followed by boiling for 10 minutes in an SDS buffer for denaturation. Forty micrograms of protein lysate were loaded per well on a 12% SDS gel and run at a voltage of 80 V. The separated protein was transferred onto the polyvinylidene difluoride (PVDF) membrane (Bio-Rad Laboratories). The membrane was blocked by 5% skimmed milk dissolved in Tris buffer saline (TBS) at room temperature for two hours. It was then incubated overnight with the primary antibody in TBS at 4 °C. The details of primary and secondary antibodies are mentioned in Table 4.2. The membranes were washed three times with Tris-buffered Saline, 0.05% Tween® 20 Detergent (TBS-T) at room temperature for 10 minutes each time. This was followed by the addition of an HRP-linked secondary antibody. Following incubation, membranes were again washed three times with TBS-T. The Protein band detection was done with an enhanced chemiluminescence system (Pierce ECL Western Blotting

Substrate; Thermo Fisher Scientific, Inc.). The ChemidocTM XRS+ system was used for imaging. The images were analyzed by Image Lab Software.

Table 4. 2 Details of primary and secondary antibodies (Bcl-2, Bax, Caspase-3, β-actin, Parp, Anti-rabbit IgG, HRP-linked antibody)

S.No.	Antibody	Catalogue number	Molecular weight
1.	Bcl-2	BioBharti, #BB-AB0230	34 kDa
2.	Bax	BioBharti, #BB-AB0250	20 kDa
3.	Caspase 3	CST, #14220	35 kDa
4.	β-actin	Santa Cruz, #Sc-69879	42 kDa
5.	Parp	CST, #9542	116 kDa
6.	Anti-rabbit IgG, HRP-linked antibody	CST, #7074	-

4.2.10 Statistical analysis

All experiments were performed at least thrice. The data are expressed as the mean ± SEM of these determinations. Comparisons between groups were made by either one-way or two-way analysis of variance (ANOVA) followed by the Bonferroni test. Values of $P < 0.05$ were considered to be statistically significant. All data analysis was performed using GraphPad Prism 8 software.

4.3 Results

4.3.1 Optimization and storage stability of casein nanoparticles

To increase the encapsulation efficiency, nanoparticles were synthesized with varying concentrations of casein protein and calcium chloride. Results are shown in Table 4.3. Among the formulations, lesser drug encapsulation was obtained with 5% casein (50.65%, 47.6%, 40.67%, 40.11%). Higher size (274.6, 254, 252.3, 343.8 nm) and higher PDI (0.371, 0.347, 0.272, 0.5) were shown with 3% casein. Acceptable PDI (0.261), size (230 nm), zeta (-14.4), and EE% (96.92%) were obtained with 4% casein and 50 µL of calcium chloride. The synthesized method was the same as described in Chapter 3. This chosen formulation was further studied for its storage stability.

Table 4.3 Effect of variables - casein (vol%) and $CaCl_2$ (calcium chloride) on nanoparticle size, PDi (Poly dispersity index), zeta, and EE% (encapsulation efficiency)

S.No.	Casein (Vol. %)	$CaCl_2$ (µL)	Size (nm)	PDi	Zeta (mV)	EE%
1.	5 %	20	199.2	0.233	-13.5	50.65
2.	5 %	30	229	0.121	-11.8	47.6
3.	5 %	40	236	0.175	-11.5	40.67
4.	5 %	50	242	0.158	-11.4	40.11
5.	4 %	20	226	0.33	-17.6	51.8
6.	4 %	30	215.6	0.207	-15.3	67.7
7.	4 %	40	277.4	0.33	-12.9	99.5
8.	**4 %**	**50**	**230**	**0.261**	**-14.4**	**96.92**
9.	3 %	20	274.6	0.371	-16	51.5
10.	3 %	30	254	0.347	-14.5	65.95
11.	3 %	40	252.3	0.272	-13.6	65.15
12.	3 %	50	343.8	0.5	-12.5	98.07

According to the results shown in Fig 4.1 (A and B), The size of nanoparticles was consistent within one month at least. No significant change was found in PDI with the optimized nanoformulations until the 30th day. Zeta potential was also seen as unchanged during storage (Table 4.4).

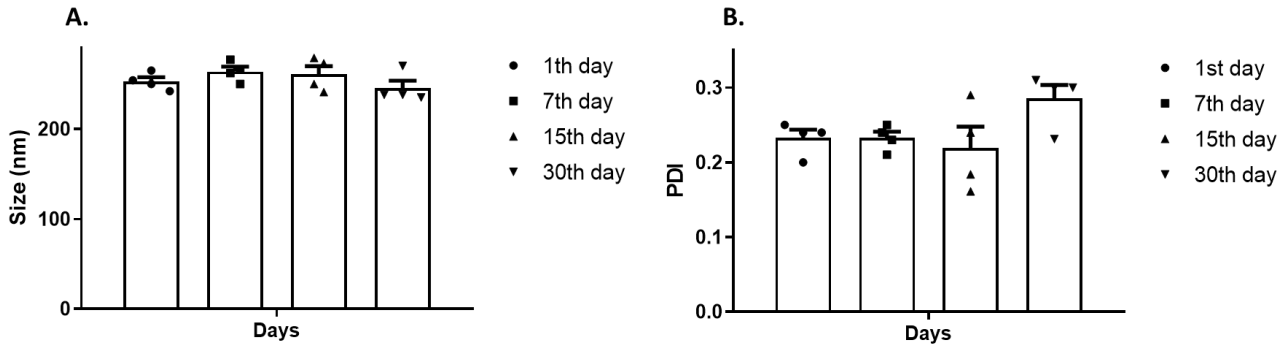

Figure 4. 1 Storage stability of nanoparticles at 4 ^{0}C**. A.** Measurement of the size of nanoparticles on 1, 7th, 15th, and 30th day **B.** Measurement of nanoparticles' PDi (Polydispersity index) on 1, 7th, 15th, and 30th day.

Table 4.4 Measurement of the zeta potential of nanoparticles on 1, 7th, 15th, and 30th day (1 month)

Days	Zeta (mv) ± S.D
1st day	-13.4 ± 1.6
7th day	-13.9 ± 0.65
15th day	-14 ± 0.8
1 month	-14.33 ± 0.57

4.3.2 Effect of sorafenib-loaded casein nanoparticles (SFN-CasNPs) on HepG2 cell morphology

The effect of SFN and SFN-CasNPs on HepG2 cells was examined morphologically by phase contrast microscopy after 24 hours of treatment. As shown in Fig. 4.2, many treated cells were shrunken, rounded, granular with indistinct margins, and irregular. A concentration-dependent cell detachment and floatation of cells were also observed. Consequently, the cell density was reduced as the concentration increased from 5 μM to 15 μM compared to the untreated control cells. A similar effect was observed with either free or encapsulated drug treatment. These unprecedented changes in cell morphology are the characteristic features of apoptosis. The untreated control HepG2 cells were well spread and adhered, depicting their normal morphology.

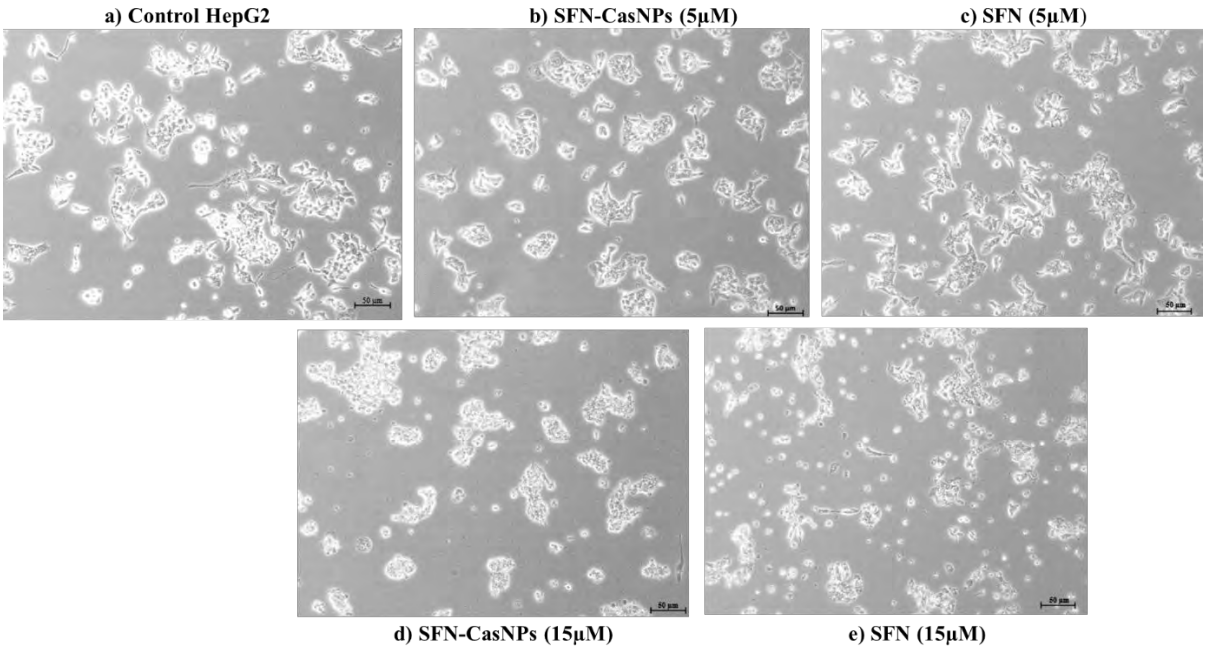

Figure 4. 2 Inverted phase contrast microscopy of HepG2 cells. (a) control HepG2 cells (b) SFN-CasNPs (5 µM) (c) SFN (5 µM) (d) SFN-CasNPs (15 µM) (e) SFN (15 µM). The scale bar is 50 µm.

4.3.3 Effect of SFN-CasNPs on DNA Fragmentation

We performed a DNA fragmentation assay to check whether the cell death was indeed caused by apoptosis (Fig 4.3). The characteristic pattern of the DNA ladder appeared when the HepG2 cells were treated with SFN-CasNPs (lanes 4 & 5). The fragmenting of DNA was almost similar to the pattern observed when cells were treated with increasing concentrations of free drug (SFN), except a higher concentration of free drug was extremely detrimental (lanes 6 & 7). However, no DNA fragments were observed in the cells treated with only casein protein (lane 3) or the untreated control HepG2 cells (lane 2). The DNA marker is displayed in lane 1.

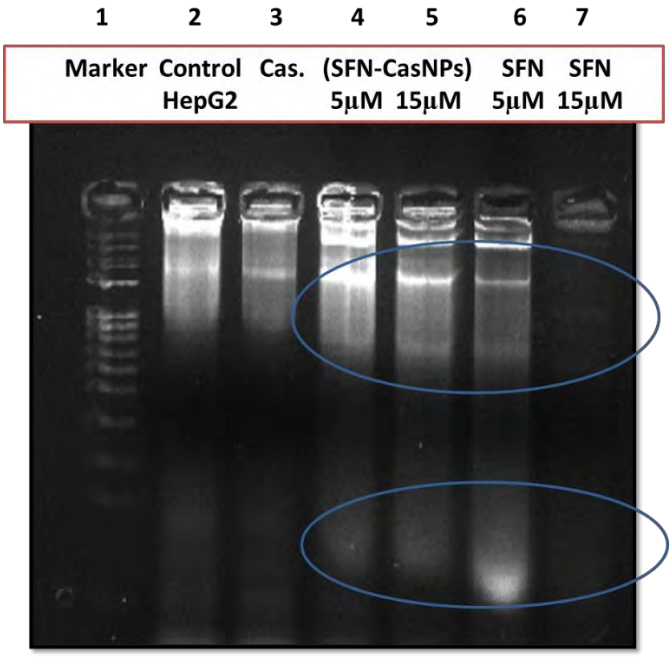

Figure 4. 3 DNA fragmentation assay in HepG2 cells. Lane 1: standard DNA ladder; lane 2: Untreated control cells; lane 3: casein-treated cells; lane 4 and lane 5: SFN-CasNPs (5 µM and 15 µM); lane 6 and lane 7: free SFN treatment at a concentration of 5 µM and 15 µM

4.3.4 Effect of SFN-CasNPs on apoptosis and cell cycle phase distribution by flow cytometry analysis

Apoptosis induction by SFN-CasNPs was further studied using Annexin PI assay. Fig.4.4 a. depicts the proportion of viable cells and cells in the early/ late stage of apoptosis. In control HepG2 cells (left), the viability was 99.37%, whereas, in the SFN-CasNPs treated cells, the viability declined to 72.67%. However, unencapsulated (free) sorafenib (SFN) drug at 15 uM concentration caused more cytotoxicity, i.e., lesser viability (55.82%). In the SFN-CasNPs, the early apoptotic population of cells was 7.83%, and the late apoptotic cell population was 18.79 %. Treatment with only SFN showed slightly more cell population in early (9.46 %) and late apoptosis (30.9%). When compared, no significant difference was found in apoptotic HepG2 cell populations when treated with both SFN and SFN-CasNPs.

Fig.4. 4 displays a quantitative description of apoptotic cells after treatment. It can be observed that HepG2 cells, upon treatment with both SFN-CasNPs and only SFN showed an increase in the percentage of apoptotic cells as compared to control cells. The impact was more by only SFN than an encapsulated drug, although both were statistically significant.

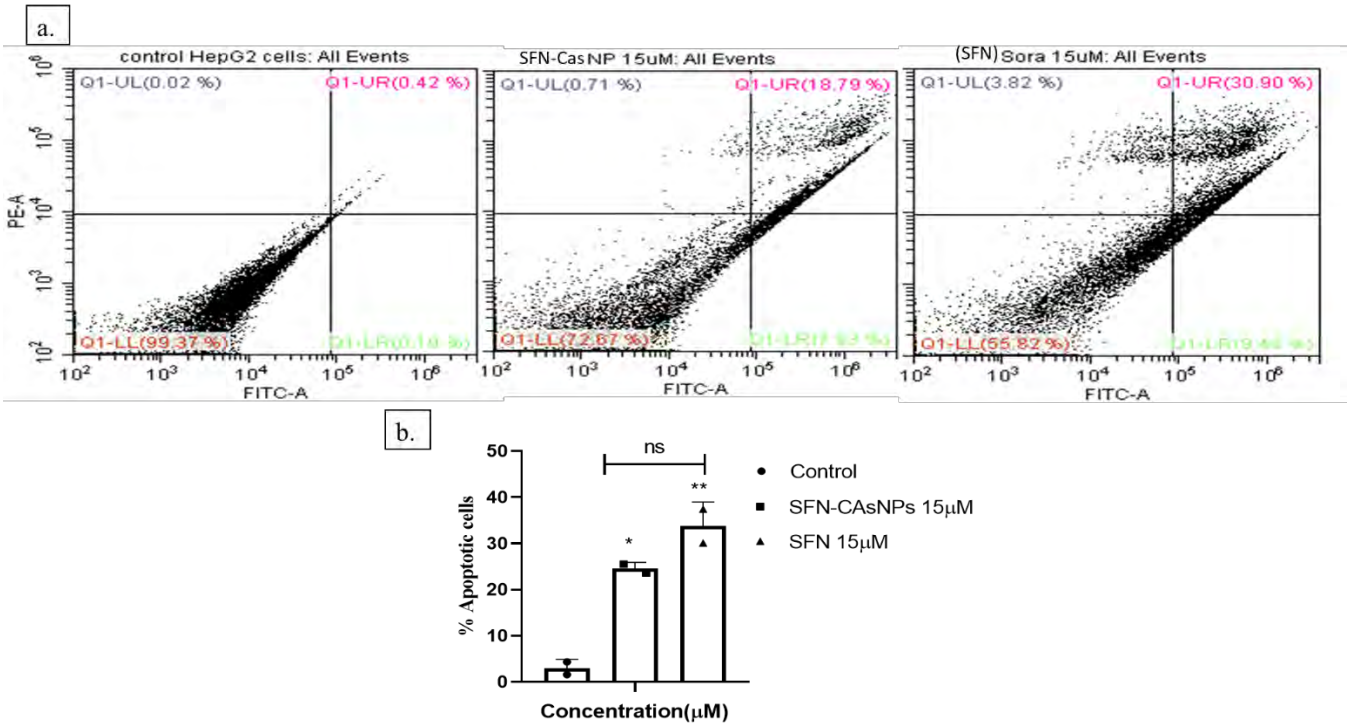

Figure 4. 4 Flow cytometric analysis of apoptotic HepG2 cells by annexin pi assay

a. Depicts control HepG2 cells (panel 1); HepG2 cells treated with SFN-CasNPs (panel 2), SFN (panel 3). [Upper left (UL): Percentage of necrotic cells; Upper right (UR): Percentage of late apoptotic cells; Lower right: Percentage of early apoptotic cells viable cells; and Lower left (LL) -Percentage of viable cells].

b. Percentages of apoptotic cells after 24 h of treatment. Data are presented as mean ± standard error mean, and each measurement was repeated two times independently. **P<0.01, *P<0.05. **Abbreviation-**. FITC - fluorescein isothiocyanate, PE – phycoerythrin.

Fig 4.5 a. demonstrates the distribution of the cells in different phases of the cell cycle, including the detection of cells in the sub-G1 phase. As shown in Fig.4.5 (a and b), treatments with free SFN or SFN-CasNPs caused an increase in the sub-G1 phase cell population, which might represent the DNA fragmentation and apoptotic cell population. The sub-G1 population increased significantly as compared to control cells in both types of treatments. Also, the number of cells in the S phase was significantly decreased.

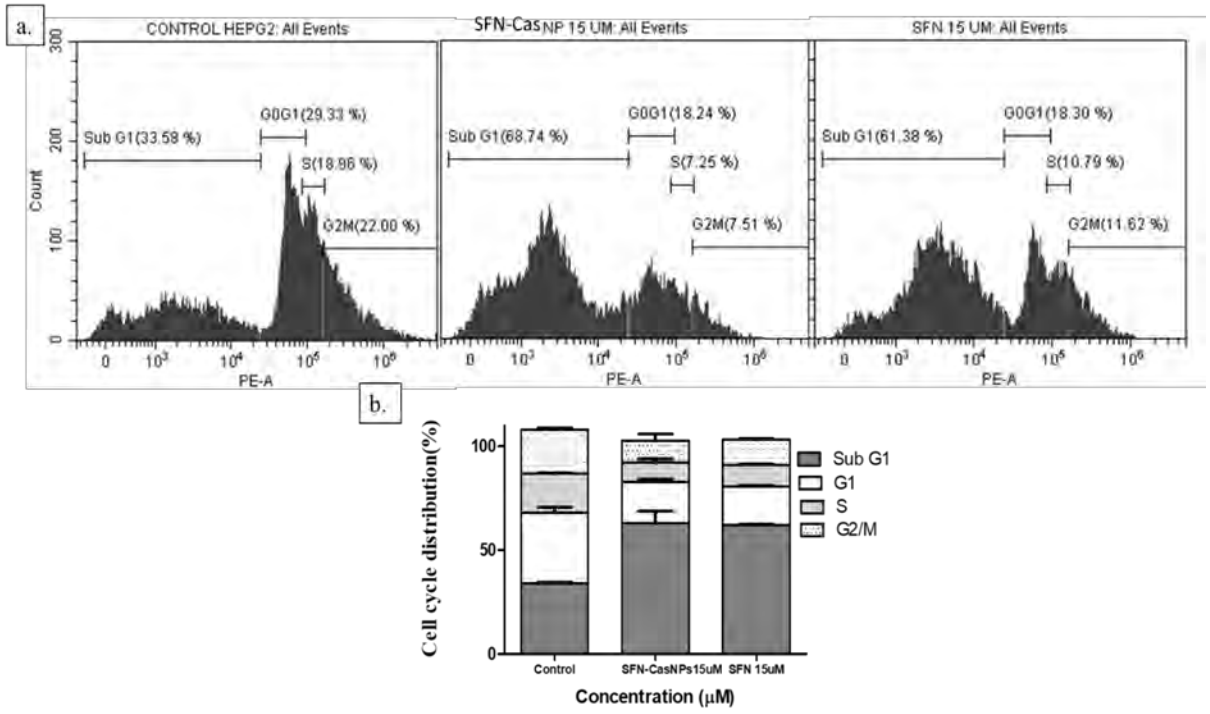

Figure 4.5 Cell cycle analysis of HepG2 cells using flow cytometer

a. Fluorescence intensity of Propidium Iodide (PI) in Control HepG2 cells; HepG2 cells treated SFN-CasNPs (15 μM) and SFN (15 μM).

b. Percentage of cells in each phase of the cell cycle. The data are presented as mean ± standard error mean (SEM) of three independent experiments.

4.3.5 Effect of sorafenib loaded casein nanoparticle on reactive oxygen species (ROS) production

In this experiment, we wanted to determine whether ROS is involved in cell death induced by treatment with the drug sorafenib, either in its free or encapsulated form. As shown in Fig 4.6, sorafenib-loaded casein nanoparticles significantly increased ROS production (6-fold) at the highest dose (20 μM) in HepG2 cells. It was observed that free sorafenib also increased ROS production (4-fold) in the absence of NAC treatment. Also, in experiments, cells were treated with NAC (a ROS scavenger) before the drug treatment to block the intracellular ROS generated in cells. Subsequently, sorafenib's effect on cell viability was studied.

In contrast, the pretreatment of cells with NAC led to a significantly suppressed production of intracellular ROS at 20 μM in both cases: sorafenib encapsulated nanoparticles and free sorafenib. At lower concentrations, such as 10 μM and 15 μM, no significant increase in ROS in the

encapsulated nanoparticles was observed either in the absence or the presence of NAC. Free sorafenib significantly increased ROS production in (-NAC) HepG2 cells at 10 µM and 15 µM concentrations compared to (+NAC) and control HepG2 cells.

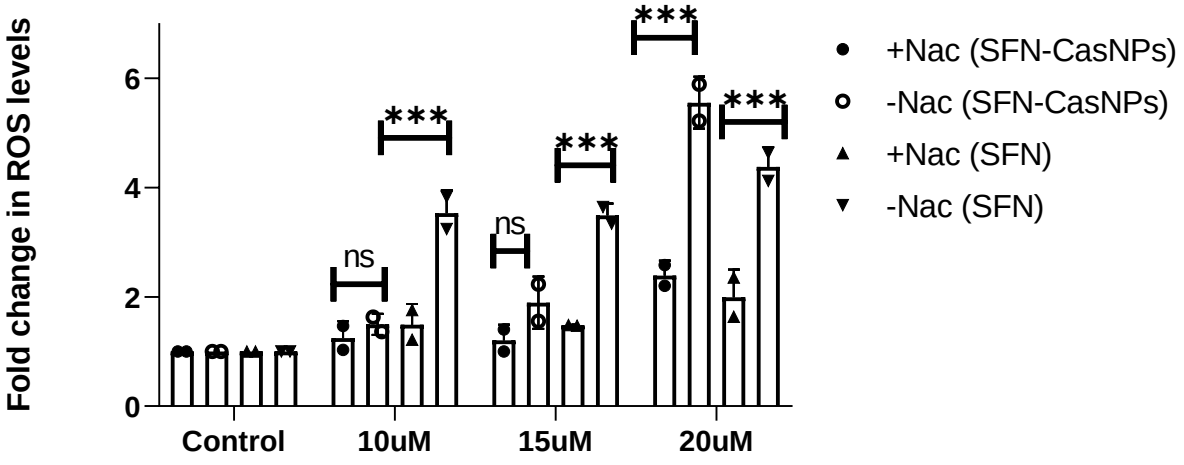

Figure 4. 6 Fold change in ROS generation by HepG2 cells on treatment with SFN and SFN-CasNPs for 24 h in the presence and absence of NAC, a ROS scavenger. Statistical analyses were carried out using one-way ANOVA (***P < 0.001, comparison between +NAC vs –NAC).

As shown in Fig 4.7, the viability of cells increased significantly when NAC was added before treatment as compared to cells without treatment of NAC. This effect was observed when the free drug or drug-loaded nanoparticles treatment was given. It is interesting to note that change occurs in the cell viability in dose-dependent in both cases. It can be noted that pretreatment with NAC has consistently increased cell viability, further suggesting an intracellular ROS-dependent cell death induced by sorafenib in an encapsulated and free form.

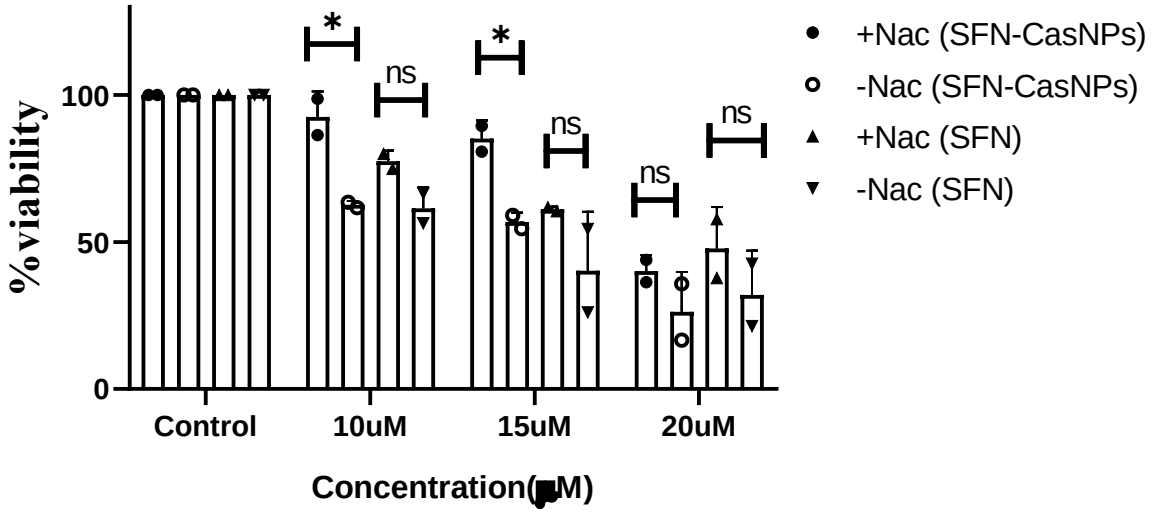

Figure 4. 7 The effect of ROS on HepG2 cell viability by MTT assay. Mean and ± SEM of 3 experiments was plotted, and statistical analyses were carried out using one-way ANOVA (**P < 0.01, ***P < 0.001 vs control)

4.3.6 Effect of sorafenib on the expression of apoptosis-related genes at the transcriptional level by Real-time PCR analysis

Here we have studied the effect of SFN-CasNPs on four apoptosis-related genes, namely, p53, Bax, caspase 3, and Bcl-2. Real-time PCR results showed that mRNA levels of p53 gene expression were significantly upregulated at a higher dose (15 μM) of the encapsulated drug compared to control cells. Whereas in lower doses, treatment with the drug in either encapsulated or free form led to downregulation of p53 expression. Fig 4.8 (a) thus indicates a low dosage may not be effective. p53 is an essential classical tumour suppressor gene, and its upregulated expression is associated with tumour cell apoptosis. Caspase 3 and Bax genes are pro-apoptotic genes responsible for the induction of apoptosis, whereas Bcl-2 is anti-apoptotic. Significant upregulation of caspase 3 gene expression can be observed in free sorafenib-treated cells at only the higher concentration of 15 μM compared to control HepG2 cells (Fig. 4.8 b). At the same time, no significant difference in upregulated caspase gene expression was found in SFN-CasNPs treated cells at either concentration. It was observed that the pro-apoptotic Bax gene expression increased significantly, for both cases, at the dose of 15 μM compared to control. In contrast, lower doses of treatment had no impact (Fig. 4.8 (d). mRNA expression of anti-apoptotic gene Bcl-2 decreased significantly in treated cells at both doses compared to control HepG2 cells (Fig. 4.8 (c). These

changes showed that sorafenib treatment (in a free and encapsulated form) significantly affected some apoptosis-related genes at appropriate concentrations. It further substantiates the induction of induced apoptosis in HepG2 cells by both forms of treatment.

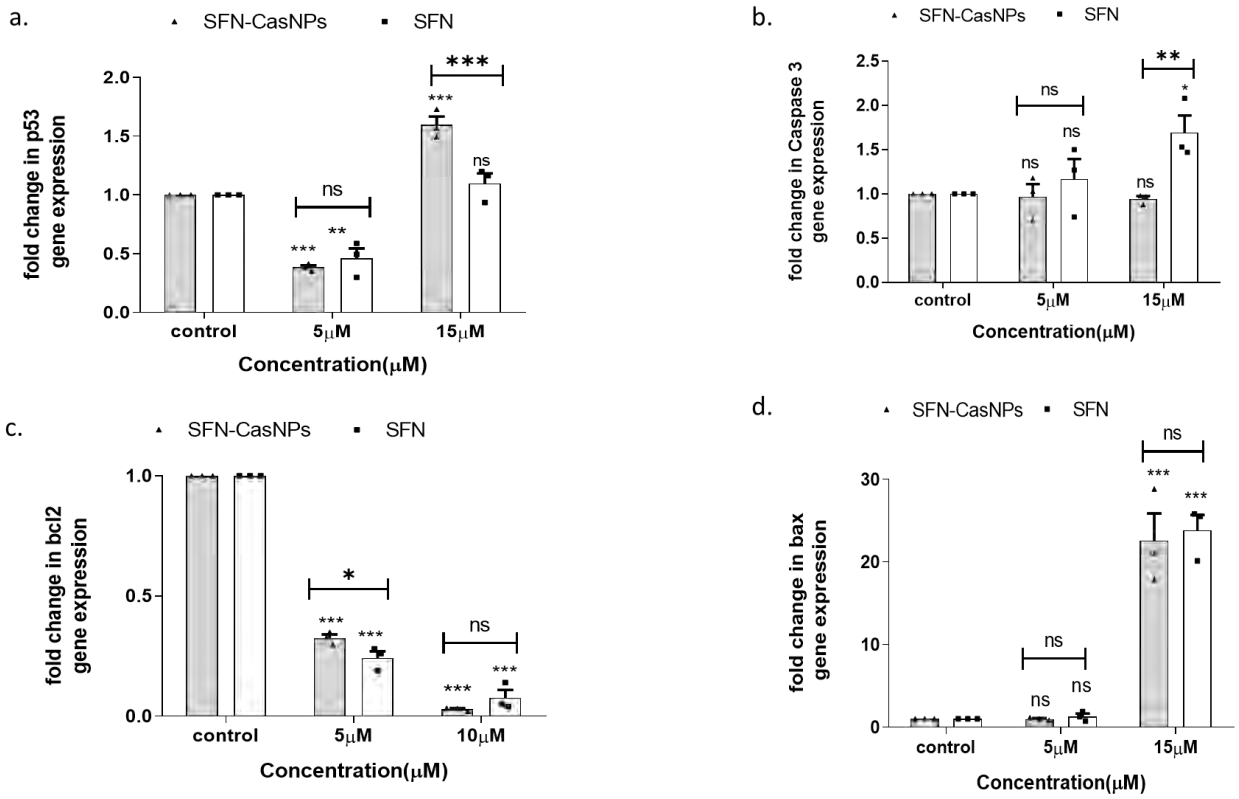

Figure 4.8 Apoptotic mRNA expression determined by qPCR assay. HepG2 cells were treated with SFN and SFN-CasNPs (5 μM) and (15 μM) for 24 h. Data of qPCR were normalized against β-Actin. Data were expressed as mean ± standard error mean. (* $P < 0.05$, ** $P < 0.01$ vs control). ns indicates a non-significant difference

4.3.7 Effect of sorafenib on the expression of apoptosis-related proteins by western blot

To better understand the mechanism of apoptosis at a translational level, the expression of vital anti and pro-apoptotic proteins, namely, Bax, Bcl-2, Parp, and Caspase-3, were examined by western blot analysis. After 24 hrs of treatment, the expression of pro-apoptotic protein Bax protein was slightly increased in drug-loaded Nps (SFN-CasNPs) and free drug (SFN) as compared to control cells (without any treatment) as shown in Fig. 4.9 (a). The anti-apoptotic protein Bcl-2 showed a slight decrease in protein expression in both treatment groups compared to the control in Fig. 4.9 (b). Parp protein is involved in DNA repair and apoptosis. During apoptosis, numerous DNA strand breaks can lead to PARP activation (Pazzaglia et al. 2020). Upon analysis, a slight

decrease in parp protein expression was observed in treated cells, as shown in Fig. 4.9(c). Caspase-3 expression was downregulated significantly in SFN as compared to control cells. Decreased caspase 3 protein expression was also observed in SFN-CasNPs (Fig. 4.9 (d).

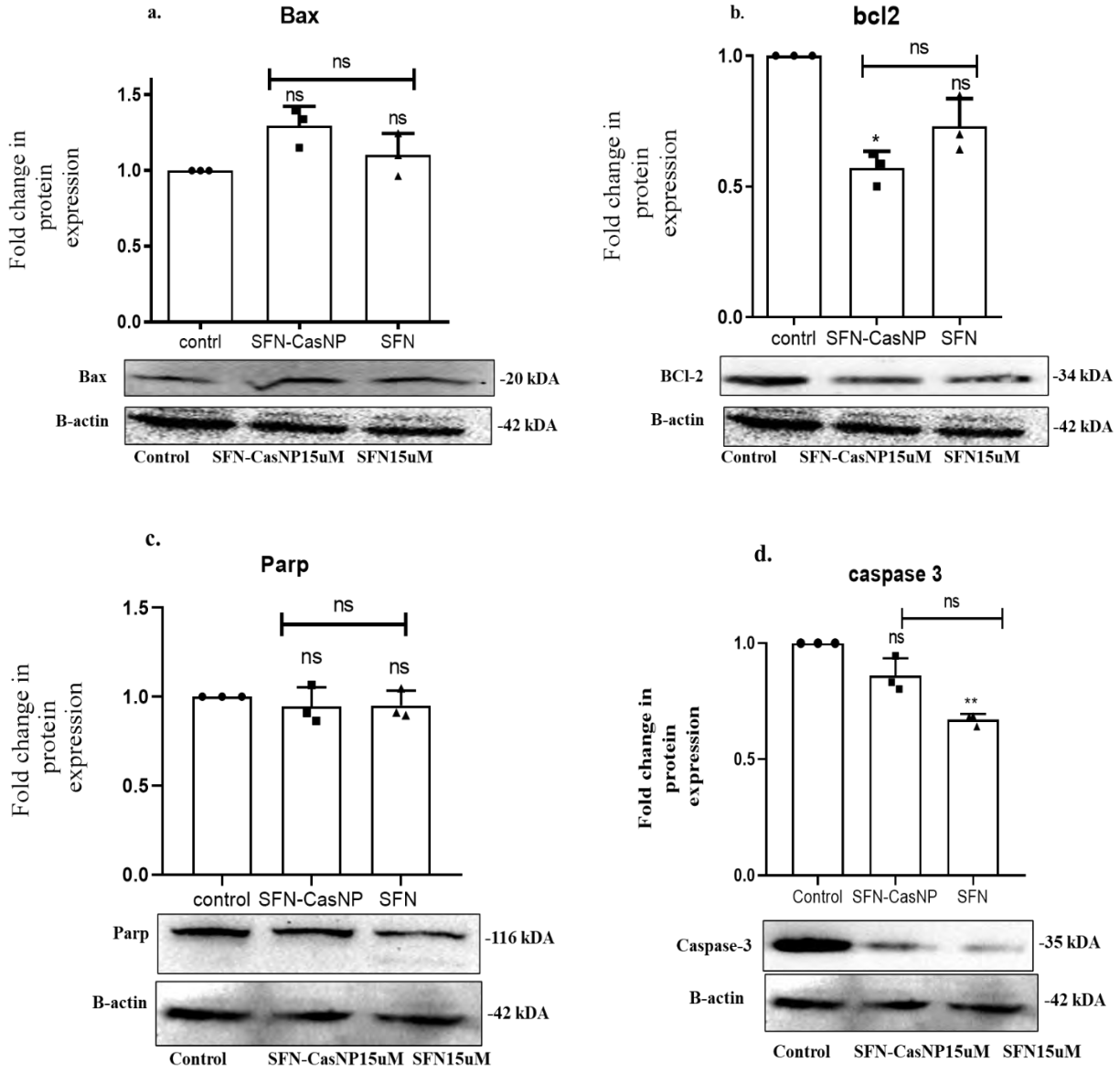

Figure 4. 9 Expression of apoptotic proteins in cells treated for 24 h with SFN-CasNPs (15 µM), SFN (15 µM) (represent sorafenib drug) with respect to control. Results showing representative gel images exhibiting bands of (a) Bax, (b) Bcl-2, (c) Parp, and (d) Caspase-3. The corresponding β-actin bands have also been depicted. Also graphically represented is the quantification of the expressed protein. Data were expressed as mean± standard error mean. *P < 0.05 as compared with control. ns is non-significant.

4.3.8 Effect of sorafenib-loaded casein nanoparticles on normal HEK cell morphology and viability

We also checked the effect of SFN-CasNPs and free SFN on the morphology and viability of noncancerous cells, taking HEK 293 as a model of normal cells. The untreated control cells depicted normal elongated epithelial morphology and appeared healthy (Fig. 4.10 (a). When treated with free SFN drug (15 μM), cells became round, clumped, and partially detached (Fig 4.10 (c). The cells had a significantly reduced confluency compared to untreated controls and were no longer adherent, thus suggesting cell death. This was in contrast to the treatment of cells with SFN-CasNPs. Now, most of the cells were quite confluent, in elongated shape (normal epithelial morphology), and looked healthy (Fig 4.10 (b) to HEK 293 cells.

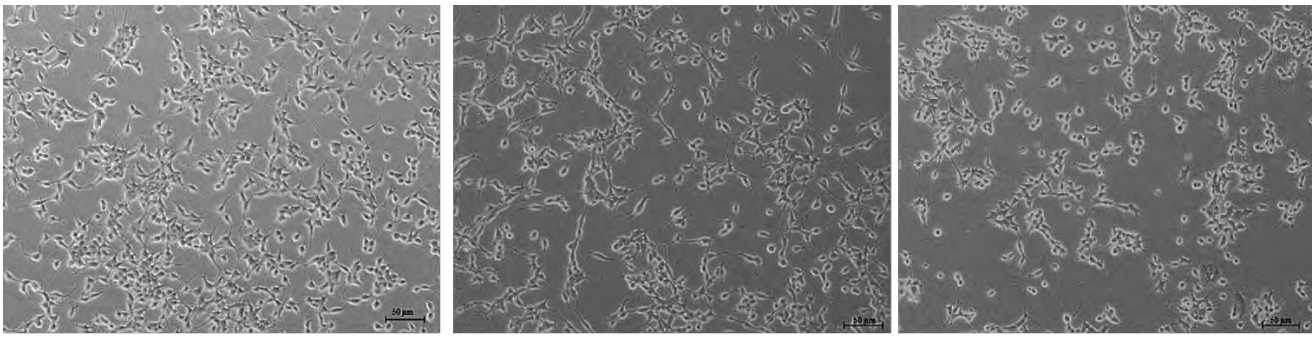

(a) Control HEK 293 cells (b) SFN-CasNPs (15μM) (c) SFN (15μM)

Figure 4. 10 Cell morphology of HEK 293 cells (a) Untreated control cells (b) Cells treatment with 15 μM SFN-CasNPs (c) Cells treatment with 15 μM SFN. Images were taken in a Zeiss™ inverted phase contrast microscope. The scale bar is 50 μm.

In the MTT assay, too, the percentage viability of cells when treated with 15 μM of sorafenib loaded casein np was 76.8% and with free sorafenib was 53.1%, respectively. Similarly, when cells were treated with a higher dose (20 μM) concertation of sorafenib-loaded casein nanoparticle (NP), casein np without the drug (CNP), and sorafenib, their percentage viability further decreased to 63.27%, 82.29%, and 37.14% respectively shown in Fig 4.11. It may be noted that the toxicity of casein-loaded sorafenib was less than the free drug at all the concentrations studied in HEK cells. The therapeutic index of sorafenib was 1.095, and for sorafenib-loaded casein nanoparticles, it was 2.6845 i.e., more than double the free drug, thus indicating its higher safety.

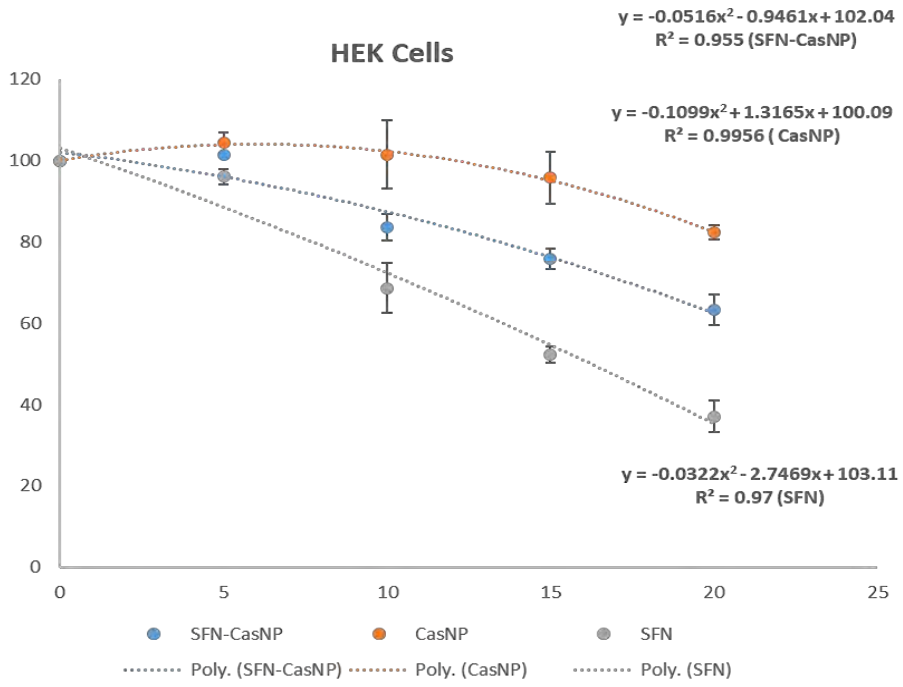

Figure 4. 11 Percentage cell viability of HEK 293 upon drug treatment. SFN-CasNPs represent sorafenib encapsulated casein NPs, and CasNPs represent casein NPs without drug. Statistical analysis was done using 2 way ANOVA (Mean ± SEM (n=3)

4.4 Discussion

In our study, we observed that variables such as the amount of casein protein and calcium chloride volume were the factors that affected the particle size, zeta potential, size distribution, and percentage drug encapsulation efficiency of the SFN-CasNPs. Calcium binding to casein protein is pH-dependent and generally binds at pH 7 or above (Zittle et al. 1958). Calcium was used as a cross-linker. Fifty microliters of 10 mM calcium chloride were found to bind efficiently with casein to form denser casein micelles with satisfying size, zeta potential, and drug encapsulation efficiency.

Treatment of HepG2 cells with sorafenib in either encapsulated or free form significantly affects its morphology. It also reduced the cell density in a dose-dependent manner as compared to untreated control cells. These results are consistent with the previously reported *in vitro* study showing morphological changes in HepG2 upon sorafenib treatment in lung cancer, NCI-H292 cells (Kuo et al. 2022), and gastric cancer cells (Tao et al. 2014).

Apoptosis is characterized by cell shrinkage, blebbing, chromatin condensation, and DNA fragmentation (Elmore 2007; He et al. 2009). Our study demonstrated that sorafenib encapsulated in casein nanoparticles and free sorafenib induced more apoptosis-mediated cell death than control cells when monitored by DNA fragmentation and annexin pi assay. In apoptosis cells, phosphatidylserine (PS) becomes exposed to the external cellular environment. Annexin V conjugated FITC has a high affinity for binding PS and thus is used to identify the apoptotic cells, an early apoptosis marker. Cells stained with propidium iodide (PI), a non-cell-permeable DNA dye, indicate necrotic cells (Demchenko 2013). In our study, cells stained with PI and annexin V-FITC demonstrated later-stage apoptosis and early necrosis. Cell cycle analysis by flow cytometry revealed a significantly greater accumulation of cells in the sub-G1 phase after treatment with 15 μM sorafenib and sorafenib-loaded casein nanoparticles as compared to untreated control cells. This may indicate that sorafenib encapsulating in casein nanoparticles induces cell cycle arrest in the sub-G1 phase as efficiently as sorafenib treatment. It has been suggested that the “Sub-G1" peak represents oligonucleosomal DNA fragments (Wlodkowic et al. 2009). A study was conducted in which sorafenib caused G1 arrest and S phase decrease and induced apoptosis in human synovial sarcoma cells (Peng et al. 2009). During normal cell division, the checkpoints present between the phases of the cell cycle control its progression. Anticancer drugs targeting the cell cycle phase can help inhibit the uncontrolled proliferation of cancer cells and also initiate their apoptosis.

Reactive oxygen species are one of the essential factors that play a role in the induction of apoptosis. In our study, we explored whether ROS are involved in sorafenib-induced apoptosis. Our results demonstrated that treatment with sorafenib and sorafenib-loaded nanoparticles leads to the production of ROS in HepG2 cells in a dose-dependent manner. Similarly, the cell viability also decreased with an increase in ROS. Moreover, NAC, the ROS inhibitor, reversed these effects, thus confirming the ROS-mediated pathways being the cause of the induced cell death. Even in some other earlier studies, sorafenib has been reported to produce ROS and induce cell death also in humans (HepG2) and murine cell lines (Hepa 1.6) (Coriat et al. 2012).

The control of apoptosis has been linked to the expression of anti and pro-apoptotic genes at a transcriptional and translational level. Here, the gene expression studies were used to gain insight

into the expression of key regulators that play an important role in cell apoptosis and its associated molecular mechanisms. Our work showed that at an upregulated p53, Bax and Caspase-3 mRNA expression were consistent with the p53 mRNA expression in treated HepG2 cells at the transcriptional level**.** Similar Bax upregulation and Bcl-2 protein downregulation at the translational level have been observed in our western blot results**.** On the other hand, a reverse effect was found in the Bcl-2 mRNA expression, as expected by an anti-apoptotic gene. This requires further investigation.

According to earlier studies, p53 has its effect by binding with the cellular stress-induced damaged DNA, leading to cell cycle arrest (Ozaki et al. 2011). Furthermore, studies suggest that sorafenib induced cancer cell apoptosis by activating the mitochondria-mediated intrinsic pathway (Zhang et al. 2008). The mitochondria-mediated mode of the cell death pathway is a vital mode of the programmed cell death pathway (Kiraz et al. 2016). In response to DNA damage, p53 (tumour suppression protein) induces apoptosis by translocating to the mitochondria, where it forms inhibitory complexes with Bax (Bcl-2 associated X protein) and Bcl-2 (B-cell lymphoma-2), causing the permeabilization of the mitochondrial membrane to release cytochrome c and induce caspase-dependent cell death (Vaseva et al. 2009). The Bcl-2 family of proteins plays a crucial role in the induction and regulation of apoptosis. Bax is a pro-apoptotic protein that resides in the outer mitochondrial membrane (Kale et al. 2018), while Bcl-2 and Bcl-X proteins can inhibit apoptosis**.** Studies showed that the up-regulation of Bax caused the permeabilization of the mitochondria membrane to release cytochrome C and initiated a caspases cascade, resulting in cell death.

On the other hand, the inhibition of pro-caspase 3 in the cells directly targeted the mitochondria, leading to cell death (Jürgensmeier et al. 1998). Caspases are the key proteins represented by a family of cysteine proteases that modulate the apoptotic response (Julien et al. 2017). Caspase-3 is a key executioner of apoptosis, which is activated via both extrinsic and intrinsic apoptotic pathways. Multiple types of activated caspases cleave respective cellular substrates, ultimately leading to cell death. Importantly, caspase-3 was reported to be crucial for PARP cleavage and DNA fragmentation, which are hallmarks of apoptosis (Brentnall et al. 2013). PARP, a DNA repair enzyme activated by DNA damage, has been used as a biochemical marker of apoptosis**.** A loss of PARP enzyme activity will accelerate cellular instability and inhibit tumour growth (Jagtap et al.

2005; Morales et al. 2014). In our study, the western blot analysis showed a slight decrease in PARP and caspase 3 expressions with drug-encapsulated casein nanoparticles when compared to control cells. These findings in our study suggest that sorafenib may induce HepG2 cell death through the intrinsic apoptotic pathway.

Sorafenib is an approved therapeutic drug for advanced HCC known to prolong the survival of patients (Huang et al. 2020). However, sorafenib, when taken orally, suffers from aqueous insolubility and is associated with a variety of side effects, including hypersensitivity, rashes, weakness, and gastrointestinal disturbances (Brose et al. 2014; Kim et al. 2011). In our study, the cytotoxicity of casein loaded with sorafenib was also tested on normal kidney cells HEK 293 and the therapeutic index was evaluated. Here camel milk casein encapsulated sorafenib was found to be less toxic and had a less adverse effect on HEK 293 cell morphology and cell viability when compared to unencapsulated free sorafenib drug. The therapeutic index of sorafenib-loaded casein nanoparticles was 2.45 folds times more than sorafenib. We feel that casein, a natural polymer, may help limit the side effects of the sorafenib drug, as shown enhanced therapeutic index when encapsulated. This also indicates that camel milk casein is an efficient drug delivery system against HepG2 cells.

4.5 Conclusion

The physical parameters for optimized nanoparticle size, zeta, and encapsulation efficiency were studied in this part of the thesis. They were also studied for their stability upon storage. Furthermore, SFN-CasNPs were evaluated *in vitro* for treating liver cancer, taking HepG2 cells as a model system. Here we report induction of apoptosis by sorafenib drug and sorafenib-loaded casein nanoparticle in HepG2 cells as tested by annexin pi assay, G1 cell cycle arrest, DNA fragmentation, and ROS-induced cell death. Further, the down-regulation of Bcl2 and up-regulation of Bax and caspase-3 genes confirmed mitochondrial apoptotic cell death. The cytotoxicity of camel milk casein encapsulated sorafenib was also checked in normal kidney cells (HEK293). It was also observed that its encapsulation in natural and biocompatible casein protein also reduced its potential side effects. Our study highlights the potential of camel milk casein for a hydrophobic drug like sorafenib *in vitro* without compromising the drug's efficiency.

Chapter-5: To conduct *in vivo* pharmacokinetics and biodistribution studies of sorafenib loaded camel milk casein nanoparticle

5.1 Introduction

Sorafenib, an FDA-approved tyrosine kinase inhibitor drug, is the first-line treatment for HCCand advanced renal cell carcinoma (RCC) (Narayanan et al. 2014). It inhibits tumour cell proliferation and prevents tumour angiogenesis (H. Zhang et al. 2022). Sorafenib is administered orally in patients with a high dose (400 mg) in advanced stages of HCC disease when no other treatment options are feasible (Mammatas et al. 2020). However, sorafenib is classified in the Biopharmaceutics Classification System (BCS) as class II according to its solubility and permeability. Sorafenib is known to have high permeability but poor aqueous solubility and limited oral absorption. Thus *in vivo,* dissolution is the critical determinant of absorption and bioavailability (Yasuhiro Tsumea et al. 2014). Upon reaching its target organ, sorafenib metabolizes in the liver, reducing oral bioavailability by 38%. Moreover, after administration, patients suffer from several adverse side effects such as skin toxicity, diarrhoea, fatigue, hypertension, etc. (Ye et al. 2014). Due to this, the efficacy of sorafenib is reduced, and patient compliance may be compromised.

Nanoparticulate size causes an increase in surface area and increased dissolution, thus helping in high bioavailability, improved *in vivo* pharmacokinetics and better passive tumour targeting (Hoshyar et al. 2016). Many synthetic polymers, liposomes, silica, and metallic nanoparticles have been developed to improve the delivery of sorafenib (Kong et al. 2021). Still, the natural nanocarrier for the delivery of sorafenib is yet to be reported.

Pharmacokinetics is the study of how the body interacts with administered drugs for the entire duration of exposure, from the moment of their administration to elimination from the body. Together study of pharmacokinetics and biodistribution study of any drug helps analyze plasma or tissue drug concentration profiles. Whereas biodistribution study is the distribution of drugs from the systemic circulation throughout the body and its quantification. Biodistribution is fundamental to identifying target organs for monitoring drug safety and efficacy (Currie 2018).

Casein is a major mammalian milk phosphoprotein. It is a natural carrier of calcium and phosphate because of its micellar structure. Casein micelles are spherical, with an average size of 300 nm,

varying among mammalian species (Runthala et al. 2023). The importance of the natural biomolecule casein micelles lies in their encapsulation of both hydrophobic and hydrophilic bioactive molecules (Ranadheera et al. 2016). Therefore, casein nanoparticles have been explored as various nutraceutical and drug delivery systems. Micelle formation has become an essential approach for preparing i.v. formulations of the poorly water-soluble drug (X. Li et al. 2011). Micelles of camel milk casein (20-300 nm) are found to have a larger average size as compared to bovine casein micelles (40-160 nm) (Swelum et al. 2021). Camel milk casein is more stable and possesses highly hydrophobic β-casein and thus can be used as a better alternative to bovine casein because of having increased solubility and bioavailability of hydrophobic drugs via hydrophobic interactions. Reports suggest that camel milk exhibits unique physical, nutritional, and technological properties compared to other species of milk, mainly bovine (Mohamed et al. 2020). Moreover, a casein micelle enables intravenous injection of poorly soluble anti-cancer drugs by incorporating them inside its hydrophobic core (Elzoghby et al. 2013). Moreover, the degradation products of casein have health benefits, like the reduction of oxidative stress (Behrouz et al. 2022).

The objective of the present work is to develop, characterize and evaluate the capability of camel milk casein nanoparticles as carriers for the *in vivo* delivery of sorafenib. In this chapter, we optimized the already synthesized drug-loaded nanoparticle for *in vivo* study. Further, the lyophilized casein-loaded sorafenib nanoparticles were characterized in terms of size, zeta potential, and PDI. We also calculated the drug encapsulation efficiency and drug loading efficiency of this system. These synthesized drug-loaded casein nanoparticles were evaluated for their efficiency by determining various pharmacokinetic parameters and performing biodistribution studies in mice after intravenous administration. This bioanalytical study method of sorafenib estimation was evaluated in mice plasma, liver, lungs, kidney, heart, and spleen using HPLC.

5.2 Methodology

5.2.1 Preparation and characterization of sorafenib-loaded camel milk casein nanoparticles

Drug-loaded nanoparticles were synthesized with little modifications from the earlier procedure (Mittal et al. 2021). Briefly, 4 mL of 5 per cent of casein solution was taken, and 4 mg/mL of sorafenib solution was added. Calcium chloride was added as a cross-linker and stirred on a magnetic stirrer for 6-7 hours to evaporate the organic solvent ethanol. The nanoparticles formed

were subsequently lyophilized using a Labconco™ FreeZone™ Triad Freeze Dryer. For characterization, the lyophilized nanoparticles were reconstituted in Milli-Q water and size, PDI, and zeta potential were measured.

5.2.2 Determination of drug encapsulation efficiency and drug loading

For determining drug loading in nanoparticles, 20 mg of lyophilized nanoparticles were mixed with 1 mL of methanol and sonicated to release the drug into the organic solvent. The resulting solution was centrifuged, a clear supernatant was analyzed with UV- Vis spectroscopy at 265 nm, and drug encapsulation was determined as described earlier.

Drug loading in nanoparticles = (Mass of SFN in NP / Mass of NP recovered)

5.2.3 Animal-related details

Experimental animals (Swiss albino mice) weighing 28–38 g were purchased from a Central Animal Facility, BITS Pilani. Animals were caged and provided with a controlled environment of temperature conditions (25 ± 2 °C), 12 h day/light cycle. They were given standard Ad libitum feeding and water throughout the study. Before the initiation of this study, protocols were reviewed and approved by the Institutional Animal Ethics Committee (IAEC), Birla Institute of Technology and Science (BITS-Pilani), Pilani campus, Rajasthan, India (IAEC/RES/28/3).

5.2.4 Formulation of sorafenib for *in vivo* studies

The stock solution of sorafenib (4 mg/mL) was prepared according to the reported study (Yang et al. 2016). Four milligrams of sorafenib was dissolved in a stock solution containing an equal volume (100 µL) of Chremophore EL, 100 µL ethanol and 800 µL of saline (0.9 % NaCl). After the addition of Chremophore EL and ethanol, the solution was vortexed at high speed for 5 minutes until the sorafenib was completely dissolved. A clear sorafenib solution was obtained and stored at 4 °C for further use.

5.2.5 Bioanalytical method development by high-performance liquid chromatography (HPLC)

The chromatography was conducted by a reversed-phase HPLC methodology. The HPLC system (Agilent 1260 infinity II) equipped with a quaternary pump, autosampler, thermostated column compartment, UV-visible detector and fluorescence detector was used. A bioanalytical method was developed to isolate sorafenib from mice plasma and tissues. Chromatographic separation of

the drug was performed using a C18 column, Infinity Lab Poroshell 120 (4.6×150 mm, 4-Micron). The mobile phase was used in isocratic mode. It consisted of acetonitrile and 10 mM potassium dihydrogen phosphate buffer in a ratio (60:40, v/v). The mobile phase was filtered and sonicated for 20 minutes before use. A flow rate of 0.8 mL/min was optimized, and detection was done at a wavelength of 264 nm for sorafenib and 227 nm for the internal standard drug paclitaxel. The injection volume for each sample was set at 60 µL, and the run time was 10 minutes.

5.2.5.1 Sample preparation

The stock solution of the drug (1 mg/mL) was prepared in methanol to establish the standard curve of sorafenib. 200 µL of blood was withdrawn from mice, and the organs under study, namely the liver, spleen, kidney, heart, and lung, were dissected. A pictorial representation of the methodology of sample preparation for pharmacokinetic and biodistribution study has also been depicted in Fig 5.1. An aliquot (10 µL) for each diluted sorafenib solution (1000-20000 ng/mL) was spiked with 80 µL of blank plasma and tissue homogenate, yielding 100 to 2000 ng/mL concentrations. Also, 10 µL of paclitaxel (internal standard) was added at a concentration of 2 µg/mL. Subsequently, the tissue homogenates or plasma samples were treated with 300 µL of methanol and vortexed for 7-10 minutes to precipitate the constituent proteins. The obtained suspensions were centrifuged at 12,000 rpm for 20 min, and the clear supernatant was injected into the HPLC system. The calibration curve of sorafenib and the linear regression equation was established.

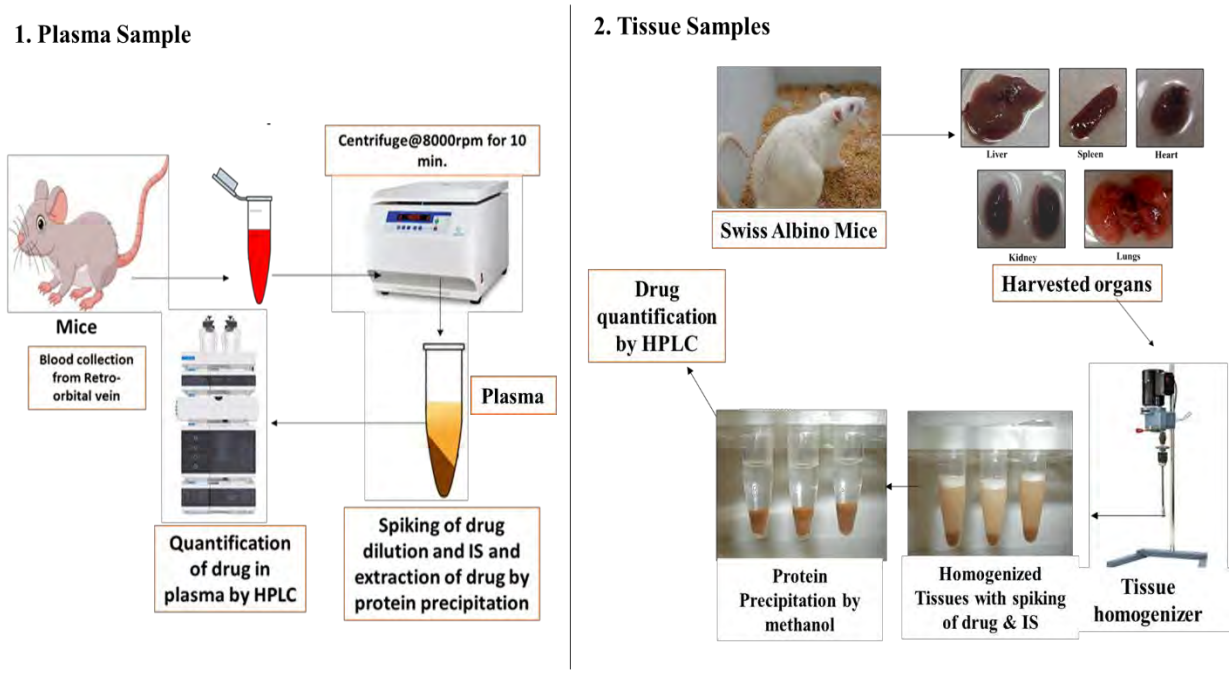

Figure 5. 1 Pictorial methodology of sample preparation for pharmacokinetic and biodistribution study 1. Method of plasma sample preparation for the bioanalytical method development of sorafenib drug for pharmacokinetic study. 2. Method of tissue sample preparation for the bioanalytical method development of sorafenib drug for biodistribution study

5.2.6 *In vivo* pharmacokinetic analysis of sorafenib and sorafenib-loaded camel milk casein nanoparticles in Swiss albino mice

Healthy Swiss albino mice (25-32 g) were used in the study, as described earlier. Mice were divided into two groups, with nine mice in each group. The first group was treated with sorafenib (SFN), and the next with sorafenib-loaded casein nanoparticles (SFN-CasNPs). Mice were injected via the tail vein with free drug solution and nanoformulation with a 20 mg/kg/5 mL dose. Blood (200 µL) at different time points, namely, 0.0833 h, 0.25 h, 1 h, and 2 h, 4 h, 8 h, 12 h and 24 h were collected from the retro-orbital plexus of mice post-injection. EDTA (10%) was used as an anticoagulant. Plasma was separated immediately after blood collection by centrifugation at 6000 rpm for 10 minutes at 4°C. The protein precipitation method, as described earlier, was used to determine the amount of sorafenib in mice plasma. Furthermore, this methodology has also been depicted figuratively below (Fig 5.2). Sorafenib concentration at each time point was determined by the high-performance liquid chromatography (HPLC) method, as described above. The experiment was performed in triplicates.

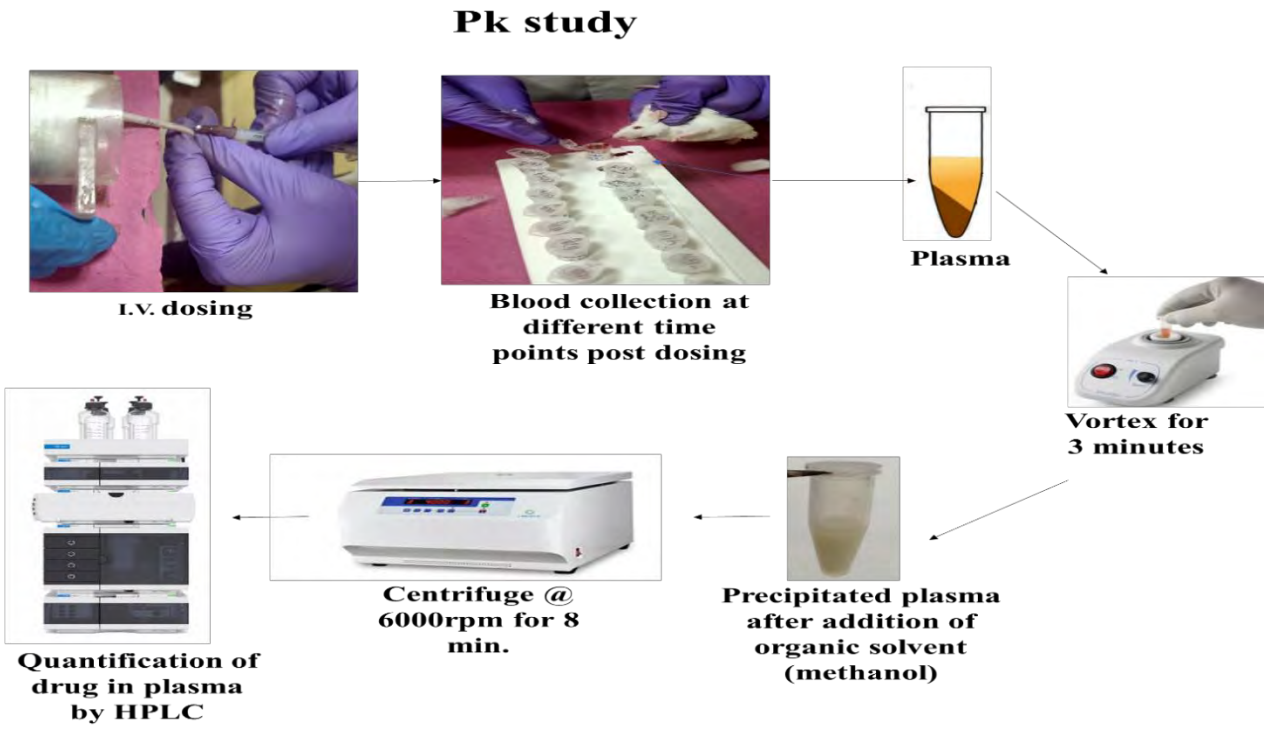

Figure 5. 2 Pictorial methodology of pharmacokinetic study (Pk) of sorafenib drug in mice plasma

5.2.6.1 Pharmacokinetic Analysis

Different pharmacokinetic parameter analyses were carried out using the Phoenix WinNolin CerteraTM (Pharsight, USA). The non-compartmental analysis (NCA) and trapezoidal model were employed for the pharmacokinetic parameter analysis. These parameters included the C_0 (drug concentration at time 0), AUC (area under the plasma concentration-time curve), maximum plasma concentration (Cmax), Z_λ (elimination rate constant), the elimination half-life ($T_{1/2}$), mean residence time (MRT), Vss_{obs} (volume of distribution per kilogram), clearance (CL), and C_{max} (maximum observed plasma concentration).

5.2.7 *In vivo* biodistribution study of sorafenib and its casein nanoparticles

The mice were divided into two groups with a sample size of six per group. The first group was for free drug-treated mice, whereas the next group was for sorafenib-loaded casein nanoparticle treatment. In both these groups, 200 µL of sorafenib solution and sorafenib encapsulated in casein nanoparticles of dose (20 mg/Kg) were given intravenously into the tail vein, respectively. After administration of the free drug and its nanoparticle, mice were sacrificed at three different time points (0.5, 6, and 12 hrs). The animals were sacrificed, and different organs like the liver, lungs, heart, kidney, and spleen were harvested, as shown in the methodology figure above in Fig 5.2.

Further, harvested organs were thoroughly washed with phosphate buffer saline (PBS), weighed, and homogenized with PBS in a (w/v) ratio of 1:1. The concentration of the sorafenib in tissue homogenate was determined based on the peak area with reference to the linear regression equation in the calibration curve of different tissue samples.

5.2.8 Statistical analysis

In this study, all experiments were performed in triplicate, and the data are presented as the mean ± standard deviation of these values. Significant differences between the two groups were evaluated by a two-way ANOVA followed by the Bonferroni post-test using GraphPad Prism 8.0 software. Values of $P < 0.05$ were considered statistically significant.

5.3 Results

5.3.1 Characterization of camel milk casein nanoparticles synthesized for *in vivo* studies

After lyophilization, we characterized the synthesized reconstituted freeze-dried casein nanoparticles; the results of the same are shown in Table 5.1. Results confirmed that the mean size, PDI, and zeta potential were approximately the same as the sorafenib-loaded casein nanoparticles prepared earlier. Particle size was in the range of 230 nm with 0.27 PDI and -16.6 mV zeta potential. The drug encapsulated in casein nanoparticles was also observed to be high, i.e., around 92%.

Table 5.1 Characterization of physical properties of sorafenib-loaded camel milk casein nanoparticles (SFN-CasNPs). Data has been expressed as the triplicate values, mean ± standard deviation (S.D).

Sample	Size(nm) ± S.D	PDI ± S.D	Zeta potential ± S.D (mV)	Drug loading± S.D	EE% ± S. D
SFN-CasNPs	230.3 ± 20	0.27 ± 0.02	-16.6 ± 2.5	2.22 ± 1.3	92% ± 10

5.3.2 Calibration curve analysis of sorafenib obtained in mice plasma and tissue homogenates for pharmacokinetic and biodistribution studies

For the pharmacokinetics and biodistribution studies, the quantity of sorafenib was determined in mice's plasma, liver, spleen, heart, kidney, and lungs by HPLC. Chromatograms of blank mice plasma, plasma spiked with paclitaxel (IS), plasma spiked with sorafenib, and the internal standard (IS) have been depicted in Fig. 5.3. As shown in the chromatogram SFN peak is well separated

from the IS peak exhibiting retention times of 6.5 and 4.2 minutes, respectively. The mobile phase consisted of acetonitrile and potassium dihydrogen phosphate buffer in the ratio of 60:40. The peak for SFN and IS was detected at wavelengths 264 nm and 227 nm, respectively.

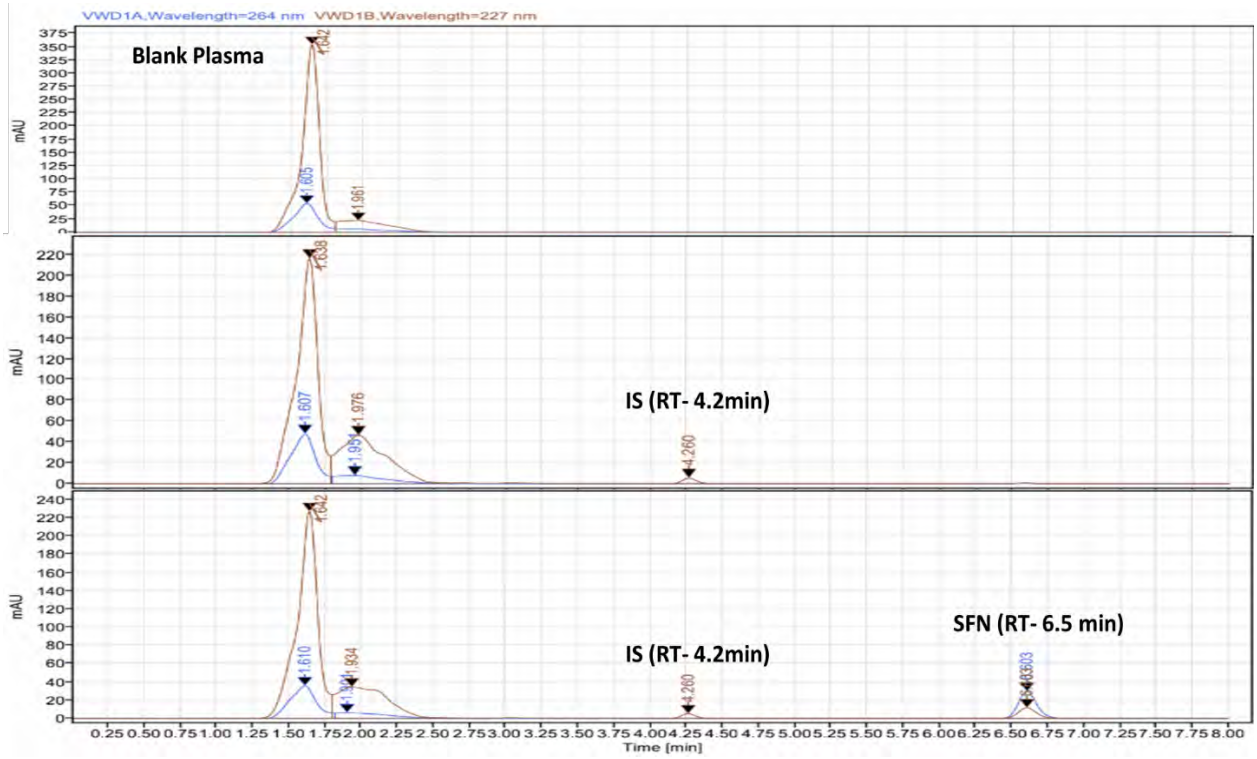

Figure 5. 3 Chromatograms of a blank mice plasma, plasma sample spiked with paclitaxel as internal standard (IS), and plasma sample spiked with sorafenib and IS

After the HPLC method development, the peak area ratio of sorafenib to IS was calculated. A calibration curve of sorafenib was constructed for plasma, kidney, spleen, liver, heart and lungs, respectively, as shown in Fig. 5.4. They showed good linearity ($R^2 = 0.99$) over a concentration range from 100 ng/mL to 2000 ng/mL. The mobile phase and chromatographic conditions were the same for the mice plasma and tissues.

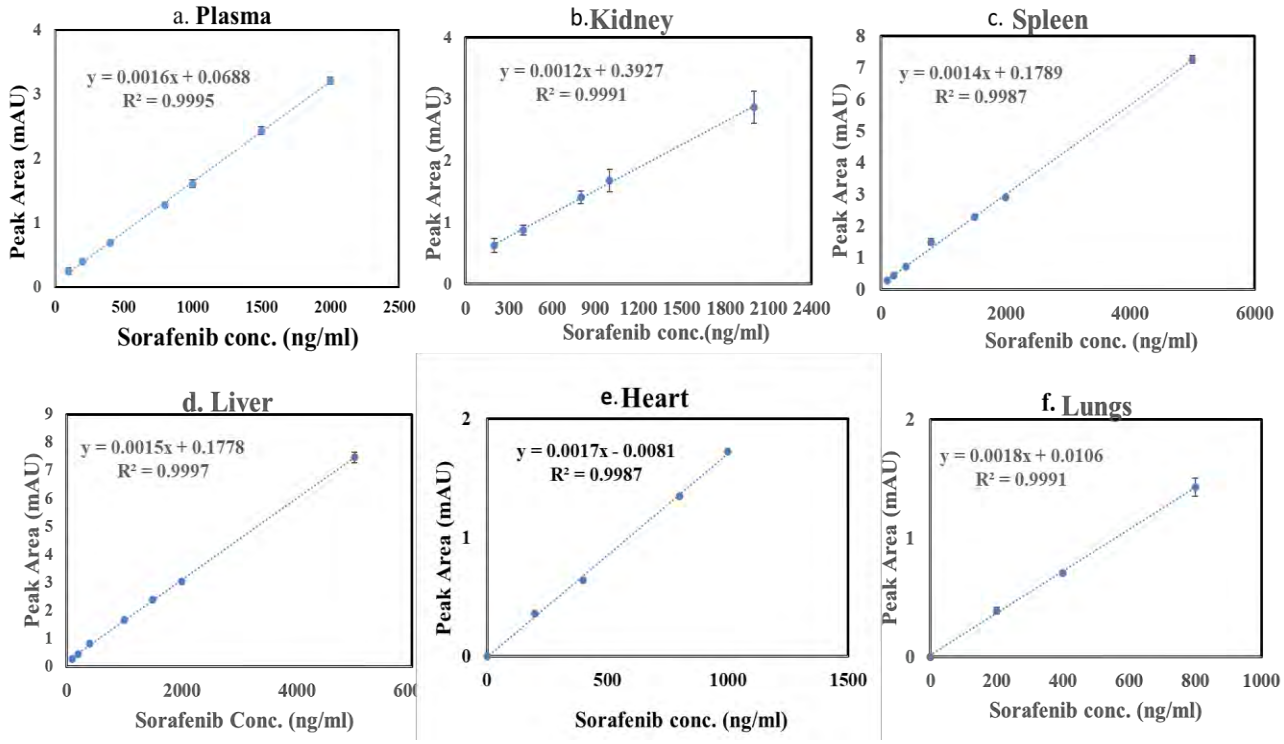

Figure 5. 4 Standard curves and correlation coefficients of quantitated sorafenib obtained from Plasma, Liver, Kidney, Spleen, Heart and Lungs, respectively

5.3.3 *In vivo* Pharmacokinetic profile of sorafenib in swiss albino mice

In vivo, the pharmacokinetic study was performed in Swiss albino mice for up to 24 hours. The variation of mean plasma drug concentration with time profile and correspondingly determined pharmacokinetic parameters have been shown in Fig. 5.5 and Table 5.2. The graph shows that for all time points studied, the plasma concentrations of intravenously applied sorafenib were significantly lower than sorafenib encapsulated in casein nanoparticles. This indicates an increased bioavailability of sorafenib in plasma when loaded in casein nanoparticles.

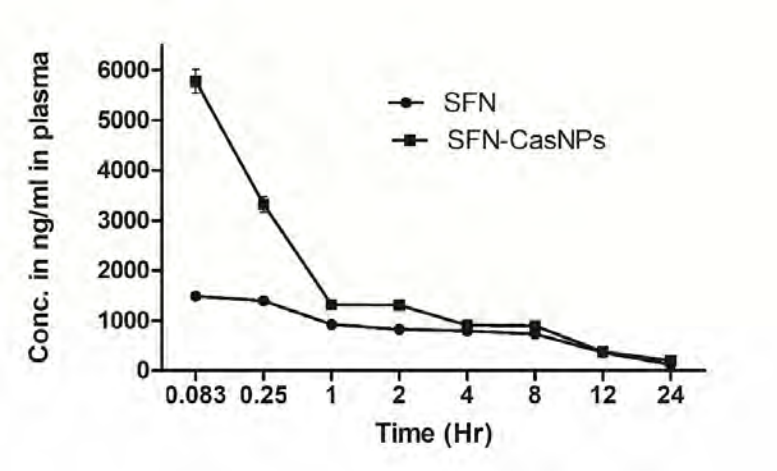

Figure 5. 5 Pharmacokinetic profile of Plasma sorafenib after intravenous administration of sorafenib (SFN) and sorafenib loaded casein nanoparticles (SFN-CasNPs) in Swiss albino mice (dose - 20 mg/kg)

Pharmacokinetic parameters (Table 5.2) revealed a dramatic elevation in the maximum concentration (C_{max}) of sorafenib-loaded casein nanoparticles in plasma. It was 3.8 times higher in drug-loaded nanoparticles than free sorafenib. There was also an enhancement in the AUC when sorafenib was encapsulated in casein nanoparticles. These results indicate an improved bioavailability of sorafenib in an encapsulated form compared to free sorafenib, as observed earlier. A decrease in the elimination rate constant of sorafenib was also observed in the case of encapsulated sorafenib nanoformulation. The time to reach the maximum concentration (T_{max}) was similar for both.

The MRT of SFN-CasNPs was also found to be almost similar to unencapsulated or free SFN. The clearance of SFN loaded in casein nanoparticles was 1.43 times lower than that of free SFN, whereas its volume of distribution was found to be 1.34 times lower. Furthermore, the half-time ($t_{1/2}$) of SFN-CasNPs increased to 8.21 h, while for free SFN, the $t_{1/2}$ was 6.82 h.

Table 5.2 Pharmacokinetic parameters of sorafenib (SFN) and sorafenib loaded casein nanoparticles (SFN-CasNPs) (20 mg/kg) in mice after intravenous administration

Parameters	Unit	SFN (n=4)	SFN-CasNPs (n=4)
C_0 (drug concentration at time 0)	ng/mL	1659.95 ±159.37	7636.78 ± 813.6***
AUC (area under the plasma concentration-time curve)	hr*ng/mL	12760.76 ± 467.58	18213.3 ± 237***
MRT (mean residence time)	hr	10.3 ± 0.18	11 ± 0.11***
Z_λ (elimination rate constant; Ke)	1/hr	0.1016 ± 0.002	0.084 ± 0.0005
C_{max} (maximum observed plasma concentration)	ng/mL	1514.464 ± 71.57	5778.08 ± 402.88***
CL_{obs} (Clearance)	mL/hr/kg	1569.425 ± 57.88	1098.28 ± 14.33
Vss_{obs} (volume of distribution per kilogram)	mL/kg	16160.02 ± 343.97	12043.23 ± 270.5***
$T_{1/2}$ (elimination half-life)	1/hr	6.82 ± 0.14	8.21 ± 0.05***

5.3.4 *In vivo* biodistribution profile of sorafenib and sorafenib-loaded camel milk casein nanoparticles

Mice were administered with sorafenib and sorafenib encapsulated in casein nanoparticles by the I.V. route in the tail vein. The kidney, heart, spleen, liver, and lungs were harvested, and concentrations of the sorafenib were quantified at 0.5 h, 6 h, and 12 h. The results are depicted in Fig.6. At 0.5 hours, the highest concentration of sorafenib-loaded casein nanoparticles was found in the liver among all harvested organs, followed by the kidney, lungs, spleen, and heart. During the same period, the free sorafenib drug was highest in the heart, followed by the liver, kidney, spleen, and lungs. At the 6th hour, the concentration of sorafenib-loaded casein nanoparticles in the liver did not decrease much compared to 0.5 hours. The concentration of drug-loaded nanoparticles was found to be decreased gradually in other organs in a pattern like liver> lungs>spleen>kidney>heart at 6th hours. Along with the liver, free sorafenib concentration was significantly higher in the lungs, heart, and spleen at the 6th hour than the encapsulated form. In the kidney, no significant difference in concentration of free sorafenib is found at the 6th hour. At the 12th hour, concentrations of both sorafenib-loaded casein nanoparticles and free drug were

found to be decreased in the liver, lungs, kidney, spleen, and heart compared to 0.5 hour and 6th hour.

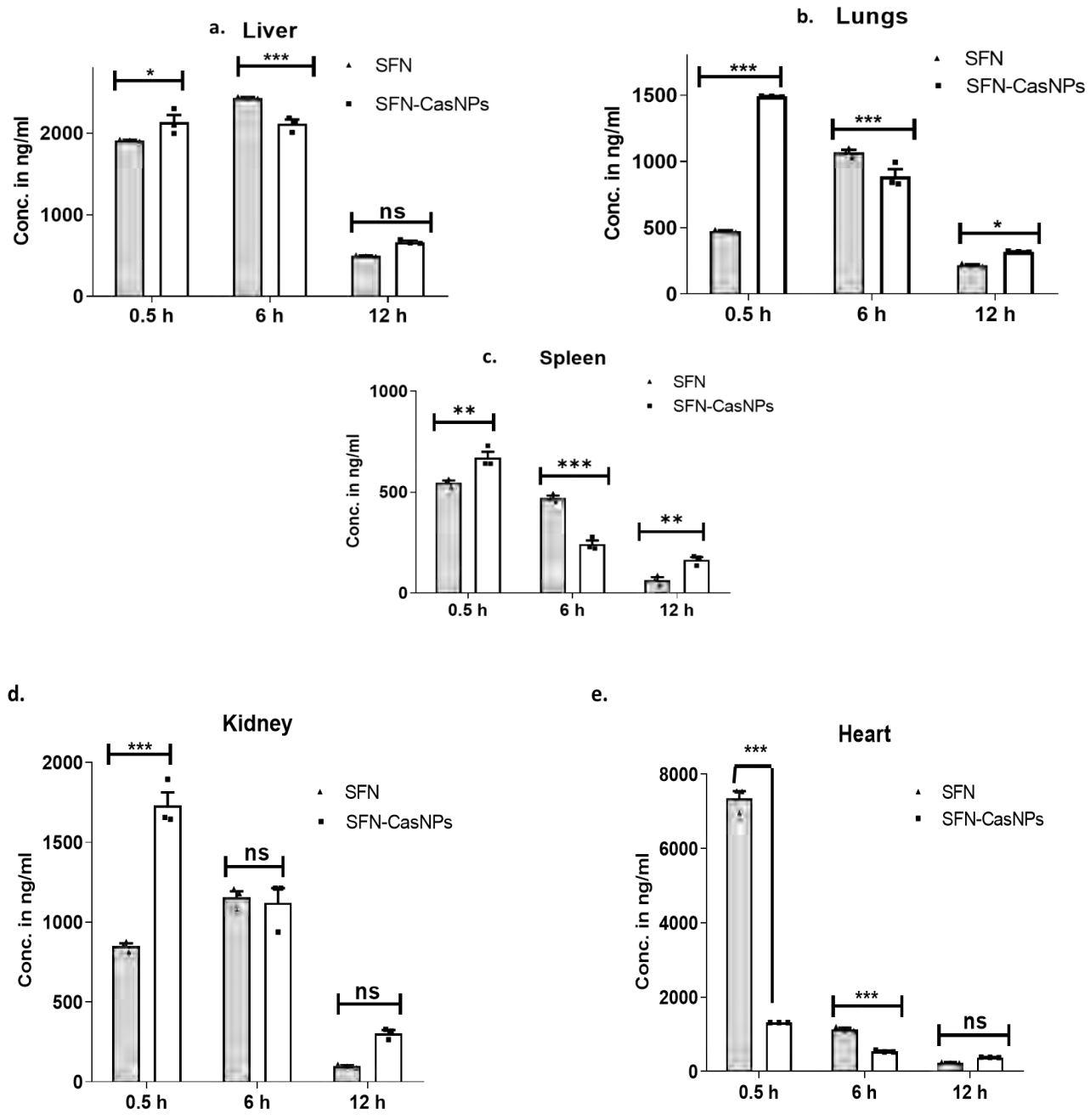

Figure 5. 6 Biodistribution profile of sorafenib (SFN) and sorafenib loaded casein nanoparticles (SFN-CasNPs) at different time points (0.5 h, 6 h, 12 h) in a. Liver, b. Lungs, c. Spleen, d. Kidney, e. Heart in Swiss albino mice after IV dose of 20 mg/Kg. Data are presented as mean ± standard error mean (SEM), (n=3). *** P<0.001, **P<0.01, *P<0.05 and ns = non-significant

5.4 Discussion

SFN-CasNPs were characterized for their size, zeta potential, PDI, drug loading, and encapsulation efficiency before the intravenous administration to the mice for the pharmacokinetic and biodistribution studies. Particle size was 230 nm with 0.27 PDI and -16.6 mV zeta potential. They have been shown to encapsulate a good amount of sorafenib, around 92%. According to other studies on casein micelles' size and hydrophilic properties, the average size of casein micelles ranges from 50 to 500 nm, with a 280-380 nm average diameter in camel casein (Habtegebriel et al. 2020). Also, the presence of a negative charge stabilizes the micellar structure (Seifu 2023). The PDI value indicates nanoparticle size distribution and stability (Liu et al. 2020). In our study, the PDI of SFN-CasNPs was also in an acceptable range (0.1-0.3). It also showed that casein nanoparticles can be lyophilized without using any cryoprotectant. Similar characterization parameters of casein nanoparticles carrying celecoxib (Madan et al. 2020) and doxorubicin (Gandhi et al. 2019) have been reported. In our study, we report that the sorafenib encapsulation in camel milk casein was remarkably high. This study confirms the minimum drug loss and assured authenticity for better delivery in less volume.

The overall bioanalytical data suggested that the SFN peak was well separated from the plasma and internal standard peaks without interference. The KH_2PO_4 buffer and acetonitrile (40:60, v/v) used in the mobile phase were found to be suitable for sorafenib. A similar mobile phase chromatographic condition for sorafenib has been reported previously (Heinz et al. 2011). Therefore, this system could be successfully applied to the present pharmacokinetic and biodistribution study.

Sorafenib is an oral anticancer drug targeted against liver and kidney cancer. Sorafenib is insoluble in water or other buffered solutions at various pH values (pH 1.2 - 7.4). The absolute bioavailability of sorafenib is very low and has been reported in the literature to be only around 8.43% (Zhang et al. 2014). The relative oral bioavailability of sorafenib tablets is also only 38% (Liu et al. 2016). In the present study, camel milk casein nanoparticles are developed to enhance the pharmacokinetics and biodistribution of sorafenib intravenously given to healthy mice.

A significant increase in the maximum concentration of sorafenib-loaded camel milk casein nanoparticles in plasma (C_{max}), $AUC_{0–24,}$ and a longer half-life suggested elongating the circulation time of SFN in plasma compared to free SFN. Negative charge and outer hydrophilic kappa casein

chains stabilize the circulatory system. These results also support previously reported studies indicating that casein nanoparticles had hemocompatibility and immunocompatibility, which were suitable for IV administration (Narayanan et al. 2014). Another study proved that after *in vivo* intravenous administration of flutamide casein (FLT-CAS) nanoparticles, CAS nanoparticles exhibited a longer circulation time, delayed blood clearance, and extended half-life of FLT when compared with free FLT (Elzoghby et al. 2013). Our study suggests that the camel milk casein nanoparticles are biocompatible and can act as long-circulating drug delivery systems of hydrophobic anticancer drugs like sorafenib.

In the biodistribution part of our study, we observed that free SFN accumulation in the heart was extremely high (as compared to SFN-CasNPs). The high availability of free sorafenib in the heart could cause cardiotoxicity. Thus, encapsulation would be a better option. However, the drug concentration in the liver and kidney for sorafenib-casein nanoparticles was higher than in the spleen, heart, and lungs up to the 12^{th} hour of the study. This indicated that the particle size of nanoparticles favours the high affinity towards the liver and kidney. This also shows that with targeted ligands against liver receptors, targeted casein nanoparticles loaded with sorafenib can be further synthesized and explored to specifically target the liver to avoid any non-specific biodistribution of sorafenib.

5.5 Conclusion

In this novel study, we encapsulated sorafenib in camel milk casein nanoparticles by a simple and reproducible synthesis method. We tested the efficiency of this formulation in healthy Swiss albino mice. Furthermore, a bioanalytical HPLC method was successfully developed to determine sorafenib in mice plasma, liver, kidney, heart, spleen, and lungs. The *in vivo* pharmacokinetic study showed that SFN-CasNP enhanced the circulation of the drug in plasma and thus has the potential to improve the bioavailability of the hydrophobic drug sorafenib. Also, encapsulation significantly reduced the availability of sorafenib in the heart, thus reducing the chances of cardiotoxicity being induced by the drug. Lastly, the accumulation of SFN- CasNPs in the liver and kidney could further facilitate their use for clinical application.

Chapter 6: Conclusion, Limitations and Future Prospects

6.1 Conclusion

In this study, we isolated the casein protein from camel milk, and then we formulated calcium chloride-linked camel casein nanoparticles by a simple and non-toxic method. Sorafenib drug was successfully encapsulated into camel casein nanoparticles. Synthesized nanoparticles were well characterized in terms of particle size, morphology, zeta potential, polydispersity index, and drug encapsulation efficiency. We evaluated their cytotoxicity against human hepatocarcinoma cells (HepG2 cells) *in vitro*. Underlying mechanisms of apoptosis have been investigated in HepG2 cells by conducting assays such as DNA fragmentation, ROS generation, and annexin pi. Subsequently, the effect of the drug-loaded nanoparticles on cell cycle phase distribution has also been studied.

Furthermore, the gene expression of apoptosis-related genes, namely p53 (tumour suppression protein), caspase-3, bcl2 (B-cell lymphoma-2), and bax (Bcl-2 associated X protein), was also studied at the transcriptional and translational levels. The cell viability was also calculated in normal cells (HEK 293), and then the therapeutic index was also calculated. The bioanalytical method was developed by HPLC. The pharmacokinetic profile and tissue distribution of the nanoparticles were determined in healthy Swiss albino mice.

For the sake of brevity, given below is the chapter-wise conclusion of our study.

In accordance with the first objective of the study

- We were able to successfully develop the casein nanoparticles in the free form and its encapsulated form (by adopting calcium chloride linkage) with a simple and reproducible preparation method. These spherical-shaped nanoparticles were prepared within the size range of 160–230 nm, were negatively charged, had -20 mV zeta potential and were with uniform dispersity (PDI - 0.23).
- MTT results show that encapsulation of sorafenib in SFN-CasNPs leads to a decrease in the IC_{50} concentration (9 μM), thus increased cytotoxicity at a lower dose, as compared to the free sorafenib (15 μM)
- Fluorescence microscopy shows that encapsulated SFN showed higher cellular uptake in HepG2 cells.

This chapter indicated that the nanoparticles developed had properties of acceptable particle size and spherical shape. They had a higher cytotoxicity as compared to free drug.

The second objective of the study pertained to the cytotoxicity of the developed drug-encapsulated nanoparticles. This revealed that the mechanism of cytotoxicity induction by sorafenib drug and sorafenib-loaded casein nanoparticle-treated HepG2 cells was apoptosis.

- This was tested by phase contrast microscopy, where it exhibited apoptosis-specific changed morphology and a reduced cell number. There was a significantly increased annexin pi-positive apoptotic cell population, fragmented DNA and arrest in the G1 phase of the cell cycle, indicating the same.
- Accumulation of ROS in HepG2 cells on drug treatment was an indication of drug-induced cell death or apoptosis.
- There was an increased mRNA expression of p53, Bax and caspase-3 upon treatment with both, at the transcriptional level whereas at a translational level, they upregulated apoptotic proteins like Bax and decreased the anti-apoptotic protein bcl2. This indicates a mitochondria-associated apoptotic cell death.
- The cytotoxicity of SFN-CasNP was also reduced when checked in normal kidney cells (HEK 293). The therapeutic index of this SFN-CasNPs (2.68) was also more than the free sorafenib (1.09), ensuring better drug safety and efficacy upon encapsulation.

From this chapter, it is also concluded that its encapsulation in natural and biocompatible casein protein would reduce its potential side effects. Our study highlights the potential of casein as a carrier for a hydrophobic drug like sorafenib *in vitro* without compromising the drug's efficiency. The fundamental intent of drug delivery systems to improve the therapeutic index of biologically active agents is also achieved through this study.

In the third objective of the study, the bioanalytical HPLC method of sorafenib drug has been successfully developed to determine drug concentration in plasma, heart, spleen, lungs, liver, and kidneys.

- *In vivo* pharmacokinetic study showed that SFN-CasNP enhanced the circulation of the drug in plasma in terms of increased t-half (8.21 hr) and area under curve (AUC). The AUC of the loaded

nanoparticle increased by 1.42 times, indicating better absorption than that of the free drug. Thus, newly developed nanoparticles have the potential to improve the bioavailability of the hydrophobic drug sorafenib.

- It was observed that the SFN-CasNPs accumulated in the liver and kidney, which could further facilitate their use for clinical application.
- The accumulation of encapsulated drug in the heart was significantly lower than the free drug, thus indicating a reduced risk of cardiotoxicity. The latter was a limiting factor in the efficiency of the free sorafenib.

This chapter indicates the efficiency of sorafenib loaded camel milk casein nanoparticles in transporting sorafenib in Swiss albino mice. It suggests that this system is suitable for drug delivery in the liver and kidney.

In conclusion, this study highlighted the importance of nanoformulation design for poorly soluble drugs like sorafenib. Camel milk casein protein seems to be an appropriate and effective carrier for the solubility enhancement of sorafenib. The structural and physicochemical properties of casein facilitate its functionality in drug delivery systems. Overall, in this study we have been able to develop sorafenib encapsulated camel milk casein nanoparticle, characterize it and evaluate its efficacy against the hepatic cell line HepG2. Our study indicates a very promising prospect of this molecule for liver chemotherapy. The limitations and future prospects of this study follow ahead.

6.2 Limitations

The development of HCC involves the aberration of many intricate signalling mechanisms. There are several molecular mechanisms involved in the action of any drug, including sorafenib. These mechanisms have not been explored in this thesis. Furthermore, many clinical cancer cases cannot be successfully treated because of the emergence of multi-drug resistance (MDR). Herein, such mechanisms have not been explored with reference to sorafenib. More precise information on the nanoparticle's size and shape could be determined by another valuable method, i.e., transmission electron microscopy (TEM), which has not been used here. Moreover, it could be more informative to see the accumulation of the sorafenib-encapsulated casein nanoparticles in tumour-bearing mice if could have been used in pharmacokinetics and biodistribution studies.

6.3 Future perspective

Active drug targeting by attaching a specific ligand against the receptor expressed on cancer cells can help a nanocarrier system to get through biological barriers, reduce the system's overall toxicity, and boost the therapeutic effect. For future studies, a transferrin ligand can be conjugated to casein nanoparticles to specifically target the liver cancer cells and increase the rate of intracellular drug absorption. It would help in dose reduction and further prevent adverse effects of sorafenib. Applying this approach to sorafenib-encapsulated casein nanoparticles would further increase the potential of our nanocarrier system. Also, for the translation of sorafenib-loaded casein nanoparticle activity studies to clinical studies, it is necessary to conduct the pharmacokinetic and pharmacodynamic studies *in vivo* studies in a tumour mice model while also including efficacy-related studies. After that, this study can perhaps be tested further in preclinical drug development and clinical trials.

References

Ahmed O. Elzoghby, Mona A. Abdelmoneem, Islam A. Hassanin, Mahmoud M. Abd Elwakil, Manar A. Elnaggar, Sarah Mokhtar, Jia-You Fang, Kadria A. Elkhodairy. 2020. "Lactoferrin, a Multi-Functional Glycoprotein: Active Therapeutic, Drug Nanocarrier & Targeting Ligand." *Biomaterials Journal* (263):120355. doi: https://doi.org/10.1016/j.biomaterials.2020.120355.

Alexis, Frank, Eric Pridgen, Linda K. Molnar, and Omid C. Farokhzad. 2008. "Factors Affecting the Clearance and Biodistribution of Polymeric Nanoparticles." *Molecular Pharmaceutics* 5(4):505–15. doi: 10.1021/mp800051m.

Alsehli, Mosa. 2020. "Polymeric Nanocarriers as Stimuli-Responsive Systems for Targeted Tumor (Cancer) Therapy: Recent Advances in Drug Delivery." *Saudi Pharmaceutical Journal* 28:255–65. doi: 10.1016/j.jsps.2020.01.004.

Ananthakrishnan, Ashwin, Veena Gogineni, and Kia Saeian. 2006. "Epidemiology of Primary and Secondary Liver Cancers." *Seminars in Interventional Radiology* 23(1):47–63. doi: 10.1055/s-2006-939841.

Antosiewicz, Jan M., and David Shugar. 2016. "UV–Vis Spectroscopy of Tyrosine Side-Groups in Studies of Protein Structure. Part 2: Selected Applications." *Biophysical Reviews* 8(2):163–77. doi: 10.1007/s12551-016-0197-7.

Arti, Sonika, Monika Bharti, Vaneet Kumar, Saruchi, Vikrant Rehani, and Jitender Dhiman. 2022. *Drug Nanocrystals as Nanocarrier-Based Drug Delivery Systems*. Elsevier Inc.

Ashkan Madadlou, Mohammad Ebrahimzadeh Mousavi, Zahra Emam-Djomeh, David Sheehan, Mohammadreza Ehsani. 2009. "Alkaline PH Does Not Disrupt Re-Assembled Casein Micelles." *Food Chemistry* 116(4):929–32. doi: 10.1016/j.foodchem.2009.03.048.

Atri, Maliheh S., Ali A. Saboury, Ali A. Moosavi-Movahedi, Bahram Goliaei, Yahya Sefidbakht, Hamid Hadi Alijanvand, Ahmad Sharifzadeh, and Amir Niasari-Naslaji. 2011. "Structure and Stability Analysis of Cytotoxic Complex of Camel α-Lactalbumin and Unsaturated Fatty Acids Produced at High Temperature." *Journal of Biomolecular Structure and Dynamics* 28(6):919–28. doi: 10.1080/07391102.2011.10508618.

Babos, György, Emese Biró, Mónika Meiczinger, and Tivadar Feczkó. 2018. "Dual Drug Delivery of Sorafenib and Doxorubicin from PLGA and PEG-PLGA Polymeric Nanoparticles." *Polymers* 10(8):1–12. doi: 10.3390/polym10080895.

Balogh, Julius, David Victor Iii, Sherilyn Gordon, Xian Li, R. Mark Ghobrial, and Howard P. Monsour Jr. 2016. "Hepatocellular Carcinoma: A Review." *Journal of Hepatocellular Carcinoma* Volume 3:41–53.

Behrouz, Sepide, Saeideh Saadat, Arghavan Memarzia, Hadi Sarir, Gert Folkerts, and Mohammad Hossein Boskabady. 2022. "The Antioxidant, Anti-Inflammatory and Immunomodulatory Effects of Camel Milk." *Frontiers in Immunology* 13(April):1–17. doi: 10.3389/fimmu.2022.855342.

Brentnall, M., Rodriguez-Menocal, L., De Guevara, R.L., Cepero, E., Boise, L. H. 2013. "Caspase-9, Caspase-3 and Caspase-7 Have Distinct Roles during Intrinsic Apoptosis." *BMC Cell Biology* 14(1):1–9.

Brose, Marcia S., Catherine T. Frenette, Stephen M. Keefe, and Stacey M. Stein. 2014. "Management of Sorafenib-Related Adverse Events: A Clinician's Perspective." *Seminars in Oncology* 41(SUPPL. 2):S1–16. doi: 10.1053/j.seminoncol.2014.01.001.

Bteich, Fernand, and Adrian M. Di Bisceglie. 2019. "Current and Future Systemic Therapies for Hepatocellular Carcinoma." *Gastroenterology and Hepatology* 15(5):266–72.

Chang, Young, Soung Won Jeong, Jae Young Jang, and Yong Jae Kim. 2020. "Recent Updates of Transarterial Chemoembolilzation in Hepatocellular Carcinoma." *International Journal of Molecular Sciences* 21(21):1–20. doi: 10.3390/ijms21218165.

Cheng, Zhe, Maoyu Li, Raja Dey, and Yongheng Chen. 2021. "Nanomaterials for Cancer Therapy: Current Progress and Perspectives." *Journal of Hematology and Oncology* 14(1):1–27. doi: 10.1186/s13045-021-01096-0.

Chew, Sue Anne, Stefania Moscato, Sachin George, Bahareh Azimi, and Serena Danti. 2019. "Liver Cancer: Current and Future Trends Using Biomaterials." *Cancers* 11(12).

Cirstoiu-Hapca, A., F. Buchegger, N. Lange, L. Bossy, R. Gurny, and F. Delie. 2010. "Benefit of Anti-HER2-Coated Paclitaxel-Loaded Immuno-Nanoparticles in the Treatment of Disseminated Ovarian Cancer: Therapeutic Efficacy and Biodistribution in Mice." *Journal of Controlled Release* 144:324–31. doi: 10.1016/j.jconrel.2010.02.026.

Coriat, Romain, Carole Nicco, Christiane Cheŕeau, Olivier Mir, Jér̂ome Alexandre, Stanislas Ropert, Bernard Weill, Stanislas Chaussade, François Goldwasser, and Fred́éric Batteux. 2012. "Sorafenib-Induced Hepatocellular Carcinoma Cell Death Depends on Reactive Oxygen Species Production in Vitro and in Vivo." *Molecular Cancer Therapeutics* 11(10):2284–93. doi: 10.1158/1535-7163.MCT-12-0093.

Currie, Geoffrey M. 2018. "Pharmacology, Part 2: Introduction to Pharmacokinetics." *Journal of Nuclear Medicine Technology* 46(3):221–30. doi: 10.2967/jnmt.117.199638.

Davoodi, Seyed Hossein, Roghiyeh Shahbazi, Saeideh Esmaeili, Sara Sohrabvandi, Amir Mohamamd Mortazavian, Sahar Jazayeri, and Aghdas Taslimi. 2016. "Health-Related Aspects of Milk Proteins." *Iranian Journal of Pharmaceutical Research* 15(3):573–91.

Deepa, Perinkulam Ravi, Suryanarayanan Vandhana, Udayakumar Jayanthi, and Subramanian

Krishnakumar. 2012. “Therapeutic and Toxicologic Evaluation of Anti-Lipogenic Agents in Cancer Cells Compared with Non-Neoplastic Cells.” *Basic and Clinical Pharmacology and Toxicology* 110:494–503. doi: 10.1111/j.1742-7843.2011.00844.x.

Demchenko, Alexander P. 2013. “Beyond Annexin V: Fluorescence Response of Cellular Membranes to Apoptosis.” *Cytotechnology* 65(2):157–72. doi: 10.1007/s10616-012-9481-y.

Deo, S. V. S., Jyoti Sharma, and Sunil Kumar. 2022. “GLOBOCAN 2020 Report on Global Cancer Burden: Challenges and Opportunities for Surgical Oncologists.” *Annals of Surgical Oncology* 29(11):6497–6500. doi: 10.1245/s10434-022-12151-6.

Din, Fakhar ud, W, Aqar Aman, Izhar Ullah, Omer Salman Qureshi, Omer Mustapha, Shumaila Shafique, and Alam Zeb. 2017. “Effective Use of Nanocarriers as Drug Delivery Systems for Treatment of Selected Tumors.” *International Journal of Nanomedicine* 7291–7309. doi: 10.2147/IJN.S146315.

Duan, Wendu, and Yan Liu. 2018. “Targeted and Synergistic Therapy for Hepatocellular Carcinoma: Monosaccharide Modified Lipid Nanoparticles for the Co-Delivery of Doxorubicin and Sorafenib.” *Drug Design, Development and Therapy* 12:2149–61. doi: 10.2147/DDDT.S166402.

Dubey, Uma, Science Pilani, Anyaa Mittal, Science Pilani, Suman Kapur, and Science Pilani. 2015. “Therapeutic Potential of Camel Milk.” (September 2018). doi: 10.9755/ejfa.2015-04-122.

Edis, Zehra, Junli Wang, Muhammad Khurram Waqas, Muhammad Ijaz, and Munazza Ijaz. 2021. “Nanocarriers-Mediated Drug Delivery Systems for Anticancer Agents: An Overview and Perspectives.” *International Journal of Nanomedicine* 16:1313–30. doi: 10.2147/IJN.S289443.

Ejigah, Victor, Oluwanifemi Owoseni, Perpetue Bataille-Backer, Omotola D. Ogundipe, Funmilola A. Fisusi, and Simeon K. Adesina. 2022. “Approaches to Improve Macromolecule and Nanoparticle Accumulation in the Tumor Microenvironment by the Enhanced Permeability and Retention Effect.” *Polymers* 14(2601). doi: 10.3390/polym14132601.

Elmore, Susan. 2007. “Apoptosis: A Review of Programmed Cell Death.” *Toxicologic Pathology* 35(4):495–516. doi: 10.1080/01926230701320337.

Elzoghby, Ahmed O., Maged W. Helmy, Wael M. Samy, and Nazik A. Elgindy. 2013. “Novel Ionically Crosslinked Casein Nanoparticles for Flutamide Delivery: Formulation, Characterization, and in Vivo Pharmacokinetics.” *International Journal of Nanomedicine* 8:1721–32. doi: 10.2147/IJN.S40674.

Esmaili, Mansoore, S. Mahmood Ghaffari, Zeinab Moosavi-Movahedi, Malihe Sadat Atri, Ahmad Sharifizadeh, Mohammad Farhadi, Reza Yousefi, Jean Marc Chobert, Thomas Haertlé, and

Ali Akbar Moosavi-Movahedi. 2011. “Beta Casein-Micelle as a Nano Vehicle for Solubility Enhancement of Curcumin; Food Industry Application.” *LWT - Food Science and Technology* 44:2166–72.

Farah, Z., and M. Rüegg. 1989. “The Size Distribution of Casein Micelles in Camel Milk.” *Food Microstructure* 8(2):211–16.

Gandhi, Sona, and Indrajit Roy. 2019. “Doxorubicin-Loaded Casein Nanoparticles for Drug Delivery: Preparation, Characterization and in Vitro Evaluation.” *International Journal of Biological Macromolecules* 121:6–12. doi: 10.1016/j.ijbiomac.2018.10.005.

Głąb, Tomasz Konrad, and Janusz Boratyński. 2017. “Potential of Casein as a Carrier for Biologically Active Agents.” *Topics in Current Chemistry* 375(4). doi: 10.1007/s41061-017-0158-z.

Gupta, Swati, and Pankaj Kumar. 2012. *Drug Delivery Using Nanocarriers: Indian Perspective*. Vol. 82.

Guzmán-Mejía, Fabiola, Marycarmen Godínez-Victoria, Daniel Efrain Molotla-Torres, and Maria Elisa Drago-Serrano. 2023. “Lactoferrin as a Component of Pharmaceutical Preparations: An Experimental Focus.” *Pharmaceuticals* 16(2):1–20. doi: 10.3390/ph16020214.

Habtegebriel, Haileeyesus, Michael Wawire, Volker Gaukel, and Martha L. Taboada. 2020. “Comparison of the Viscosity of Camel Milk with Model Milk Systems in Relation to Their Atomization Properties.” *Journal of Food Science* 85(10):3459–66. doi: 10.1111/1750-3841.15451.

Al haj, Omar A., and Hamad A. Al Kanhal. 2010. “Compositional, Technological and Nutritional Aspects of Dromedary Camel Milk.” *International Dairy Journal* 20(12):811–21. doi: 10.1016/j.idairyj.2010.04.003.

Hanahan, Douglas, and Robert A. Weinberg. 2000. “The Hallmarks of Cancer.” *Cell* 100(1):57–70.

Hartke, Justin, Matthew Johnson, and Marwan Ghabril. 2017. “The Diagnosis and Treatment of Hepatocellular Carcinoma.” *Seminars in Diagnostic Pathology* 34(2):153–59. doi: 10.1053/j.semdp.2016.12.011.

Haug, Anna, Arne T. Høstmark, and Odd M. Harstad. 2007. “Bovine Milk in Human Nutrition - A Review.” *Lipids in Health and Disease* 6:1–16. doi: 10.1186/1476-511X-6-25.

He, Bin, Nan Lu, Zheng Zhou. 2009. “Cellular and Nuclear Degradation during Apoptosis.” *Current Opinion in Cell Biology* 21(6):900–912. doi: 10.1016/j.ceb.2009.08.008.Cellular.

Heinz, Werner J., Kathrin Kahle, Annegret Helle-Beyersdorf, Diana Schirmer, Ulrike Lenker, Daniela Keller, Peter Langmann, and Hartwig Klinker. 2011. “High-Performance Liquid

Chromatographic Method for the Determination of Sorafenib in Human Serum and Peritoneal Fluid." *Cancer Chemotherapy and Pharmacology* 68(1):239–45. doi: 10.1007/s00280-010-1474-y.

Hejmady, Siddhanth, Rajesh Pradhan, Amit Alexander, Mukta Agrawal, Gautam Singhvi, Bapi Gorain, Sanjay Tiwari, Prashant Kesharwani, and Sunil Kumar Dubey. 2020. "Recent Advances in Targeted Nanomedicine as Promising Antitumor Therapeutics." *Drug Discovery Today* 25(12):2227–44. doi: 10.1016/j.drudis.2020.09.031.

Hoshyar, Nazanin, Samantha, Hongbin Han Gray, &. Gang, and Bao. 2016. "The Effect of Nanoparticle Size on in Vivo Pharmacokinetics and Cellular Interaction Nanoparticle-Based." 11:673–92.

Huang, An-tian, Jun Du, Zhi-yong Liu, Guang-cong Zhang, Weinire Abuduwaili, and Jia-yan Yan. 2022. "Sorafenib-Loaded Cu 2 − x Se Nanoparticles Boost Photothermal – Synergistic Targeted Therapy against Hepatocellular Carcinoma." *Nanomaterials* 12(3191). doi: 10.3390/nano12183191.

Huang, Ao, Xin Rong Yang, Wen Yuan Chung, Ashley R. Dennison, and Jian Zhou. 2020. "Targeted Therapy for Hepatocellular Carcinoma." *Signal Transduction and Targeted Therapy* 5(1). doi: 10.1038/s41392-020-00264-x.

Huang, Daniel Q., Philippe Mathurin, Helena Cortez-Pinto, and Rohit Loomba. 2023. "Global Epidemiology of Alcohol-Associated Cirrhosis and HCC: Trends, Projections and Risk Factors." *Nature Reviews Gastroenterology and Hepatology* 20(1):37–49. doi: 10.1038/s41575-022-00688-6.

Ikeda, Masafumi, Chigusa Morizane, Makoto Ueno, Takuji Okusaka, Hiroshi Ishii, and Junji Furuse. 2018. "Chemotherapy for Hepatocellular Carcinoma: Current Status and Future Perspectives." *Japanese Journal of Clinical Oncology* 48(2):103–14. doi: 10.1093/jjco/hyx180.

Jagtap, Prakash, and Csaba Szabo. 2005. "Poly(ADP-Ribose) Polymerase and the Therapeutic Effects of Its Inhibitors." *Nature Reviews Drug Discovery* 4(5):421–40. doi: 10.1038/nrd1718.

Jindal, Aastha, Anusha Thadi, and Kunwar Shailubhai. 2019. "Hepatocellular Carcinoma: Etiology and Current and Future Drugs." *Journal of Clinical and Experimental Hepatology* 9(2):221–32. doi: 10.1016/j.jceh.2019.01.004.

Johnston, Michael P., and Salim I. Khakoo. 2019. "Immunotherapy for Hepatocellular Carcinoma: Current and Future." *World Journal of Gastroenterology* 25(24):2977–89. doi: 10.3748/wjg.v25.i24.2977.

Julien, Olivier, and James A. Wells. 2017. "Caspases and Their Substrates." *Cell Death and*

Differentiation 24(8):1380–89. doi: 10.1038/cdd.2017.44.

Jürgensmeier, Juliane M., Zhihua Xie, Quinn Deveraux, Lisa Ellerby, Dale Bredesen, and John C. Reed. 1998. "Bax Directly Induces Release of Cytochrome c from Isolated Mitochondria." *Proceedings of the National Academy of Sciences of the United States of America* 95(9):4997–5002. doi: 10.1073/pnas.95.9.4997.

Kale, Justin, Elizabeth J. Osterlund, and David W. Andrews. 2018. "BCL-2 Family Proteins: Changing Partners in the Dance towards Death." *Cell Death and Differentiation* 25(1):65–80. doi: 10.1038/cdd.2017.186.

Kalyanaraman, Balaraman, Victor Darley-Usmar, Kelvin JA Davies, Phyllis A. Dennery, Henry Jay Forman, Matthew B. Grisham, Giovanni E. Mann, Kevin Moore, L. Jackson Roberts II and Harry Ischiropoulo. 2012. "Measuring Reactive Oxygen and Nitrogen Species with Fluorescent Probes: Challenges and Limitations." *Free Radical Biology and Medicine* 52(1):1–6. doi: 10.1016/j.freeradbiomed.2011.09.030.Measuring.

Kappeler, Stefan, Zakaria Farah, and Zdenko Puhan. 1999. "Sequence Analysis of Camelus Dromedarius Milk Caseins." *InterJournal of Dairy Research* (9):481–86. doi: 10.1017/S0022029997002847.

Kim, Dong Ha, In Pyeong Son, Jin Woong Lee, Hye In Lee, Beom Joon Kim, and Myeung Nam Kim. 2011. "Sorafenib (Nexavar̄, BAY 43-9006)-Induced Hand-Foot Skin Reaction with Facial Erythema." *Annals of Dermatology* 23(1):119–22. doi: 10.5021/ad.2011.23.1.119.

Kiraz, Yağmur, Aysun Adan, Melis Kartal Yandim, and Yusuf Baran. 2016. "Major Apoptotic Mechanisms and Genes Involved in Apoptosis." *Tumor Biology* 37(7):8471–86. doi: 10.1007/s13277-016-5035-9.

Kong, Fan Hua, Qi Fa Ye, Xiong Ying Miao, Xi Liu, Si Qi Huang, Li Xiong, Yu Wen, and Zi Jian Zhang. 2021. "Current Status of Sorafenib Nanoparticle Delivery Systems in the Treatment of Hepatocellular Carcinoma." *Theranostics* 11(11):5464–90. doi: 10.7150/thno.54822.

Krishna, Kowthavarapu V, Sunil Kumar Dubey, Gautam Singhvi, Gaurav Gupta, and Prashant Kesharwani. 2021. "MAPK Pathway : Potential Role in Glioblastoma Multiformurgery." *Interdisciplinary Neurosurgery: Advanced Techniques and Case Management* 23:100901. doi: 10.1016/j.inat.2020.100901.

Krishna, Kowthavarapu Venkata, Ranendra Narayan Saha, and Sunil Kumar Dubey. 2020. "Biophysical, Biochemical, and Behavioral Implications of ApoE3 Conjugated Donepezil Nanomedicine in a Aβ1-42Induced Alzheimer's Disease Rat Model." *ACS Chemical Neuroscience* 11(24):4139–51. doi: 10.1021/acschemneuro.0c00430.

Krishna, Kowthavarapu Venkata, Geetika Wadhwa, Amit Alexander, Neha Kanojia, Ranendra Narayan Saha, Ritushree Kukreti, Gautam Singhvi, and Sunil Kumar Dubey. 2019. "Design

and Biological Evaluation of Lipoprotein-Based Donepezil Nanocarrier for Enhanced Brain Uptake through Oral Delivery." doi: 10.1021/acschemneuro.9b00343.

Kudo, Masatoshi. 2020. "Recent Advances in Systemic Therapy for Hepatocellular Carcinoma in an Aging Society: 2020 Update." *Liver Cancer* 9(6):640–62. doi: 10.1159/000511001.

Kumar, Devendra, Manish Kumar Chatli, Raghvendar Singh, Nitin Mehta, and Pavan Kumar. 2016. "Enzymatic Hydrolysis of Camel Milk Casein and Its Antioxidant Properties." *Dairy Science and Technology* 96(3):391–404. doi: 10.1007/s13594-015-0275-9.

Kumari, Sonali, Saad M. Ahsan, Jerald M. Kumar, Anand K. Kondapi, and Nalam M. Rao. 2017. "Overcoming Blood Brain Barrier with a Dual Purpose Temozolomide Loaded Lactoferrin Nanoparticles for Combating Glioma (SERP-17-12433)." *Scientific Reports* 7(1):1–13. doi: 10.1038/s41598-017-06888-4.

Kuo, Jung Yu, Ching Lung Liao, Yi Shih Ma, Chao Lin Kuo, Jaw Chyun Chen, Yi Ping Huang, Wen Wen Huang, Shu Fen Peng, and Jing Gung Chung. 2022. "Combination Treatment of Sorafenib and Bufalin Induces Apoptosis in NCI-H292 Human Lung Cancer Cells In Vitro." *In Vivo* 36(2):582–95. doi: 10.21873/INVIVO.12741.

Large, Danielle E., Jonathan R. Soucy, Jacob Hebert, and Debra T. Auguste. 2019. "Advances in Receptor-Mediated, Tumor-Targeted Drug Delivery." *Advanced Therapeutics* 2(1800091). doi: 10.1002/adtp.201800091.

Li, Daojin, Mei Zhu, Chen Xu, and Baoming Ji. 2011. "Characterization of the Baicalein E- Bovine Serum Albumin Complex without or with Cu 2+ or Fe 3+ by Spectroscopic Approaches." *European Journal of Medicinal Chemistry* 46(2):588–99. doi: 10.1016/j.ejmech.2010.11.038.

Li, Liang, and Hongyang Wang. 2016. "Heterogeneity of Liver Cancer and Personalized Therapy." *Cancer Letters* 379(2):191–97. doi: 10.1016/j.canlet.2015.07.018.

Li, Xinru, Yanhui Zhang, Yating Fan, Yanxia Zhou, Xiaoning Wang, Chao Fan, Yan Liu, and Qiang Zhang. 2011. "Preparation and Evaluation of Novel Mixed Micelles as Nanocarriers for Intravenous Delivery of Propofol." *Nanoscale Research Letters* 6(1):1–9. doi: 10.1186/1556-276X-6-275.

Li, Yuhua, Qiang Meng, Mengbi Yang, Dongyang Liu, Xiangyu Hou, Lan Tang, Xin Wang, Yuanfeng Lyu, Xiaoyan Chen, Kexin Liu, Ai Ming Yu, Zhong Zuo, and Huichang Bi. 2019. "Current Trends in Drug Metabolism and Pharmacokinetics." *Acta Pharmaceutica Sinica B* 9(6):1113–44. doi: 10.1016/j.apsb.2019.10.001.

Li, Zihuang, Ling Ye, Jingwen Liu, Daizheng Lian, and Xianming Li. 2020. "Sorafenib-Loaded Nanoparticles Based on Biodegradable Dendritic Polymers for Enhanced Therapy of Hepatocellular Carcinoma." *International Journal of Nanomedicine* 15:1469–80. doi:

10.2147/IJN.S237335.

Liou, Geou Yarh, and Peter Storz. 2010. *Reactive Oxygen Species in Cancer*. Vol. 44.

Liu, Chengxia, Ting Ting Jiang, Zhi Xiang Yuan, and Yu Lu. 2020. "Self-Assembled Casein Nanoparticles Loading Triptolide for the Enhancement of Oral Bioavailability." *Natural Product Communications* 15(8). doi: 10.1177/1934578X20948352.

Liu, Chengyu, Zhen Chen, Yuejie Chen, Jia Lu, Yuan Li, Shujing Wang, Guoliang Wu, and Feng Qian. 2016. "Improving Oral Bioavailability of Sorafenib by Optimizing the 'Spring' and 'Parachute' Based on Molecular Interaction Mechanisms." *Molecular Pharmaceutics* 13(2):599–608. doi: 10.1021/acs.molpharmaceut.5b00837.

Liu, Chun Yu, Kuen Feng Chen, and Pei Jer Chen. 2015. "Treatment of Liver Cancer." *Cold Spring Harbor Perspectives in Medicine* 5(9):1–16. doi: 10.1101/cshperspect.a021535.

Liu, Li, Yichen Cao, Charles Chen, Xiaomei Zhang, Angela McNabola, Dean Wilkie, Scott Wilhelm, Mark Lynch, and Christopher Carter. 2006. "Sorafenib Blocks the RAF/MEK/ERK Pathway, Inhibits Tumor Angiogenesis, and Induces Tumor Cell Apoptosis in Hepatocellular Carcinoma Model PLC/PRF/5." *Cancer Research* 66(24):11851–58. doi: 10.1158/0008-5472.CAN-06-1377.

Liu, Qingguan, Yuxue Sun, Qiang Cui, Jianjun Cheng, A. Killpartrik, Alyssa H. Kemp, and Mingruo Guo. 2022. "Characterization, Antioxidant Capacity, and Bioaccessibility of Coenzyme Q10 Loaded Whey Protein Nanoparticles." *Lwt* 160:113258. doi: 10.1016/j.lwt.2022.113258.

Llovet, Josep M., and Jordi Bruix. 2008. "Molecular Targeted Therapies in Hepatocellular Carcinoma." *Hepatology* 48(4):1312–27. doi: 10.1002/hep.22506.Molecular.

Llovet, Josep M., Sergio Ricci, Vincenzo Mazzaferro, Philip Hilgard, Edward Gane, Jean-Frédéric Blanc, Andre Cosme de Oliveira, Armando Santoro, Jean-Luc Raoul, Alejandro Forner, Myron Schwartz, Camillo Porta, Stefan Zeuzem, Luigi Bolondi, Tim F. Greten, Peter R. Galle, Jean-François Seitz, Ivan Borbath, Dieter Häussinger, Tom Giannaris, Minghua Shan, Marius Moscovici, Dimitris Voliotis, and Jordi Bruix. 2008. "Sorafenib in Advanced Hepatocellular Carcinoma." *New England Journal of Medicine* 359(4):378–90. doi: 10.1056/nejmoa0708857.

Lohcharoenkal, Warangkana, Liying Wang, Yi Charlie Chen, and Yon Rojanasakul. 2014. "Protein Nanoparticles as Drug Delivery Carriers for Cancer Therapy." *BioMed Research International* 2014. doi: 10.1155/2014/180549.

Lynch, Shalini S. 2022. "Drug Efficacy and Safety." *MSD Manual Professional Edition*.

M. Corzo-Martínez1, M. Mohan1, J. Dunlap2, and F. Harte3. 2015. "Effect of Ultra-High Pressure Homogenization on the Interaction between Bovine Casein Micelles and Ritonavir."."

Pharmaceutical Research 32(3):1055–71. doi: 10.1007/s11095-014-1518-9.

M.G. Sosa-Herrera, I.E. Lozano-Esquivel, Y.R. Ponce de León-Ramírez, L. P. Martínez-Padilla. 2012. "Effect of Added Calcium Chloride on the Physicochemical and Rheological Properties of Aqueous Mixtures of Sodium Caseinate / Sodium Alginate and Respective Oil-in-Water Emulsions." *Food Hydrocolloids* 29(1):175–84. doi: 10.1016/j.foodhyd.2012.02.017.

Ma, Andi, Bernhard Biersack, Nils Goehringer, Bianca Nitzsche, and Michael Höpfner. 2022. "Novel Thienyl-Based Tyrosine Kinase Inhibitors for the Treatment of Hepatocellular Carcinoma." *Journal of Personalized Medicine* 12(5). doi: 10.3390/jpm12050738.

Madan, Jyotsana R., Izharahemad N. Ansari, Kamal Dua, and Rajendra Awasthi. 2020. "Formulation and in Vitro Evaluation of Casein Nanoparticles as Carrier for Celecoxib." *Advanced Pharmaceutical Bulletin* 10(3):408–17. doi: 10.34172/apb.2020.049.

Mahala Neelam, Aastha Mittal, Manohar lal, and Uma S. Dubey. 2023. "Chromatographic Purification of Proteins with Cytotoxic Potential from Camel Milk against Cervical Cancer Cell Line." *Journal of Camel Practice and Research* 30(1):1–9.

Mahala Neelam, Mittal Aastha, Dubey S. Uma. 2022. "Medicinal Potential of Camel Milk Lactoferrin." in *IntechOpen*.

Mahala, Neelam, Aastha Mittal, Manohar Lal, and Uma S. Dubey. 2022. "Isolation and Characterization of Bioactive Lactoferrin from Camel Milk by Novel PH-Dependent Method for Large Scale Production." *Biotechnology Reports* 36(e00765). doi: 10.1016/j.btre.2022.e00765.

Mammatas, L. H., A. S. Zandvliet, M. Rovithi, R. J. Honeywell, E. L. Swart, G. J. Peters, C. W. Menke-van der Houven van Oordt, and H. M. W. Verheul. 2020. "Sorafenib Administered Using a High-Dose, Pulsatile Regimen in Patients with Advanced Solid Malignancies: A Phase I Exposure Escalation Study." *Cancer Chemotherapy and Pharmacology* 85(5):931–40. doi: 10.1007/s00280-020-04065-5.

Mandlik, Deepa S., Satish K. Mandlik, and Heena B. Choudhary. 2023. "Immunotherapy for Hepatocellular Carcinoma: Current Status and Future Perspectives." *World Journal of Gastroenterology* 29(6):1054–75. doi: 10.3748/wjg.v29.i6.1054.

Marcellin, Patrick, and Blaise K. Kutala. 2018. "Liver Diseases: A Major, Neglected Global Public Health Problem Requiring Urgent Actions and Large-Scale Screening." *Liver International* 38(December 2017):2–6. doi: 10.1111/liv.13682.

Mart, Joel, Maricarmen Hern, M. Abraham, T. Guillermo, and Elvia Mera. 2023. "Computational Studies of Aflatoxin B 1 (AFB 1): A Review." *Toxins* 15(2):135. doi: 10.3390/toxins15020135.

Maryniak, Natalia Zofia, Egon Bech Hansen, Anne Sofie Ravn Ballegaard, Ana Isabel Sancho,

and Katrine Lindholm Bøgh. 2018. “Comparison of the Allergenicity and Immunogenicity of Camel and Cow’s Milk—A Study in Brown Norway Rats.” *Nutrients* 10(12). doi: 10.3390/nu10121903.

Maulana, Reza Achmad, Faizah Fulyani, and Gemala Anjani. 2022. “Nanocarriers System for Vitamin D as Nutraceutical in Type 2 Diabetes: A Review.” *Open Access Macedonian Journal of Medical Sciences* 10(F):427–36. doi: 10.3889/oamjms.2022.9507.

Mehla, Rita, and Shalini Arora. 2021. “Potential of Milk Protein as a Carrier of Functional Ingredients.” *Journal of Nutrition & Food Sciences* 11:242.

Méndez-Sánchez, Nahum, Alejandro Valencia-Rodríguez, Carlos E. Coronel-Castillo, and Xingshun Qi. 2021. “Narrative Review of Hepatocellular Carcinoma: From Molecular Bases to Therapeutic Approach.” *Digestive Medicine Research* 4(January 2021):15–15. doi: 10.21037/dmr-20-116.

Mittal, Aastha, Neelam Mahala, Kowthavarapu Venkata Krishna, Uma S. Dubey, and Sunil Kumar Dubey Dubey. 2021. “Calcium Chloride Linked Camel Milk Derived Casein Nanoparticles for the Delivery of Sorafenib in Hepatocarcinoma Cells.” *BIOCELL* 46:127–36.

Mohamed, Huda, Monika Johansson, Åse Lundh, Peter Nagy, and Afaf Kamal-Eldin. 2020. “Short Communication: Caseins and α-Lactalbumin Content of Camel Milk (Camelus Dromedarius) Determined by Capillary Electrophoresis.” *Journal of Dairy Science* 103(12):11094–99. doi: 10.3168/jds.2020-19122.

Mondal, Dipankar, Kausik Das, and Abhijit Chowdhury. 2022. “Epidemiology of Liver Diseases in India.” *Clinical Liver Disease* 19(3). doi: 10.1002/cld.1177.

Morales, Julio C., Longshan Li, Farjana J. Fattah, Ying Dong, Erik A. Bey, Malina Patel, Jinming Gao, and David A. Boothman. 2014. “Review of Poly (ADP-Ribose) Polymerase (PARP) Mechanisms of Action and Rationale for Targeting in Cancer and Other Diseases.” *Critical Reviews in Eukaryotic Gene Expression* 24(1):15–28. doi: 10.1615/CritRevEukaryotGeneExpr.2013006875.

Morris, Gordon A. 2002. “The Self-Assembly and Structure of Caseins in Solution.” *Biotechnology and Genetic Engineering Reviews* 19(1):357–76. doi: 10.1080/02648725.2002.10648034.

Mou, Lisha, Xiaohe Tian, Bo Zhou, Yongqiang Zhan, Jiao Chen, Ying Lu, Jing Deng, Ying Deng, Zijing Wu, Qi Li, Yi’an Song, Hongyuan Zhang, Jinjun Chen, Kuifeng Tian, Yong Ni, and Zuhui Pu. 2021. “Improving Outcomes of Tyrosine Kinase Inhibitors in Hepatocellular Carcinoma: New Data and Ongoing Trials.” *Frontiers in Oncology* 11(October):1–11. doi: 10.3389/fonc.2021.752725.

Mukthinuthalapati, V. V. Pavan Kedar, Vikash Sewram, Ntokozo Ndlovu, and Stephen Kimani.

2021. “Hepatocellular Carcinoma in Sub-Saharan Africa.” *JCO Global Oncology* 7:756–66.

Narayanan, Sreeja, Maya Pavithran, Aiswarya Viswanath, Dhanya Narayanan, Chandini C. Mohan, K. Manzoor, and Deepthy Menon. 2014. “Sequentially Releasing Dual-Drug-Loaded PLGA-Casein Core/Shell Nanomedicine: Design, Synthesis, Biocompatibility and Pharmacokinetics.” *Acta Biomaterialia* 10(5):2112–24. doi: 10.1016/j.actbio.2013.12.041.

Narvekar, Mayuri, Hui Yi Xue, June Young Eoh, and Ho Lun Wong. 2014. “Nanocarrier for Poorly Water-Soluble Anticancer Drugs - Barriers of Translation and Solutions.” *AAPS PharmSciTech* 15(4):822–33. doi: 10.1208/s12249-014-0107-x.

Nishida, Naoyo, Hirohisa Yano, Takashi Nishida, Toshiharu Kamura, and Masamichi Kojiro. 2006. “Angiogenesis in Cancer.” *Vascular Health and Risk Management* 2(3):213–19. doi: 10.2147/vhrm.2006.2.3.213.

Niu, Gang, Xiaoyuan Chen. 2010. “Vascular Endothelial Growth Factor as a Target for Antiangiogenic Therapy.” *Current Drug Targets* 8(11):1000–1017.

Olusanya, Temidayo O. B., Rita Rushdi Haj Ahmad, Daniel M. Ibegbu, James R. Smith, and Amal Ali Elkordy. 2018. “Liposomal Drug Delivery Systems and Anticancer Drugs.” *Molecules* 23(907). doi: 10.3390/molecules23040907.

Onur, Senol. 2018. “Rapid Determination and Validation of Sorafenib via UV-Visible Method in Pharmaceutical Formulations.” *Balıkesir Sağlık Bilimleri Dergisi* 7(3):87–92.

Ozaki, Toshinori, and Akira Nakagawara. 2011. “Role of P53 in Cell Death and Human Cancers.” *Cancers* 3(1):994–1013. doi: 10.3390/cancers3010994.

Paradis, Valérie, and Jessica Zucman-Rossi. 2023. “Pathogenesis of Primary Liver Carcinomas.” *Journal of Hepatology* 78(2):448–49. doi: 10.1016/j.jhep.2022.05.037.

Patra, Jayanta Kumar, Gitishree Das, Leonardo Fernandes Fraceto, Estefania Vangelie, Ramos Campos, Pilar Rodriguez, Laura Susana, Acosta Torres, Luis Armando, Diaz Torres, and Renato Grillo. 2018. “Nano Based Drug Delivery Systems : Recent Developments and Future Prospects.” *Journal of Nanobiotechnology* 1–33. doi: 10.1186/s12951-018-0392-8.

Pazzaglia, Simonetta, and Claudio Pioli. 2020. “Multifaceted Role of Parp-1 in Dna Repair and Inflammation: Pathological and Therapeutic Implications in Cancer and Non-Cancer Diseases.” *Cells* 9(1):41. doi: 10.3390/cells9010041.

Penalva, Rebeca, Irene Esparza, Maite Agüeros, Carlos J. Gonzalez-navarro, Carolina Gonzalez-ferrero, and Juan M. Irache. 2015. “Casein Nanoparticles as Carriers for the Oral Delivery of Folic Acid.” *Food Hydrocolloids* 44:399–406.

Peng, Chang Liang, Wei Guo, Tao Ji, Tingting Ren, Yi Yang, Da Sen Li, Hua Yi Qu, Xiao Li, Shun Tang, Tai Qiang Yan, and Xiao Dong Tang. 2009. “Sorafenib Induces Growth

Inhibition and Apoptosis in Human Synovial Sarcoma Cells via Inhibiting the RAF/MEK/ERK Signaling Pathway." *Cancer Biology and Therapy* 8(18):1729–36. doi: 10.4161/cbt.8.18.9208.

Petrick, Jessica L., and Katherine A. McGlynn. 2019. "The Changing Epidemiology of Primary Liver Cancer Jessica." *Current Epidemiology Reports* 6(2):104–11. doi: 10.1007/s40471-019-00188-3.

Pons, Fernando, Maria Varela, and Josep M. Llovet. 2005. "Staging Systems in Hepatocellular Carcinoma." *HPB* 7(1):35–41. doi: 10.1080/13651820410024058.

Prieto-Domínguez, Nestor, Raquel Ordóñez, Anna Fernández, Andres García-Palomo, Jordi Muntané, Javier González-Gallego, and José L. Mauriz. 2016. "Modulation of Autophagy by Sorafenib: Effects on Treatment Response." *Frontiers in Pharmacology* 7(151):1–16. doi: 10.3389/fphar.2016.00151.

Raica, Marius, and Anca Maria Cimpean. 2010. "Platelet-Derived Growth Factor (PDGF)/PDGF Receptors (PDGFR) Axis as Target for Antitumor and Antiangiogenic Therapy." *Pharmaceuticals* 3(3):572–99. doi: 10.3390/ph3030572.

Rajesh, Singh, and James W. Lillard Jr. 2009. "Nanoparticle-Based Targeted Drug Delivery." *Experimental & Molecular Pathology* 86(3):215–23. doi: 10.1016/j.yexmp.2008.12.004.Nanoparticle-based.

Ranadheera, C. S., W. S. Liyanaarachchi, Jayani Chandrapala, Muditha Dissanayake, and Todor Vasiljevic. 2016. "Utilizing Unique Properties of Caseins and the Casein Micelle for Delivery of Sensitive Food Ingredients and Bioactives." *Trends in Food Science and Technology* 57:178–87. doi: 10.1016/j.tifs.2016.10.005.

Raut, Hrushikesh, Chetana Jadhav, Karishma Shetty, Neha Laxane, Harsh P. Nijhawan, GSN Koteswara Rao, Rajasekhar Reddy Alavala, Garima Joshi, Ch Niranjan Patro, Govind Soni, and Khushwant S. Yadav. 2022. "Sorafenib Tosylate Novel Drug Delivery Systems: Implications of Nanotechnology in Both Approved and Unapproved Indications." *OpenNano* 8(November):100103. doi: 10.1016/j.onano.2022.100103.

Rodríguez, Francisco, Pablo Caruana, Noa De la Fuente, Pía Español, María Gámez, Josep Balart, Elisa Llurba, Ramón Rovira, Raúl Ruiz, Cristina Martín-Lorente, José Luis Corchero, and María Virtudes Céspedes. 2022. "Nano-Based Approved Pharmaceuticals for Cancer Treatment: Present and Future Challenges." *Biomolecules* 12(784). doi: 10.3390/biom12060784.

Rumgay, Harriet, Melina Arnold, Jacques Ferlay, Olufunmilayo Lesi, Citadel J. Cabasag, Jérôme Vignat, Mathieu Laversanne, Katherine A. McGlynn, and Isabelle Soerjomataram. 2022. "Global Burden of Primary Liver Cancer in 2020 and Predictions to 2040." *Journal of Hepatology* 77(6):1598–1606. doi: 10.1016/j.jhep.2022.08.021.

Runthala, Ashish, Mustapha Mbye, Mutamed Ayyash, Yajun Xu, and Afaf Kamal-Eldin. 2023. "Caseins: Versatility of Their Micellar Organization in Relation to the Functional and Nutritional Properties of Milk." *Molecules* 28(5):1–36. doi: 10.3390/molecules28052023.

Ryan, Michael J., Jonathon Willatt, Bill S. Majdalany, Ania Z. Kielar, Suzanne Chong, Julie A. Ruma, and Amit Pandya. 2016. "Ablation Techniques for Primary and Metastatic Liver Tumors." *World Journal of Hepatology* 8(3):191–99. doi: 10.4254/wjh.v8.i3.191.

Sabra, Sally A., Ahmed O. Elzoghby, Salah A. Sheweita, Medhat Haroun, Maged W. Helmy, Maha A. Eldemellawy, Ying Xia, David Goodale, Alison L. Allan, and Sohrab Rohani. 2018. "Self-Assembled Amphiphilic Zein-Lactoferrin Micelles for Tumor Targeted Co-Delivery of Rapamycin and Wogonin to Breast Cancer." *European Journal of Pharmaceutics and Biopharmaceutics* 128:156–69. doi: 10.1016/j.ejpb.2018.04.023.

Sadiq, Uzma, Harsharn Gill, and Jayani Chandrapala. 2021. "Casein Micelles as an Emerging Delivery System for Bioactive Food Components." *Foods* 10(8). doi: 10.3390/foods10081965.

Sahu, Abhishek, Naresh Kasoju, and Utpal Bora. 2008. "Fluorescence Study of the Curcumin - Casein Micelle Complexation and Its Application as a Drug Nanocarrier to Cancer Cells." *Biomacromolecules* 9(Figure 1):2905–12.

Salami, Maryam, Ali Akbar Moosavi-Movahedi, Faezeh Moosavi-Movahedi, Mohammad Reza Ehsani, Reza Yousefi, Mohammad Farhadi, Amir Niasari-Naslaji, Ali Akbar Saboury, Jean Marc Chobert, and Thomas Haertlé. 2011. "Biological Activity of Camel Milk Casein Following Enzymatic Digestion." *Journal of Dairy Research* 78(4):471–78. doi: 10.1017/S0022029911000628.

Seifu, Eyassu. 2023. "Camel Milk Products: Innovations, Limitations and Opportunities." *Food Production, Processing and Nutrition* 5(1). doi: 10.1186/s43014-023-00130-7.

Shetty, Vijith Vittal, and Adithi Kellarai. 2022. "Comprehensive Review of Hepatocellular Carcinoma in India: Current Challenges and Future Directions." *JCO Global Oncology* (8):1–10. doi: 10.1200/go.22.00118.

Shihong Shen, Youshen wu, Yongchun Liu, Daocheng Wu. 2017. "High Drug-Loading Nanomedicines : Progress , Current Status , and Prospects." *International Journal of Nanomedicine* 12:4085–4109.

Shubham Shitole, Santosh Waghmare, Hemant Kamble 1Dept. 2022. "Nanoparticle-Novel Drug Delivery System Microsphere: A Review." *International Journal for Research in Applied Science & Engineering Technology (IJRASET)* 10(1):9–16. doi: 10.36346/sarjap.2022.v03i02.001.

Siegel, Rebecca L., Kimberly D. Miller, Nikita Sandeep Wagle, and Ahmedin Jemal. 2023.

"Cancer Statistics, 2023." *CA: A Cancer Journal for Clinicians* 73(1):17–48. doi: 10.3322/caac.21763.

Singal, Amit G., Pietro Lampertico, and Pierre Nahon. 2020. "Epidemiology and Surveillance for Hepatocellular Carcinoma: New Trends." *Journal of Hepatology* 72(2):250–61. doi: 10.1016/j.jhep.2019.08.025.

Sona Gandhi, Indrajit Roy. 2018. "Doxorubicin-Loaded Casein Nanoparticles for Drug Delivery: Preparation, Characterization and in Vitro Evaluation." *International Journal of Biological Macromolecules 121 (2019) 6-12*.

Suman, Shubhankar, Akshay Pandey, and Sudhir Chandna. 2012. "An Improved Non-Enzymatic 'DNA Ladder Assay' for More Sensitive and Early Detection of Apoptosis." *Cytotechnology* 64(1):9–14. doi: 10.1007/s10616-011-9395-0.

Sung, Hyuna, Jacques Ferlay, Rebecca L. Siegel, Mathieu Laversanne, Isabelle Soerjomataram, Ahmedin Jemal, and Freddie Bray. 2021. "Global Cancer Statistics 2020: GLOBOCAN Estimates of Incidence and Mortality Worldwide for 36 Cancers in 185 Countries." *CA: A Cancer Journal for Clinicians* 71(3):209–49. doi: 10.3322/caac.21660.

Swelum, Ayman A., Mohamed T. El-Saadony, Mohamed Abdo, Rabee A. Ombarak, Elsayed O. S. Hussein, Gamaleldin Suliman, Ahmed R. Alhimaidi, Aiman A. Ammari, Hani Ba-Awadh, Ayman E. Taha, Khaled A. El-Tarabily, and Mohamed E. Abd El-Hack. 2021. "Nutritional, Antimicrobial and Medicinal Properties of Camel's Milk: A Review." *Saudi Journal of Biological Sciences* 28(5):3126–36. doi: 10.1016/j.sjbs.2021.02.057.

Tang, Xiaolong, Longzhou Chen, Amin Li, Shiyu Cai, Yinci Zhang, and Xueke Liu. 2018. "Anti-GPC3 Antibody-Modified Sorafenib-Loadednanoparticles Significantly Inhibited HepG2 Hepatocellular Carcinoma." *Drug Delivery* 25(1):1484–94. doi: 10.1080/10717544.2018.1477859.

Tao, Chun Lian, Hao Lin, and Shun Qing Chen. 2014. "The Regulation of ERK and P-ERK Expression by Cisplatin and Sorafenib in Gastric Cancer Cells." *Gene* 552(1):106–15. doi: 10.1016/j.gene.2014.09.019.

Toutain, P. L., and A. Bousquet-Mélou. 2004. "Bioavailability and Its Assessment." *Journal of Veterinary Pharmacology and Therapeutics* 27(6):455–66. doi: 10.1111/j.1365-2885.2004.00604.x.

Tran, Hao Thi, Long Binh Vong, Yuji Nishikawa, and Yukio Nagasaki. 2022. "Sorafenib-Loaded Silica-Containing Redox Nanoparticles for Oral Anti-Liver Fibrosis Therapy." *Journal of Controlled Release* 345(April):880–91. doi: 10.1016/j.jconrel.2022.04.002.

Tran, Tuan Hiep, Phuong Thi Thu Tran, and Duy Hieu Truong. 2023. "Lactoferrin and Nanotechnology: The Potential for Cancer Treatment." *Pharmaceutics* 15:1362. doi:

10.3390/pharmaceutics15051362.

Usmani, Afreen, Anuradha Mishra, and Mohd Ahmad. 2018. “Nanomedicines: A Theranostic Approach for Hepatocellular Carcinoma.” *Artificial Cells, Nanomedicine and Biotechnology* 46(4):680–90. doi: 10.1080/21691401.2017.1374282.

Vaseva, Angelina V., and Ute M. Moll. 2009. “The Mitochondrial P53 Pathway.” *Biochimica et Biophysica Acta (BBA)-Bioenergetics* 1787(5):414–20. doi: 10.1016/j.bbabio.2008.10.005.The.

Wang, Yifan, Si Chen, Xin Yang, Shuang Zhang, and Chunying Cui. 2021. “Preparation Optimization of Bovine Serum Albumin Nanoparticles and Its Application for Sirna Delivery.” *Drug Design, Development and Therapy* 15:1531–47. doi: 10.2147/DDDT.S299479.

William H. Gmeiner and Supratim Ghosh. 2015. “Nanotechnology for Cancer Treatment.” *Nanotechnol Rev.* 3(2):111–22. doi: 10.1515/ntrev-2013-0013.

Williams, Roger. 2006. “Global Challenges in Liver Disease.” *Hepatology* 44(3):521–26. doi: 10.1002/hep.21347.

Wlodkowic, Donald, Joanna Skommer, and Zbigniew Darzynkiewicz. 2009. “Flow Cytometry-Based Apoptosis Detection.” *Methods in Molecular Biology (Clifton, N.J.)* 559(0):19–32. doi: 10.1007/978-1-60327-017-5_2.

Xia, Xiaojing, Haowei Liu, Huixia Lv, Jing Zhang, Jianping Zhou, and Zhiying Zhao. 2017. “Preparation, Characterization, and in Vitro/Vivo Studies of Oleanolic Acid-Loaded Lactoferrin Nanoparticles.” *Drug Design, Development and Therapy* 11:1417–27. doi: 10.2147/DDDT.S133997.

Yang, Ju Dong, Lewis R. Roberts. 2010. “Epidemiology and Management of Hepatocellular Carcinoma.” *Infectious Disease Clinics* 24(4):899–919. doi: 10.1016/j.idc.2010.07.004.Epidemiology.

Yang, Ju Dong, Pierre Hainaut, Gregory J. Gores, Amina Amadou, Amelie Plymoth, and Lewis R. Roberts. 2019. “A Global View of Hepatocellular Carcinoma: Trends, Risk, Prevention and Management.” *Nature Reviews Gastroenterology and Hepatology* 16(10):589–604. doi: 10.1038/s41575-019-0186-y.

Yang, Shaomei, Bo Zhang, Xiaowei Gong, Tianqi Wang, Yongjun Liu, and Na Zhang. 2016. “In Vivo Biodistribution, Biocompatibility, and Efficacy of Sorafenib-Loaded Lipid-Based Nanosuspensions Evaluated Experimentally in Cancer.” *International Journal of Nanomedicine* 11:2329–43. doi: 10.2147/IJN.S104119.

Yasuhiro Tsumea, Deanna M. Mudiea, Peter Langguthb, Greg E. Amidona, and Gordon L. Amidona. 2014. “The Biopharmaceutics Classification System: Subclasses for in Vivo

Predictive Dissolution (IPD) Methodology and IVIVC Yasuhiro." *European Journal of Pharmaceutical Sciences* 57:152–163. doi: 10.1016/j.ejps.2014.01.009.The.

Ye, Ling, Xiaoshan Yang, Enshuang Guo, Weiying Chen, Linlin Lu, Ying Wang, Xiaojuan Peng, Tongmeng Yan, Fuyan Zhou, and Zhongqiu Liu. 2014. "Sorafenib Metabolism Is Significantly Altered in the Liver Tumor Tissue of Hepatocellular Carcinoma Patient." *PLoS ONE* 9(5):1–8. doi: 10.1371/journal.pone.0096664.

Yelubaeva, Makhpal Yelubaevna, Batyrkhan Azimkhanovich Buralkhiev, Assiya Demeukhanovna Serikbayeva, Mirash Hudretovna Narmuratova, and Shynar Yırmkızy Kenenbay. 2017. "Electrophoretic Identification of Casein in Various Types of Milk." *OnLine Journal of Biological Sciences* 17(4):348–52. doi: 10.3844/ojbsci.2017.348.352.

Yen, Chon Ho, Yin Shen Lin, and Ching Fu Tu. 2015. "A Novel Method for Separation of Caseins from Milk by Phosphates Precipitation." *Preparative Biochemistry and Biotechnology* 45(1):18–32. doi: 10.1080/10826068.2013.877030.

Yue, Qiaoli, Tongfei Shen, Changna Wang, Chaohui Gao, and Jifeng Liu. 2012. "Study on the Interaction of Bovine Serum Albumin with Ceftriaxone and the Inhibition Effect of Zinc (II)." *International Journal of Spectroscopy* 2012. doi: 10.1155/2012/284173.

Zhang, Dan, Lin Liu, Jian Wang, Hong Zhang, Zhuo Zhang, Gang Xing, Xuan Wang, and Minghua Liu. 2022. "Drug-Loaded PEG-PLGA Nanoparticles for Cancer Treatment." *Frontiers in Pharmacology* 13(August):1–12. doi: 10.3389/fphar.2022.990505.

Zhang, Huajun, Wuyang Zhang, Longying Jiang, and Yongheng Chen. 2022. "Recent Advances in Systemic Therapy for Hepatocellular Carcinoma." *Biomarker Research* 10(1):1–21. doi: 10.1186/s40364-021-00350-4.

Zhang, W., M. Konopleva, V. R. Ruvolo, T. McQueen, R. L. Evans, W. G. Bornmann, J. McCubrey, J. Cortes, and M. Andreeff. 2008. "Sorafenib Induces Apoptosis of AML Cells via Bim-Mediated Activation of the Intrinsic Apoptotic Pathway." *Leukemia* 22(4):808–18. doi: 10.1038/sj.leu.2405098.

Zhang, Zhen Hai, Xiao Pan Wang, Waddad Y. Ayman, Were L. L. Munyendo, Hui Xia Lv, and Jian Ping Zhou. 2013. "Studies on Lactoferrin Nanoparticles of Gambogic Acid for Oral Delivery." *Drug Delivery* 20(2):86–93. doi: 10.3109/10717544.2013.766781.

Zhang, Zhiwen, Baohua Niu, Jian Chen, Xinyu He, Xiaoyue Bao, Jianhua Zhu, Haijun Yu, and Yaping Li. 2014. "The Use of Lipid-Coated Nanodiamond to Improve Bioavailability and Efficacy of Sorafenib in Resisting Metastasis of Gastric Cancer." *Biomaterials* 35(15):4565–72. doi: 10.1016/j.biomaterials.2014.02.024.

Zittle, C. A., E. S. DellaMonica, R. K. Rudd, and J. H. Custer. 1958. "Binding of Calcium to Casein: Influence of PH and Calcium and Phosphate Concentrations." *Archives of*

Biochemistry and Biophysics 76(2):342–53. doi: 10.1016/0003-9861(58)90159-0.

Zwicke, Grant L., G. Ali Mansoori, and Constance J. Jeffery. 2012. "Utilizing the Folate Receptor for Active Targeting of Cancer Nanotherapeutics." *Nano Reviews* 3(18496).

Appendix I: List of Publications

A.1 Publication from Thesis

- **Aastha Mittal**, Neelam Mahala, Kowthavarapu Venkata Krishna, Uma S. Dubey, and Sunil Kumar Dubey. "Calcium chloride linked camel milk-derived casein nanoparticles for the delivery of sorafenib in hepatocarcinoma cells." Biocell 46, no. 1 (2022): 127-136. DOI:10.32604/biocell.2021.015932
- **Aastha Mittal,** Neelam Mahala, Nikhil Hanamant Dhanawade, Sunil Kumar Dubey, Uma S. Dubey. Evaluation of the cytotoxic activity of sorafenib-loaded camel milk casein nanoparticles against hepatocarcinoma cells. (Under revision)

A.2 Patent

- Uma Shukla Dubey, Neelam Mahala, **Aastha Mittal,** Manohar Lal. "Methods for Isolation of Lactoferrin from Camel Milk". Patent Application No: 202211003167, filled on 18th January 2022.

A.3 Other Publications

- Neelam Mahala, **Aastha Mittal,** Manohar Lal, and Uma S. Dubey. (2022). "Isolation and Characterization of Bioactive Lactoferrin from Camel Milk by Novel pH-Dependent Method for Large Scale Production". Biotechnology Reports, e00765. DOI: 10.1016/j.btre. 2022.e00765.
- Neelam Mahala, **Aastha Mittal,** and Uma S. Dubey. "Medicinal potential of Camel Milk Lactoferrin". In (Ed.), Dairy Processing - From Basics to Advances. IntechOpen. https://doi.org/10.5772/intechopen.108316.
- Neelam Mahala, Manohar Lal, **Aastha Mittal,** and Uma S. Dubey. Chromatographic Purification of Proteins with Cytotoxic Potential from Camel milk whey against cervical cancer cell line. Journal of Camel Practice and Research. Vol 30 No 1, p 53-61, DOI: 10.5958/2277-8934.2023.00007.3.
- Manohar Lal, Neelam Mahala, **Aastha Mittal,** Anisha Ramdas, Chetan Shrivastava and Uma S. Dubey. Studies on cytotoxic activity of camel milk whey protein as a nutraceutical against HeLa cells. Journal of Camel Practice and Research. Vol 30 No 2, p 155-164, DOI: 10.5958/2277-8934.2023.00021.8.

A.4 Posters Presented in Conferences

- **Aastha Mittal,** Uma S. Dubey "Development, characterization, and evaluation of sorafenib loaded casein nanoparticles" in "Young Scientists' Conference (YSC) as a part of India International Science Festival (IISF) 2020 on 22nd – 24th December 2020 organized by the Ministry of Science and Technology; Ministry of Earth Sciences, and Ministry of Health and Family Welfare, Govt. of India in collaboration with Vijnana Bharati (VIBHA) by Council of Scientific & Industrial Research (CSIR). YSC, IISF-2020) **(oral presentation).**
- **Aastha Mittal,** Dr.Sunil Kumar Dubey, Uma S. Dubey "Characterisation of Sorafenib loaded Casein nanoparticles" in International Conference on emerging Areas in Biosciences and Biomedical Technologies (eBBt-2) on 7-9th feb, 2020 organized by Indian Institute of Technology (IIT) Indore, India. **(Poster presentation).**
- Neelam Mahala, Manohar Lal, **Aastha Mittal**, Uma S. Dubey "Studies on Anti-Cancer Property of Proteins isolated from Camelus dromedarius Milk" in "Young Scientists' Conference (YSC) in India International Science Festival 2019 on 5th – 7th November 2019 organized at Biswa Bangla Convention Centre, Kolkata, India. (YSC, IISF-2019).
- Kumar Udit Saumya, Neelam Mahala, **Aastha Mittal,** Manohar Lal, Uma S. Dubey "Comparative Bioinformatics Analysis of Camel Milk Proteins and their Bioactive peptides with potential Anticancer and Antimicrobial activities" in "Breaking Barriers through Bioinformatics & Computational Biology" on 31st July – 1st August 2017 organized by Supercomputing Facility for Bioinformatics and Computational Biology -104- (SCFBio), IIT Delhi, India. (SCFBio-2017, IIT Delhi)
- Manohar Lal, Neelam Mahala, **Aastha Mittal,** Kumar Udit Saumya, Uma S. Dubey* "Investigation of the anti-cancer property of camel milk proteins" in "International Conference on Challenges in Drug Delivery (ICCD3)" on 2nd – 4th March 2017 organized by Department of Pharmacy at BITS-Pilani, Pilani Campus, Pilani-333031, Rajasthan, India. (ICCD3-2017, BITS-Pilani)
- Kumar Udit Saumya, Manohar Lal, Neelam Mahala, **Aastha Mittal,** Uma S. Dubey* "Analysis of mammalian milk protein-derived Peptides with Potential Anti-cancer and Anti-microbial Activities using Bioinformatics Approach" in "International Conference on Challenges in Drug Delivery (ICCD3)" on 2nd – 4th March 2017 organized by Department of Pharmacy at BITS-Pilani, Pilani Campus, Pilani333031, Rajasthan, India. (ICCD3-2017, BITS-Pilani)

A.5 Workshop Attended

- Participated in the 3rd Workshop on Analytical Instruments for Chemical & Environmental Engineers (WAICEE – 2017) organized by the Department of Chemical Engineering & IIChE Pilani Regional Centre from 10th – 11th February 2017 at BITS Pilani, Pilani Campus, Pilani-333031, Rajasthan, India.

Appendix II: Biography of guide, co-guides and candidate

A brief biography of the Supervisor

Dr. Uma S. Dubey is an Associate Professor in the Department of Biological Sciences at BITS Pilani-Pilani Campus. She has served this department for 20 years in various teaching and research-related posts. She conducted teaching and program development in the Biotechnology, Microbiology, and Environmental Sciences departments at the Institute of Life Sciences, Kanpur University. She also has a year's research experience at the Department of Plant Sciences, University of Alberta, Canada. She has done her Ph.D. in Immunology (under the supervision of Prof. S.S. Agarwal) from Sanjay Gandhi Post Graduate Institute of Medical Sciences, Lucknow.

Teaching: She has taught more than 15 courses in the Department of Biological Sciences, BITS Pilani. She has been involved in many of these course planning and development. Besides this, she has initiated two new courses in Immunology and Cancer Biology. She has coordinated the course restructuring of the M.Sc. and ME programs of the Biological Science Department as DCA Convener from 2012 -2014 and continues as a member. She has coordinated the Science, Imagination, and Discovery (SID) workshop at BITS Pilani. She has been Judging various events of APOGEE since 2006-onwards in Biological Sciences and Medical Sciences categories. She is a member of My India Team, BITS Pilani.

Her research interest is in immunology and cancer biology's theoretical and practical aspects. Specifically, in (i) Cellular Immune Responses: She has been involved in comparative studies on Lymphocyte proliferation, Natural Killer cell function, and Antibody-dependent cellular cytotoxicity at average and febrile temperatures. Also, the cell cycle proliferation kinetics of lymphocytes and cell lines is interesting. (ii) Mathematical Modelling of Immune System: She studied the interaction of various immune system components, cancer cells, and infectious agents in the presence and absence of environmental toxicants. The analysis requires theoretical, mathematical, and computational input. (iii) Cancer Biology: She is interested in studying the anticancer properties attributed to Camel milk proteins such as whey proteins & casein proteins and associated mechanisms of action. She has received a research

grant from the Department of Science and Technology (DST), Rajasthan. She singly guided Ph.D. scholars, and at present, she is guiding two more Ph.D. scholars to fulfil their thesis. She has supervised four more students as their Co-guide and is continueing to guide one more as the same. She has filed one patent, published 21 original research articles, and has three book chapters and one lab manual to her credit.

A brief biography of the Co-Supervisor -1

Dr. Sunil Kumar Dubey is presently working as the General Manager, Medical Research, R&D Healthcare Division at Emami Ltd, Kolkata. He is involved in planning and ensuring the timely execution of several preclinical and clinical studies. His expertise involves in validating the effectiveness of a vast range of healthcare products and providing business development-related insights. He is responsible for developing product concept notes, technical notes, monographs, and dossiers. His team is also involved in supporting medico-marketing, product licensing activities, and training personnel from marketing and sales teams. Collectively, his efforts are towards bridging the gap between the industry, consumers, and the scientific community.

Overall, he has more than 16 years of industrial, teaching, research, and administrative experience. Prior to this, he was Assistant Professor in the Department of Pharmacy, Birla Institute of Technology and Science (BITS), Pilani, India. He was also a visiting Assistant Research Professor in the Department of Chemical and Biomolecular Engineering at the University of Maryland, USA. Currently, he also serves as a guest faculty at various leading institutes including NIPER Guwahati, NIPER Raebareli, Jamia Hamdard, etc. He has an extensive research experience in the area of pharmacokinetic pharmacodynamic modelling and simulations, development of phytopharmaceuticals and numerous nano-technology-based platforms. He has supervised Ph.D., postgraduate and undergraduate students. He has published more than 150 articles and book chapters in renowned high-impact journals and presented papers at conferences in India and abroad. He is included in the list of ‘World’s Top 2% Most-Cited Scientists’ as per the Elsevier-Stanford University report. He has successfully completed various government and

industry-funded projects related to new product development, pharmacokinetic and pharmacodynamic investigations. All these concerted efforts have also led to the grant of patents to his name.

A brief biography of the Co-Supervisor -2

Dr. Rajeev Taliyan is a Professor in the Department of Pharmacy, Birla Institute of Technology and Science, Pilani, Pilani-campus, Rajasthan. He has completed his M.Pharm. (Pharmacology) from Punjabi University-Patiala, Punjab, and Ph.D. in Pharmacology with Prof. P.L Sharma and Late Prof. Manjeet Singh (Ex-Head, Dean, Punjabi University) from ISF College, Punjab Technical University, Punjab. His field of expertise is Cardiovascular and Neuropharmacology. Dr. Taliyan published numerous research papers in national and International reputed Journals. He delivered invited talks and attended and presented scientific papers at several national and international conferences. He is a member of the editorial board and reviewer of many reputed journals. He is also an Ex- executive member of the Indian Pharmacological Society (IPS) and is actively involved in the regional conference of IPS. He is currently a member of the Institutional Human Ethics Committee, Institutional Animal Ethics Committee (IAEC), BITS Pilani, Pilani Campus. Many prizes and awards are also in his credit, including the prestigious NAMS membership award.

A brief biography of the Candidate

Ms. Aastha Mittal did her Bachelor's (BSc. Biotechnology) and Master's (MSc. Biotechnology) from Banasthali University Newai, Rajasthan, India, in 2014 & 2016 respectively. She joined Birla Institute of Technology & Science (BITS) Pilani, Pilani Campus as a JRF in the Department of Science and Technology (DST) Rajasthan project in 2017. After that, in the same year, she enrolled in PhD, under the supervision of Prof. Uma S. Dubey and the Co-supervision of Dr. Sunil Kumar Dubey

and Prof. Rajeev Taliyan. She has worked on isolating camel milk proteins and studying their anticancer properties. She has also extended her research interest in nanoparticulate drug delivery systems in cancer. She has presented her research work as an oral and poster presentation at an international conference. She has four published research articles and filed a one patent. During her Ph.D. she was also involved in the Department's teaching activities by taking courses for first and higher-degree students of the BITS Pilani campus.